

3. SITE 503: EASTERN EQUATORIAL PACIFIC¹

Shipboard Scientific Party²

HOLE 503

Date occupied: 6 September 1979

Date departed: 7 September 1979

Time on hole: 16 hr.

Position: 4°03.04'N, 95°38.21'W

Water depth (sea level; corrected m; echo-sounding): 3672

Water depth (rig floor; corrected m; echo-sounding): 3682

Penetration (m): 4.78

Number of cores: 1

Total length of cored section (m): 4.78

Total core recovered (m): 4.78

Core recovery (%): 100

Oldest sediment cored:

Depth sub-bottom (meters): 4.78

Nature: Siliceous marl

Age: Quaternary

Measured velocity (km/s): 1.5206

Core recovery (%): 58.8

Oldest sediment cored:

Depth sub-bottom (meters): 234.74

Nature: Siliceous nannofossil ooze

Age: late Miocene

Measured velocity (km/s): 1.5567

Shear strength (g/cm²): 1119.75

HOLE 503A

Date occupied: 7 September 1979

Date departed: 11 September 1979

Time on hole: 88.3 hr.

Position: 4°04.04'N, 95°38.21'W

Water depth (sea level; corrected m; echo-sounding): 3672

Water depth (rig floor; corrected m; echo-sounding): 3682

Penetration (m): 235.0

Number of cores: 54

Total length of cored section (m): 235.0

Total core recovered (m): 138.16

Date occupied: 11 September 1979

Date departed: 13 September 1979

Time on hole: 52.0 hr.

Position: 4°03.02'N, 95°38.32'W

Water depth (sea level; corrected m; echo-sounding): 3672

Water depth (rig floor; corrected m; echo-sounding): 3682

Penetration (m): 112.8

Number of cores: 26

Total length of cored section (m): 112.8

Total core recovered (m): 94.17

Core recovery (%): 83.5

Oldest sediment cored:

Depth sub-bottom (meters): 111.12

Nature: Siliceous nannofossil ooze

Age: Lower Pliocene

Measured velocity (km/s): 1.5002

Shear Strength (g/cm²): 247.5

BACKGROUND AND OBJECTIVES

Our primary objective at Site 503 (Fig. 1) was to recover a complete, undisturbed Neogene and Quaternary section in the eastern equatorial Pacific. Site 503 is located near Site 83 in an area that contains an almost continuous pelagic record of the past 10 m.y. (Hays et al., 1972). Unfortunately, Site 83 was only spot-cored, and the recovered sediment is so badly disturbed by rotary drilling that most of the detailed record is lost. The section has an average sedimentation rate of 2.0 to 2.5 cm/k.y. with good-to-moderate preservation of all the major microfossil groups. We returned to Site 83 to core the same section, using the Hydraulic Piston Corer (HPC) to obtain an undisturbed, continuous section for high-resolution stratigraphic studies.

The quality of these HPC cores, together with the data already collected at Site 502, should allow a high-resolution intercalibration of the Neogene and Quaternary magnetostratigraphy with both Atlantic and Pacific equatorial biostratigraphy. In addition, the evolution of equatorial microfossils throughout the late Neogene and Quaternary are now available for study in one section, with excellent time control. The detailed history

¹ Prell, W. L., Gardner, J. V., et al., *Init. Repts. DSDP*, 68: Washington (U.S. Govt. Printing Office).

² Warren L. Prell (Co-Chief Scientist), Department of Geological Sciences, Brown University, Providence, Rhode Island; James V. Gardner (Co-Chief Scientist), Pacific-Arctic Branch of Marine Geology, U.S. Geological Survey, Menlo Park, California; Charles Adel-seck, Deep Sea Drilling Project, Scripps Institution of Oceanography, La Jolla, California (present address: McClelland Engineers, Ventura, California); Gretchen Blechschmidt, Lamont-Doherty Geological Observatory, Columbia University, Palisades, New York (present address: Exxon Production and Research Corp., Houston, Texas); Andrew Fleet, Department of Earth Sciences, Open University, Buckinghamshire, United Kingdom (present address: Geochemistry Branch Explor. and Prod. Division British Petroleum Research Center, Sudbury-on-Thames, Middlesex TW16 7LN United Kingdom); Lloyd Keigwin, Jr., Graduate School of Oceanography, University of Rhode Island, Kingston, Rhode Island (present address: Woods Hole Oceanographic Institution, Woods Hole, Massachusetts); Dennis Kent, Lamont-Doherty Geological Observatory, Columbia University, Palisades, New York; Michael T. Ledbetter, Department of Geology, University of Georgia, Athens, Georgia; Ulrich Mann, Institut für Sedimentforschung, Universität Heidelberg, Heidelberg, Federal Republic of Germany; Larry A. Mayer, Graduate School of Oceanography, University of Rhode Island, Kingston, Rhode Island; William R. Riedel, Geological Research Division, Scripps Institution of Oceanography, La Jolla, California; Constance Sancetta, Lamont-Doherty Geological Observatory, Columbia University, Palisades, New York; Dann Spariosu, Lamont-Doherty Geological Observatory, Columbia University, Palisades, New York; Herman B. Zimmerman, Department of Geology, Union College, Schenectady, New York.

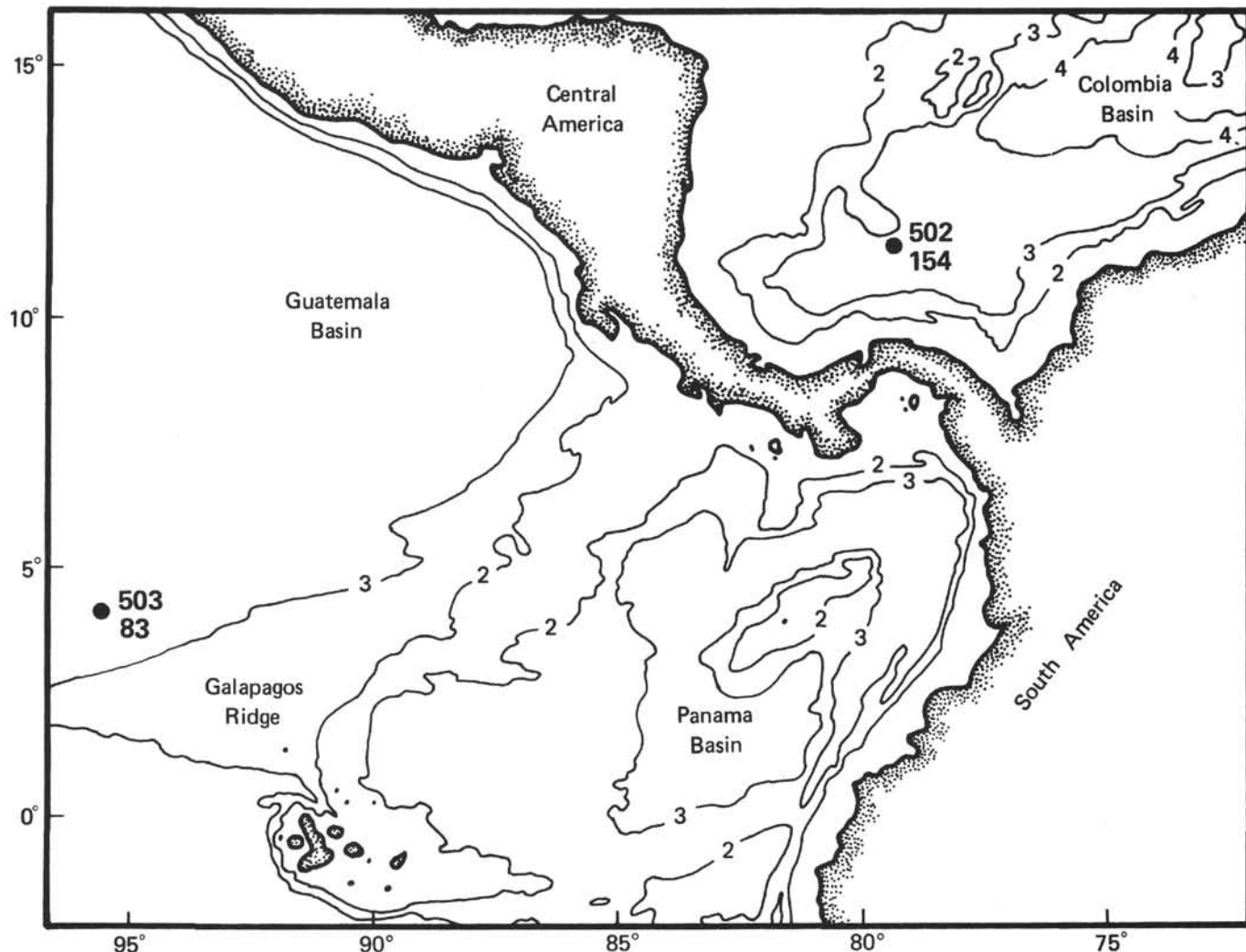


Figure 1. Location of Site 503 and Site 83 (Leg 9) in the eastern equatorial Pacific. Both sites lie on the north flank of the Galapagos Ridge within the symbol for Site 503.

of oceanographic conditions in this area, revealed by fluctuations in isotopes, calcium carbonate and opal contents, and faunal and floral assemblages, can now be studied. Sediment at Site 503, in combination with the data from Site 502, should also record changes in surface circulation and trade wind intensity. These sites also contain information on the timing of the closing of the Isthmus of Panama and initiation of Northern Hemisphere glaciation.

OPERATIONS

We departed Balboa, Panama, at 0012 hr. on 3 September 1979, deployed the geophysical gear at 0015 hr., and steamed toward the vicinity of Site 503 (Fig. 1). Our course paralleled that of *Glomar Challenger* Leg 9 (GC-9) from Site 83 (our destination) to Balboa, so we were able to follow our progress by referring to the GC-9 profiles (Fig. 2). Speed was reduced to 5 knots at 0305 hr. on 7 September because the seismic reflection profile closely resembled the profile over Site 83 (Fig. 2). We dropped the beacon at 0332 hr., retrieved the geophysical gear, and by 0400 hr. were stationed over the bea-

con. Site 503 is located at 4°04.4'N, 95°38.21'W at a water depth of 3672 meters (corrected), about 11 km east of Site 83. The track line of our approach and departure is shown in Figure 3. A summary of the drilling data is given in Table 1.

Core 1 from Hole 503 was retrieved on 7 September at 1430 hr. and was a full core. We raised the drill string 3.0 meters and started again so that the sediment/water interface would be recovered. We designated this second core Core 503A-1 and commenced coring Hole 503A. The operation was plagued with core catcher failures, especially with the flapper type, and core liner fracturing. We cored Hole 503A to a total depth of 235 meters (Core 54), then stopped to avoid piston coring basalt calculated to be at 240 meters. Recovery for Hole 503A was only 58.8%, principally because of core catcher failures. Rust contamination from the drill pipe was obvious once we started using pipe that had not been used at Site 502. This contamination caused a severe degradation of the paleomagnetic data.

Hole 503B was offset 100 meters to the southwest of Hole 503A and was cored continuously, again from

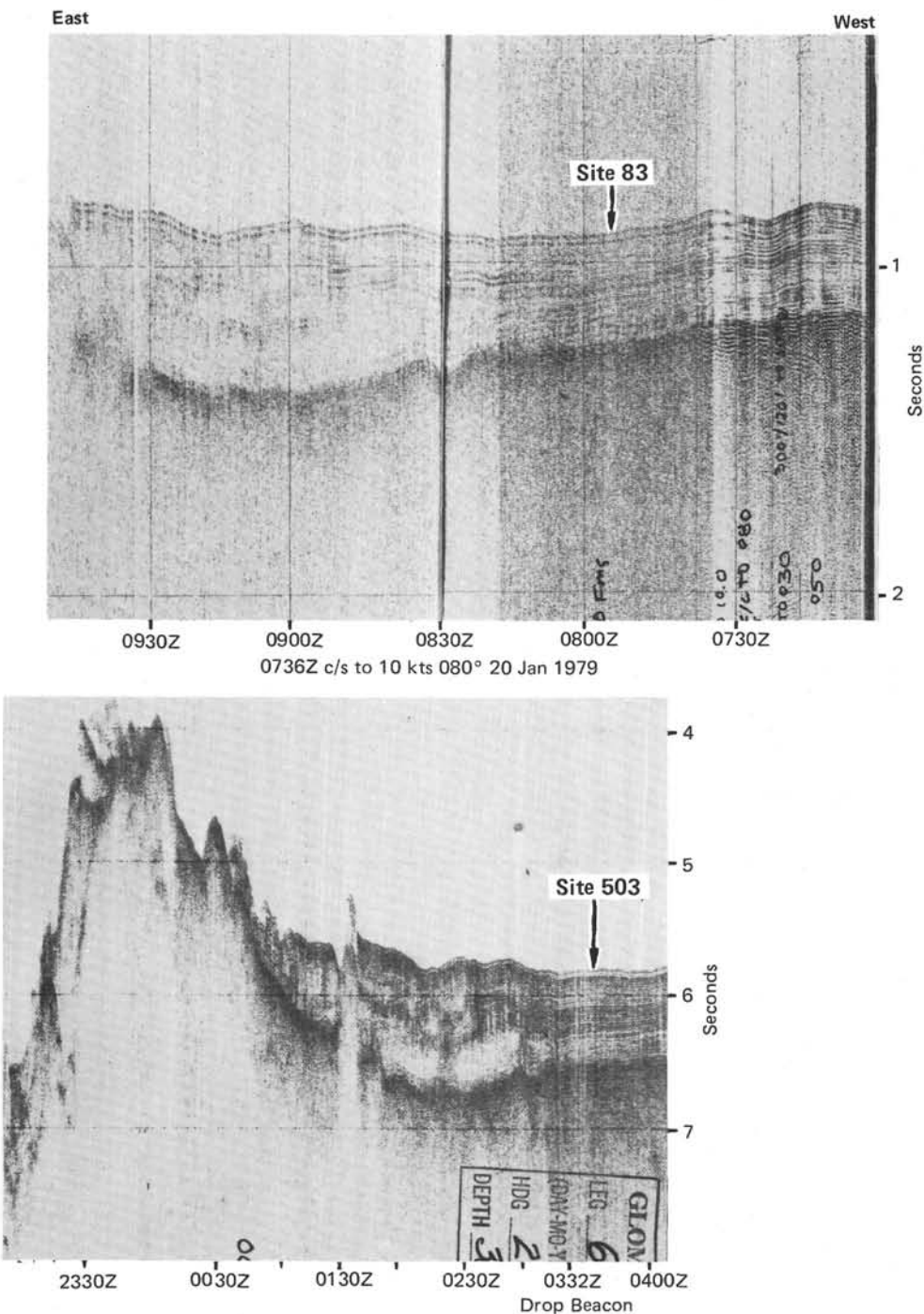


Figure 2. Seismic profiles across Site 503 (GC-68), filtered at 80/640 Hz, and Site 83 (GC-9).

the sediment/water interface. Two modifications to the HPC were made for Hole 503B: (1) We reversed the bevel on the flapper-type core catchers so that the force of the sediment on the flapper would tend to close it, and (2) we chose to use only one small shear pin rather than three. This latter change allowed the HPC to "fire" at 800 to 1000 psi rather than 1800 to 2000 psi. We felt that the shock of the HPC striking the sediment at a high velocity and its rapid deceleration at the end of the stroke may have caused some of the disturbance in Hole 503A.

These modifications were significant. The recovery at Hole 503B, both in amount and quality, was greatly improved compared with Hole 503A. However, contamination by rust continued to be a problem. Hole 503B was continuously cored from the sediment/water interface to 112.8 meters sub-bottom, with a recovery of 83.5%. We terminated coring at 0354 hr. on 13 September because of time constraints on our arrival in Salinas, Ecuador.

The geophysical gear was deployed by 1704 hr. on 13 September. We steamed to the northwest, then came

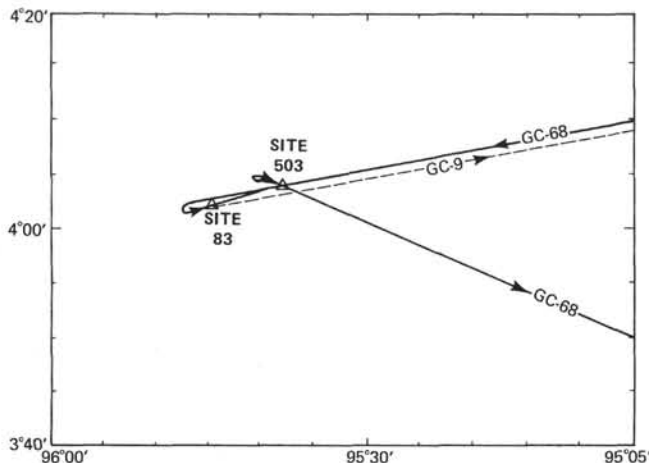


Figure 3. Approach and departure of GC 68 (solid line) from Site 503. Dashed track line is GC-9 departure from Site 83.

about and crossed over the beacon at Site 503 and continued on to the port of Salinas.

LITHOSTRATIGRAPHY

The section at Site 503 consists of one major lithologic facies that can be divided into three units. These units are defined on the basis of oxidation state and clay content of the sediment. The lithostratigraphic division of Site 503 and the ages of the units are given in Table 2. Smear slide summaries for major and minor lithologies are given in Table 3 (see Appendix, this chapter).

Major Lithofacies

The section at Site 503 is composed of three sediment types: (1) siliceous-bearing nannofossil marl, (2) calcareous siliceous ooze, and (3) siliceous nannofossil ooze. Slight variations in composition and microfossil preservation occur throughout the section but are not useful for subdivision. Color cycles, apparently with a uniform periodicity, are marked and occur throughout.

Unit A (0-8.45 m sub-bottom)

Unit A is composed of intervals of very dark grayish brown iron oxide- and silica-bearing nannofossil marl and calcareous-bearing siliceous ooze that alternates with light yellowish brown and very pale brown silica-bearing nannofossil marl and silica-bearing nannofossil ooze. Gradations between these sediment types are common. Burrows and mottles are common. Most color boundaries are gradational and/or burrowed, but some sharp boundaries occur near the base of darker lithologies.

Sediment in Unit A is uniform in composition. Clay is common (5-25%) to abundant (25-75%), but variation in clay content does not appear to correlate with color cycles. Foraminifers are common (5-25%) and moderately to poorly preserved. Nannofossils are abundant (25-75%), and diatoms and radiolarians are common (5-25%). Iron oxides are rare (1-5%) in the lighter-colored sediment and common (5-25%) in the darker-colored material. Sponge spicules, silicoflagellates, and volcanic glass sporadically occur in rare (1-5%) to trace (<1%) amounts.

Table 1. Coring summary for Site 503.

| Core No. | Date (September 1979) | Time (hr.) | Depth from Drill Floor (m) Top Bottom | Depth below Seafloor (m) Top Bottom | Length Cored (m) | Length Recovered (m) | Recovery (%) |
|------------------|-----------------------|------------|--|--|------------------|----------------------|--------------|
| Hole 503 | | | | | | | |
| 1 | 7 | | 3678.8-3083.0 | 0-4.4 | 4.4 | 4.78 | 108.6 |
| Hole 503A | | | | | | | |
| 1 | 7 | 1642 | 3679.9-3680.6 | 0-1.8 | 1.8 | 1.73 | 97.2 |
| 2 | 7 | 1823 | 3680.6-3685.0 | 1.8-6.2 | 4.4 | 3.76 | 85.5 |
| 3 | 7 | 2022 | 3685.0-3689.4 | 6.2-10.6 | 4.4 | — | — |
| 4 | 7 | 2203 | 3689.4-3693.8 | 10.6-15.0 | 4.4 | 3.15 | 71.6 |
| 5 | 7 | 2333 | 3693.8-3698.2 | 15.0-19.4 | 4.4 | 4.15 | 94.3 |
| 6 | 8 | 0123 | 3698.2-3702.6 | 19.4-23.8 | 4.4 | 0.02 | cc only |
| 7 | 8 | 0254 | 3702.6-3707.0 | 23.8-28.2 | 4.4 | 4.12 | 93.6 |
| 8 | 8 | 0417 | 3707.0-3711.4 | 28.2-32.6 | 4.4 | — | — |
| 9 | 8 | 0536 | 3711.3-3715.8 | 32.6-37.0 | 4.4 | 3.48 | 79.1 |
| 10 | 8 | 0705 | 3715.8-3720.2 | 37.0-41.4 | 4.4 | 3.64 | 82.7 |
| 11 | 8 | 0825 | 3720.2-3724.6 | 41.4-45.8 | 4.4 | 4.21 | 95.7 |
| 12 | 8 | 0947 | 3724.6-3729.0 | 45.8-50.2 | 4.4 | 3.85 | 87.50 |
| 13 | 8 | 1128 | 3729.0-3733.4 | 50.2-54.6 | 4.4 | 4.23 | 96.1 |
| 14 | 8 | 1305 | 3733.4-3737.8 | 54.6-59.0 | 4.4 | 3.26 | 74.1 |
| 15 | 8 | 1432 | 3737.8-3742.2 | 59.0-63.4 | 4.4 | 3.97 | 90.2 |
| 16 | 8 | 1605 | 3742.2-3746.6 | 63.4-67.8 | 4.4 | 3.06 | 69.5 |
| 17 | 8 | 1735 | 3746.6-3751.0 | 67.8-72.2 | 4.4 | 1.45 | 33.0 |
| 18 | 8 | 1850 | 3751.0-3755.4 | 72.2-76.6 | 4.4 | 0.06 | 1.4 |
| 19 | 8 | 2012 | 3755.4-3759.8 | 76.6-81.0 | 4.4 | 2.93 | 66.6 |
| 20 | 8 | 2315 | 3764.2-3768.6 | 81.0-85.4 | 4.4 | 4.35 | 98.9 |
| 21 | 7 | 2315 | 3764.2-3768.6 | 85.4-89.8 | 4.4 | 4.20 | 96.8 |
| 22 | 9 | 0047 | 3768.6-3773.0 | 89.8-94.2 | 4.4 | — | — |
| 23 | 9 | 0223 | 3773.0-3777.4 | 94.2-98.6 | 4.4 | 2.66 | 60.0 |
| 24 | 9 | 0342 | 3777.4-3781.8 | 98.6-103.0 | 4.4 | 4.10 | 93.4 |
| 25 | 9 | 0459 | 3781.8-3786.2 | 103.0-107.4 | 4.4 | — | — |
| 26 | 9 | 0630 | 3786.2-3790.6 | 107.4-111.8 | 4.4 | — | — |
| 27 | 9 | 0809 | 3790.6-3795.0 | 111.8-116.2 | 4.4 | 0.99 | 33.0 |
| 28 | 9 | 0953 | 3795.0-3799.4 | 116.2-120.6 | 4.4 | — | — |
| 29 | 9 | 1114 | 3799.4-3803.8 | 120.6-125.0 | 4.4 | 4.17 | 93.6 |
| 30 | 9 | 1300 | 3803.8-3808.2 | 125.0-129.4 | 4.4 | 2.86 | 69.3 |
| 31 | 9 | 1416 | 3888.2-3812.6 | 129.4-133.8 | 4.4 | 4.47 | 103.4 |
| 32 | 9 | 1529 | 3812.6-3817.0 | 133.8-138.2 | 4.4 | 0.70 | 17.0 |
| 33 | 9 | 1655 | 3817.0-3821.4 | 138.2-142.6 | 4.4 | 1.18 | 36.8 |
| 34 | 9 | 1927 | 3821.4-3825.8 | 142.6-147.0 | 4.4 | 3.56 | 88.2 |
| 35 | 9 | 2103 | 3825.8-3830.2 | 147.0-151.4 | 4.4 | 0.77 | 20.5 |
| 36 | 9 | 2240 | 3830.2-3824.6 | 151.4-155.8 | 4.4 | 3.38 | 78.6 |
| 37 | 9 | 2357 | 3834.6-3839.0 | 155.8-160.2 | 4.4 | 2.71 | 64.8 |
| 38 | 10 | 0126 | 3839.0-3843.4 | 160.2-164.6 | 4.4 | 0.06 | 1.6 |
| 39 | 10 | 0301 | 3843.4-3847.8 | 164.6-169.0 | 4.4 | 3.05 | 73.6 |
| 40 | 10 | 0420 | 3844.8-3852.2 | 169.0-173.4 | 4.4 | 1.01 | 30.9 |
| 41 | 10 | 0537 | 3852.2-3856.6 | 173.4-177.8 | 4.4 | 4.21 | 96.4 |
| 42 | 10 | 0954 | 3856.6-3861.0 | 177.8-182.2 | 4.4 | 3.99 | 91.1 |
| 43 | 10 | 1232 | 3861.0-3865.4 | 182.2-186.6 | 4.4 | 3.54 | 80.5 |
| 44 | 10 | 1354 | 3865.4-3869.8 | 186.6-191.0 | 4.4 | 3.97 | 90.2 |
| 45 | 10 | 1524 | 3869.8-3874.2 | 191.0-195.4 | 4.4 | — | — |
| 46 | 10 | 1652 | 3874.2-3878.6 | 195.4-199.8 | 4.4 | 1.15 | 26.1 |
| 47 | 10 | 1810 | 3878.6-3883.0 | 199.8-204.2 | 4.4 | 1.00 | 22.7 |
| 48 | 10 | 1940 | 3883.0-3887.4 | 204.2-208.6 | 4.4 | 3.65 | 83.0 |
| 49 | 10 | 2118 | 3887.4-3891.8 | 208.6-213.0 | 4.4 | 1.90 | 44.5 |
| 50 | 10 | 2304 | 3891.8-3896.2 | 213.0-217.4 | 4.4 | 4.35 | 98.9 |
| 51 | 11 | 0059 | 3896.2-3900.6 | 217.4-221.8 | 4.4 | 5.23 | 73.4 |
| 52 | 11 | 0215 | 3900.6-3905.0 | 221.8-226.2 | 4.4 | 3.86 | 87.7 |
| 53 | 11 | 0340 | 3905.0-3909.4 | 226.2-230.6 | 4.4 | 3.83 | 89.0 |
| 54 | 11 | 0508 | 3909.4-3913.8 | 230.6-235.0 | 4.4 | 4.15 | 94.3 |
| Total | | | | | 235.0 | 138.16 | 58.8 |
| Hole 503B | | | | | | | |
| 1 | 11 | 1048 | 3678.8-3681.6 | 0.0-2.8 | 2.8 | 2.64 | 94.3 |
| 2 | 11 | 1220 | 3681.6-3686.0 | 2.8-7.2 | 4.4 | 2.94 | 66.8 |
| 3 | 11 | 1342 | 3686.0-3690.4 | 7.2-11.6 | 4.4 | 4.35 | 99.61 |
| 4 | 11 | 1520 | 3690.4-3694.8 | 11.6-16.0 | 4.4 | 4.23 | 96.14 |
| 5 | 11 | 1702 | 3694.8-3699.2 | 16.0-20.4 | 4.4 | 4.19 | 95.23 |
| 6 | 11 | 1816 | 3699.2-3703.6 | 20.4-24.8 | 4.4 | 4.36 | 99.09 |
| 7 | 11 | 1925 | 3703.6-3708.0 | 24.8-29.2 | 4.4 | 4.20 | 95.45 |
| 8 | 11 | 2105 | 3708.0-3712.4 | 29.2-33.6 | 4.4 | 4.35 | 98.86 |
| 9 | 11 | 2231 | 3712.4-3716.8 | 33.6-38.0 | 4.4 | 0.34 | 7.72 |
| 10 | 12 | 0221 | 3716.8-3721.2 | 38.0-42.4 | 4.4 | 4.21 | 95.68 |
| 11 | 12 | 0356 | 3721.2-3725.6 | 42.4-46.8 | 4.4 | 4.57 | 103.8 |
| 12 | 12 | 0536 | 3725.6-3730.0 | 46.8-51.2 | 4.4 | 4.07 | 92.5 |
| 13 | 12 | 0707 | 3730.0-3734.4 | 51.2-55.6 | 4.4 | 3.65 | 83.86 |
| 14 | 12 | 0828 | 3734.4-3738.8 | 55.6-60.0 | 4.4 | 4.07 | 92.5 |
| 15 | 12 | 0959 | 3738.8-3743.2 | 60.0-64.4 | 4.4 | 4.29 | 97.5 |
| 16 | 12 | 1134 | 3743.2-3747.6 | 64.4-68.8 | 4.4 | 4.27 | 97.04 |
| 17 | 12 | 1252 | 3747.6-3752.0 | 68.8-73.2 | 4.4 | 3.98 | 90.45 |
| 18 | 12 | 1409 | 3752.0-3756.4 | 73.2-77.6 | 4.4 | 4.43 | 100.68 |
| 19 | 12 | 1630 | 3756.4-3760.8 | 77.6-82.0 | 4.4 | 3.71 | 84.32 |
| 20 | 12 | 1908 | 3760.8-3765.2 | 82.0-86.4 | 4.4 | 2.86 | 65.00 |
| 21 | 12 | 2029 | 3765.2-3769.6 | 86.4-90.8 | 4.4 | 4.71 | 107.05 |
| 22 | 12 | 2147 | 3769.6-3774.0 | 90.8-95.2 | 4.4 | 4.67 | 106.14 |
| 23 | 12 | 2330 | 3774.0-3778.4 | 95.2-99.6 | 4.4 | 1.17 | 26.59 |
| 24 | 13 | 0106 | 3778.4-3782.8 | 99.6-104.0 | 4.4 | 2.60 | 59.09 |
| 25 | 13 | 0230 | 3782.8-3787.2 | 104.0-108.4 | 4.4 | 2.60 | 59.09 |
| 26 | 13 | 0354 | 3787.2-3791.6 | 108.4-112.8 | 4.4 | 2.72 | 61.82 |
| Total | | | | | 112.8 | 94.17 | 83.5 |

Table 2. Lithostratigraphic summary for Site 503.

| Unit | Hole | Core/Section | Depth (m) | Sub-bottom (m) | Age (m.y.) | Description |
|------|------|---------------|--------------|-------------------|---------------|---|
| A | 503 | 1-1 to 1,CC | | | 0-0.4 | Oxidized dark brown and orange silica-bearing-nannofossil marl alternating with calcareous-bearing siliceous ooze with manganese and iron oxides-hydroxides. |
| | 503A | 1-1 to 2,CC | | | | |
| | 503B | 1-1 to 3,CC | | 0-8.45 | | |
| B | 503A | 4-1 to 52,CC | 8.45-226.2 | 8.45-226.2 | 0.4-7.5 | Reduced dark greenish to very pale greenish yellow silica-bearing nannofossil marl alternating with calcareous siliceous ooze gradational from dark at the top to light at the base. Clay content decreases down-section. |
| | 503B | 3-1 to 26,CC | | | | |
| C | 503A | 53-1 to 54,CC | 226.2-235.0 | 226.2-235.0 | 7.5-7.8 | Reduced dark greenish to pale greenish yellow siliceous nannofossil marl alternating with calcareous-silica-bearing clay. Contains pyrite and greater than 25% clay. |

The yellowish brown to brown silica-bearing nannofossil marl of Unit A overlies a pale olive silica-bearing nannofossil marl. We use this color change as the boundary between Units A and B.

Unit B (8.45-226.20 m sub-bottom)

Unit B is composed of silica-bearing nannofossil marl, calcareous siliceous ooze, and siliceous nannofossil ooze that contains small amounts of pyrite and has colors characteristic of reduced oxidation states. The unit has small-scale variations of both color and composition that have a range similar to the overall gradational trends in the section.

Color cycles in the uppermost part of the unit are in the green hue—from greenish black to light greenish gray. The colors lighten downsection, hues of yellow and yellow green beginning below 30 meters sub-bottom. Brownish hues appear below 170 meters sub-bottom as minor constituents of the total range in color; however, the overall aspect of the colors continues to lighten downsection.

Clay content in Unit B decreases with depth. Clay comprises less than 10% of the sediment in the dominant lithologies. Below 220 meters, clay content increases and exceeds 25% abundance below 226.2 meters, which marks the boundary with Unit C. Calcium carbonate content exhibits high-frequency fluctuations throughout the unit (see Gardner, this volume). Silica content is variable and does not show a consistent trend within the unit.

We chose the boundary between Units B and C where the clay content rapidly increased to more than 25%. The transition to over 25% clay abundance occurs between Cores 52 and 53 of Hole 503A at 226.2 meters sub-bottom.

Unit C (226.20-234.75 m sub-bottom)

Unit C is composed of siliceous nannofossil marl, silica-bearing nannofossil marl, and calcareous- and silica-bearing clay, all of which are enriched in clay in comparison to the overlying sediment. The colors of Unit C are somewhat darker than those of the overlying sediment. Clay is abundant (25-75%) but varies greatly. The proximity of the base of this unit to basement (we estimate the bottom of Hole 503A is within 10 m of oce-

anic crust) suggests that the clay may reflect a hydrothermal or thermal alteration of the sediment (see Baker, this volume). These basal clays are composed predominantly of smectite minerals (see Zimmerman, this volume). Foraminifers are rare (1-5%) to absent. Nannofossils are common (5-25%) to abundant (25-75%), and unspecified carbonate is common. Diatoms and radiolarians are uniformly common (5-25%). Minor amounts of pyrite, ash, and silicoflagellates make up the remainder of the sediment.

Discussion

The lithofacies at Site 503 have several interesting aspects. The abrupt change from reduced to oxidized sediment at 8.45 cm sub-bottom (see Frontispiece, this volume, and core photographs) is similar to that at Site 502 in the western Caribbean. The significance of this event is not well understood, but it apparently represents postdepositional reduction of the sediment. Clay minerals throughout the section are dominated by smectites that probably reflect halmyrolytic formation of the clays by convection of pore waters that are thermally driven. The large increase in clay mineral content in Unit C may reflect the proximity of altered basaltic rocks. Unit B has trace amounts of illite and rare amounts of chlorite and kaolinite, whereas abundant occurrences of chlorite and kaolinite and rare amounts of illite occur in Unit A. Smectite is still the dominant clay mineral; however, the small increase in detrital clay input may reflect a change in oceanographic current patterns in the Holocene.

Several horizons of dispersed ash occur throughout the section (see Ledbetter, this volume). The Miocene and lowermost Pliocene sections contain only trace amounts of ash at infrequent intervals. However, several lower Pliocene through Quaternary horizons contain abundant dispersed ash, with the greatest incidence in the uppermost Quaternary. The ash in the lowermost section is dominantly dark glass, whereas the upper section is dominated by light glass (see smear slide summary, Table 3).

Large nodules of microcrystalline rhodochrosite, $MnCO_3$, (Fig. 4) occur within Units B and C from 19.4 meters to the base of the section (last occurrence in Sample 503A-53-2, 13 cm at 227.8 m sub-bottom) (see Coleman et al., this volume). Semiindurated carbonate occurs around burrows at about 13 meters. The nodules are most abundant in the interval from 19.4 to 80 meters sub-bottom and appear to have formed around burrows. This relationship suggests that either the burrowing organism or the burrows themselves created a geochemical microenvironment favorable to the subsequent precipitation of rhodochrosite. Several nodules show not only the major burrow but additional burrows intersecting the major one.

Biogenic parts (briefly discussed and figured in the Site 502 chapter, this volume) appear scattered throughout the section in trace abundances. The most common element found is probably a hook from a squid arm (C. B. Miller, personal communication).

Bioturbation is common to abundant throughout the section (Figs. 5 and 6). Mottles commonly are “reaction

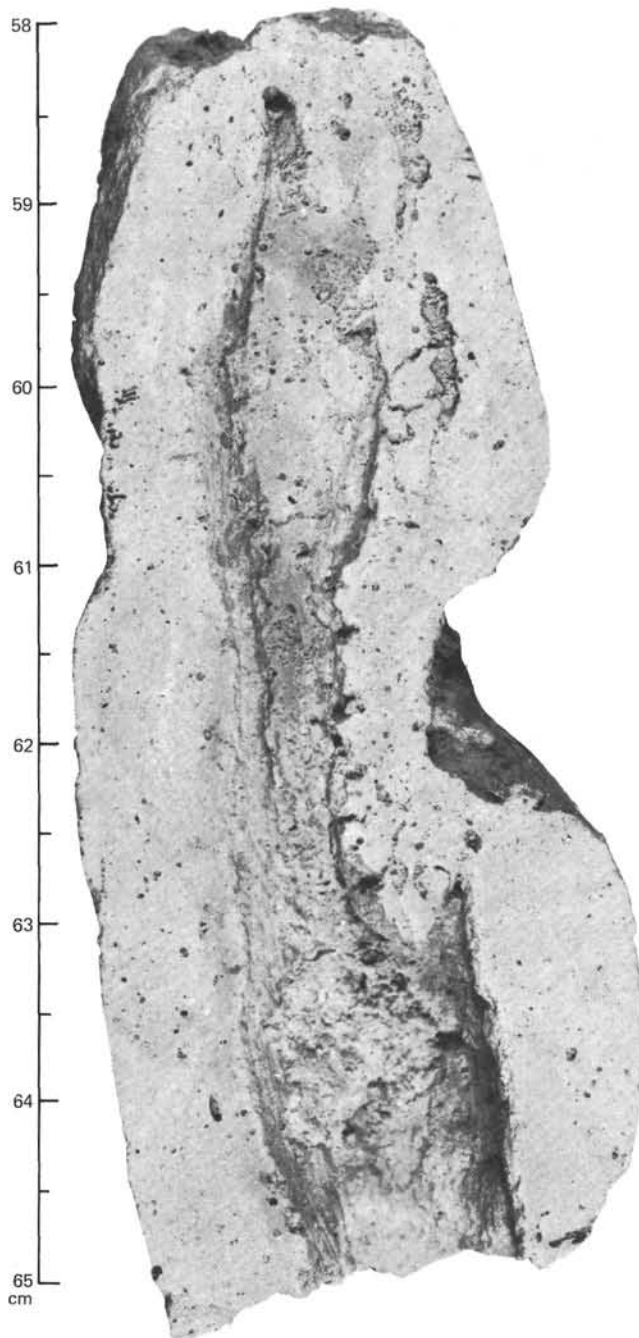


Figure 4. Rhodochrosite nodule from Sample 503B-2, 58–65 cm. The nodule apparently formed around a burrow.

rims" around burrows. In some instances, concentric millimeter-thick dark laminae enriched in pyrite encircle burrows. Intense bioturbation occurs in numerous intervals. Burrows are most evident at sharp color changes and they are very often pyritized. *Zoophycus* are common throughout the section. Open burrows are common in Unit B (Fig. 6) from 9.3 to 64 meters sub-bottom. These burrows have cemented walls that are generally pyritized. Fecal pellets occur in one burrow at 9.3 meters (Fig. 6).

Color cycles are a dominant feature of this section. The color changes reflect lithologic composition, espe-

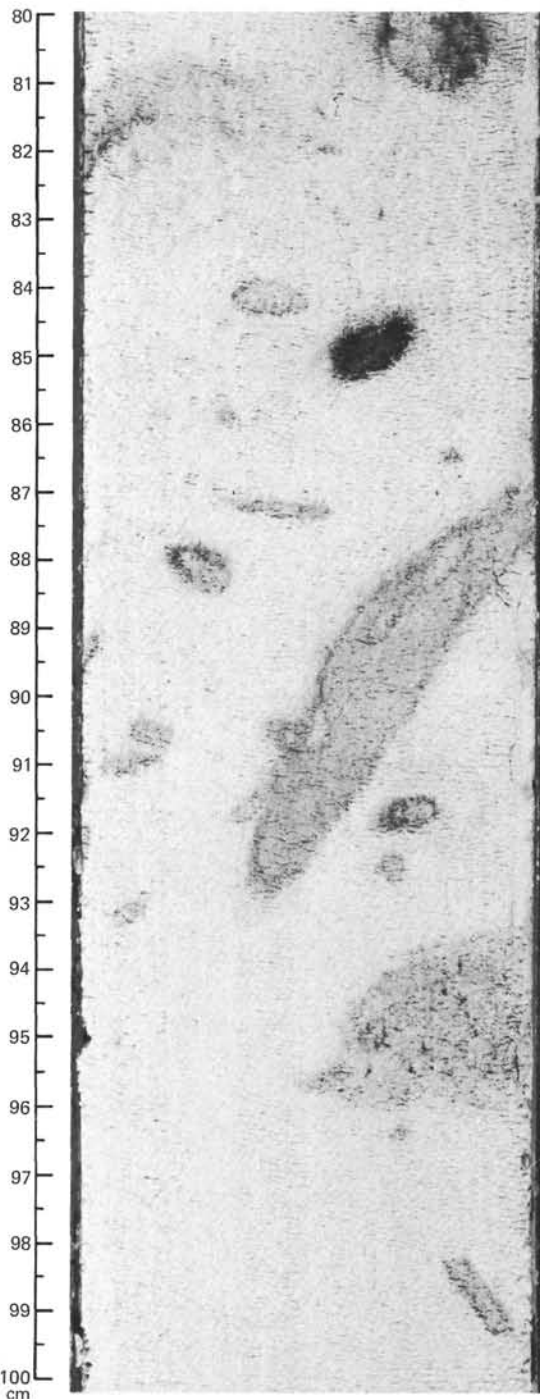


Figure 5. Example of undisturbed burrows in Sample 24A-2, 80–100 cm at approximately 100 meters sub-bottom. Little to no distortion occurs along the sides of the core.

cially carbonate content. We measured the lengths of the color cycles as the distance between the tops of consecutive layers of the same shade (Fig. 7). The lengths of the cycles in Hole 503A show a wide range that may reflect a change in sedimentation rates. A shift to longer cycles occurs at the bottom of Hole 503A (Fig. 7). A single strong mode occurs at 80 to 100 cm per color cycle down to 110 meters depth. This corresponds to a periodicity of 32 to 40 k.y. per cycle if we use an estimate of a 2.5

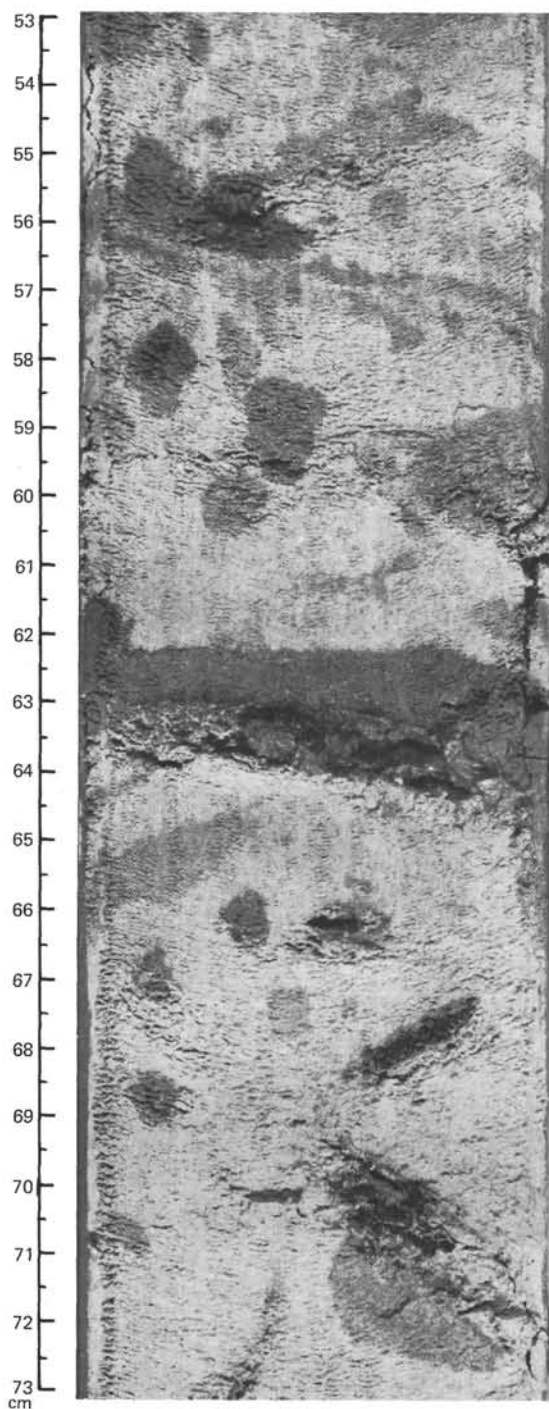


Figure 6. Open burrows and a burrow filled with fecal pellets in Sample 503B-3-2, 53–73 cm (approximately 9 m sub-bottom). These structures illustrate the undisturbed nature of HPC cores. See frontispiece, this volume, for a color photograph of these features.

cm/k.y., for the sedimentation rate. This estimate is slightly biased to shorter periodicities, because we ignored the layer at the top and the bottom of each core and the change of the longer rather than the shorter cycles straddling core breaks is greater. Carbonate content also shows a cyclic variation (Fig. 8) (Gardner, this volume), with periodicities similar to those of color cycles.

Our lithostratigraphic subdivision differs from that at Site 83 (Hays et al., 1972). The lithostratigraphy at Site 83 is subdivided into three formations (Clipperton Oceanic Formation, San Blas Oceanic Formation, and Line Island Oceanic Formation), and the San Blas Oceanic Formation is further subdivided into three units. Our subdivision of the section is compared to that of Site 83 in Table 4. Our Unit A can be correlated with the Clipperton Oceanic Formation. Unit B correlates roughly with the San Blas Oceanic Formation but differs in some aspects. We do not recognize the increased carbonate content in the upper section of our Unit B that was noted by Hays et al. (1972) in their Unit 1 of the San Blas Oceanic Formation. We also did not detect a change in the frequency of burrowing in our Unit B that had been noted in Unit 3 of the San Blas Oceanic Formation. The carbonate nodules that are so abundant at Site 503 apparently were not found at Site 83. We believe these differences are simply the result of the differences in quality of HPC versus rotary-drilled samples. Our Unit C correlates to an unrecovered interval above the Line Islands Oceanic Formation at Site 83. Site 503 did not penetrate a facies that correlates to the Line Islands Oceanic Formation at Site 83.

PHYSICAL PROPERTIES

Standard DSDP methods (Boyce, 1976, 1977) were used for the analyses of physical properties at Site 503 (see Introduction and Explanatory Notes for details). Zones of obvious sediment disturbance were not sampled or analyzed. Vane shear and penetrometer measurements were made on split cores. One sample per core (usually from Section 2) of known volume was taken and sealed with rubber cement. A 2-minute GRAPE count was run on these subsamples. They were then refrigerated in sealed containers to await additional analysis ashore. A detailed discussion of the results appears in Mayer (this volume).

Low values of shear strength occur in the uppermost section at Site 503 (Fig. 9). The expected increase of shear strength with depth, however, occurs only to a depth of about 15 meters, where a value of about 400 gm/cm² occurs. Shear strength below this depth remains fairly constant but with small variations down to about 210 meters sub-bottom. Shear strength rapidly increases at about 210 meters to a maximum of 1686 g/cm² at 224 meters. The lack of an increase in shear strength with depth in the upper 200 meters of the sediment column implies that the sediment is extremely undercompacted. This is consistent with the associated high porosities and water contents. The cause of the undercompaction may be the high percentage of biogenous silica. The spiny biogenous tests may mechanically interlock to form a supporting framework. The small variations about the mean in shear strength may be due to subtle lithologic changes. The rapid increase in shear strength at 210 meters probably reflects the increase in the clay content (see Lithostratigraphy) together with the collapse of the interlocking framework due to the weight of the overburden, the dissolution and

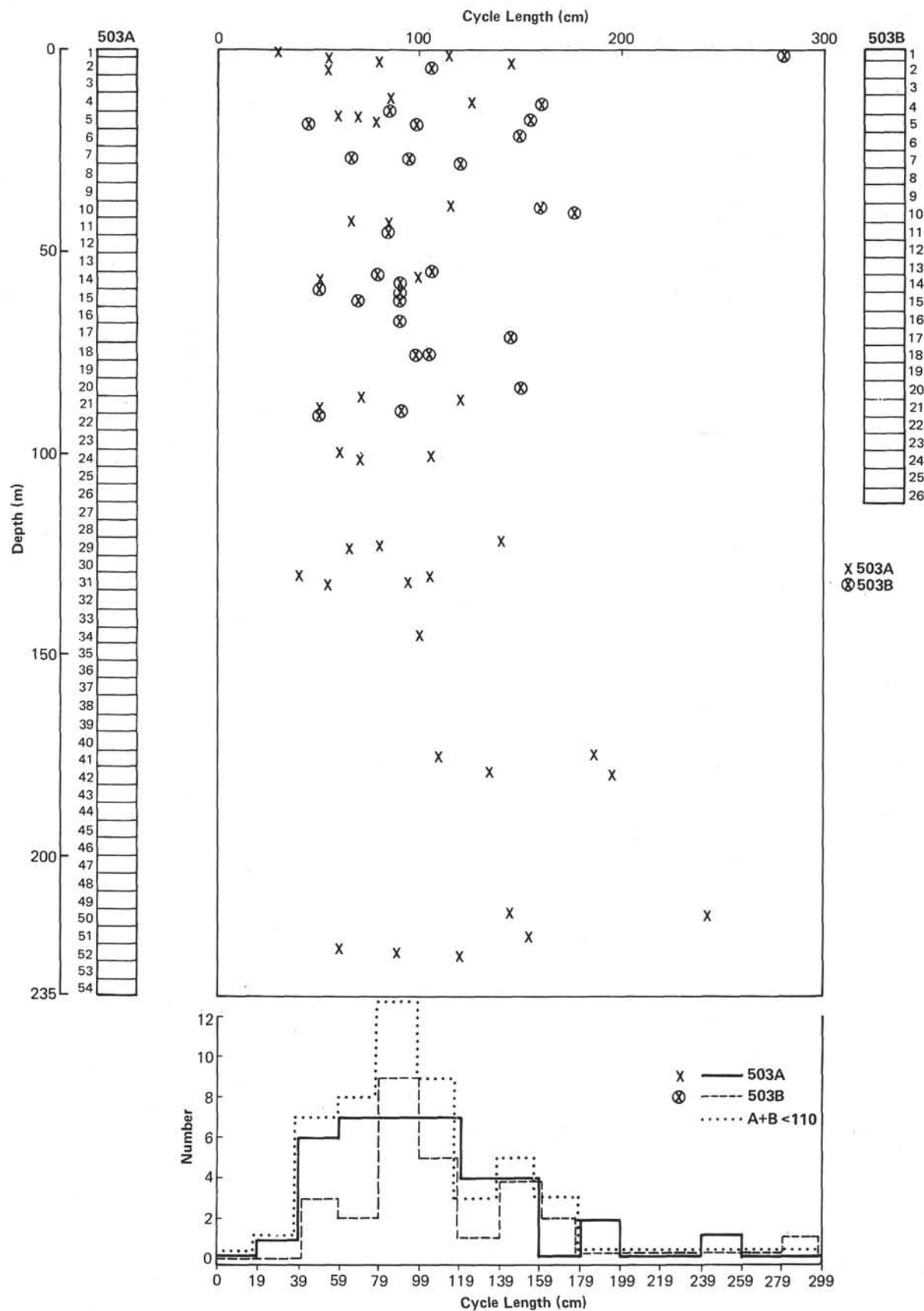


Figure 7. The distribution of the length (cm) of color cycles versus sub-bottom depth (m) in Holes 503A and 503B. A histogram of cycle length is also shown. Note the strong mode at 80–100 cm for the combined data at depths less than 110 meters.

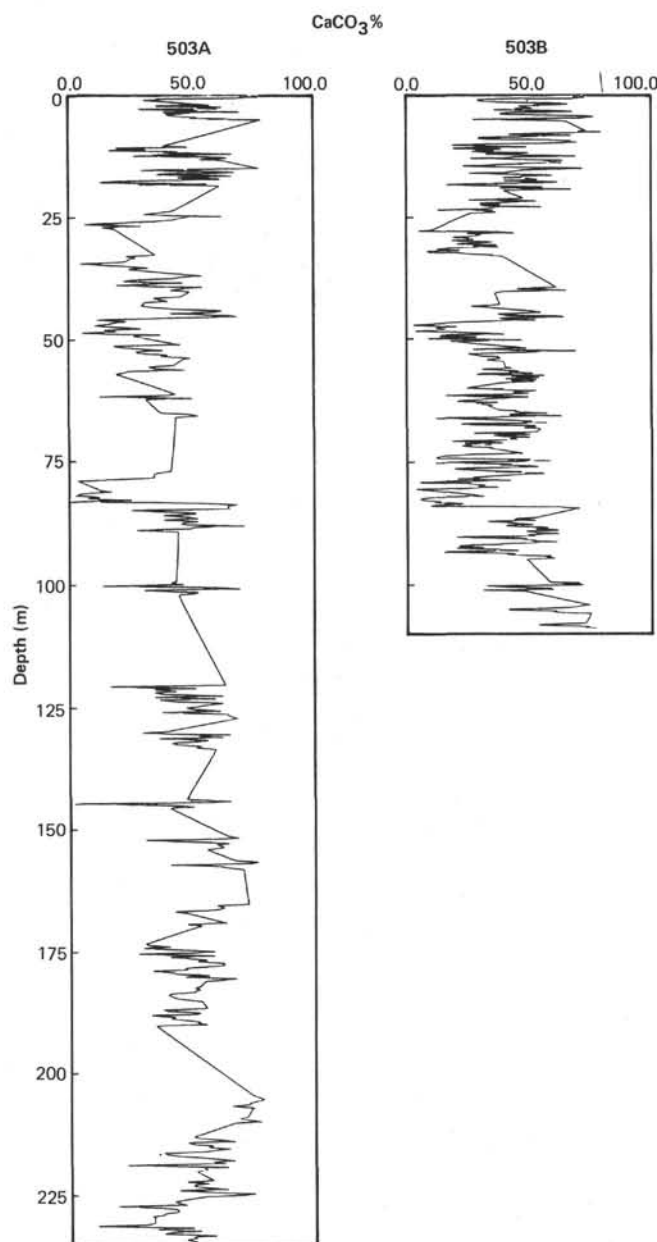


Figure 8. The variation of calcium carbonate content with sub-bottom depth in Holes 503A and 503B. (From Gardner, this volume.)

Table 4. Correlation of lithostratigraphic units between Site 83 and Site 503.

| Site 503 | | Site 83 | |
|-------------------------|-----------|--|--|
| Lithostratigraphic Unit | Depth (m) | Lithostratigraphic Unit | Depth (m) |
| Unit A | 0-8.5 | Clipperton Oceanic Fm. | 0-12.6 |
| Unit B | 8.5-226.2 | San Blas Oceanic Fm. Unit 1 Unit 2 Unit 3 | 12.6-222 12.6-49.6 49.6-150.0 150.0-222.0 |
| Unit C | 226.2-235 | Line Islands Oceanic Fm. | 232.9-234.4 |

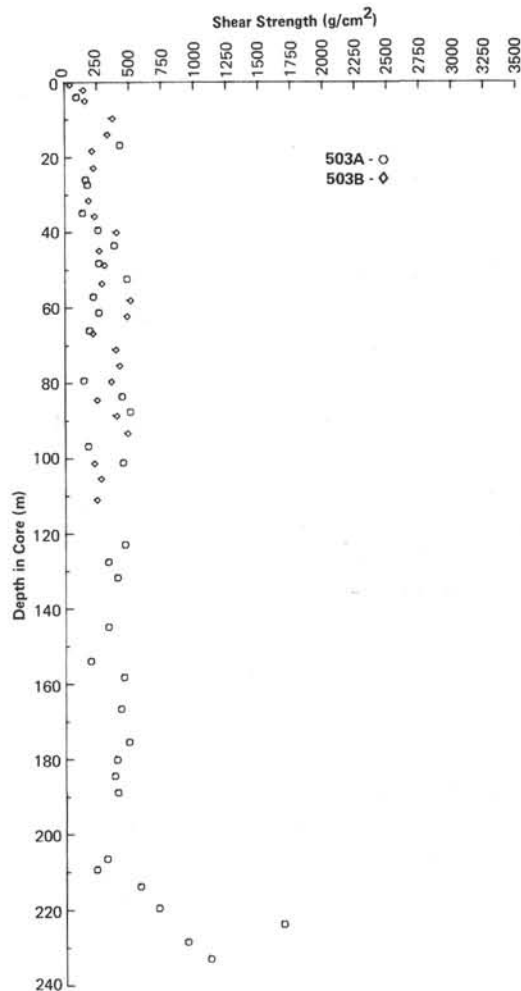


Figure 9. The variation of shear strength (g/cm^2) with sub-bottom depth in Holes 503A and 503B.

reprecipitation of silica, or possibly a thermal effect caused by proximity to basement. Biostratigraphy virtually eliminates a major hiatus at this depth.

In order to place the vane shear measurements in the proper perspective, shear strengths were determined on several calibration samples. Each sample was run ten times with the utmost of care. The shear strength of day-old Jewish rye bread dough (without seeds) was found to be $47.53 \text{ g}/\text{cm}^2$. Cream cheese proved to have a strength of $66.13 \text{ g}/\text{cm}^2$. Ginger cookie dough had values of $70.26 \text{ g}/\text{cm}^2$. A value could not be determined for lime jello, probably because of the large pineapple inclusions interspersed throughout the host material. Several attempts were made to measure the shear strength of chocolate chip cookie dough, but in each case the cookies were eaten before a measurement could be made.

The penetrometer data (Fig. 10) also indicate that the section is undercompacted, although the data seem to be slightly more sensitive to small amounts of compaction that have occurred. The general trend shows a very gentle decrease in penetration down to about 210 meters after a rapid decrease from very high ($> 4.4 \text{ cm}$) values

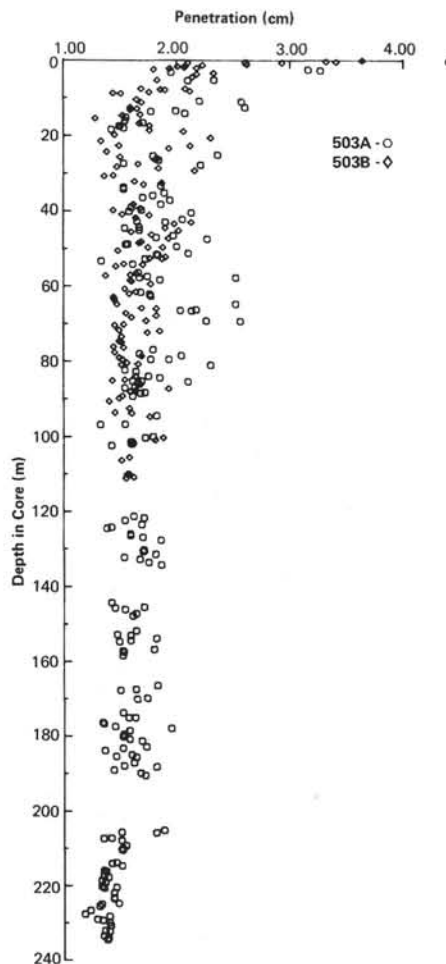


Figure 10. The variation in penetrometer penetration (cm) with sub-bottom depth in Holes 503A and 503B.

in the uppermost sediment. Very large-scale, high-frequency fluctuations in penetration are superimposed on this trend. These fluctuations appear to be the result of lithologic variations. High-frequency fluctuations end below 210 meters sub-bottom, and penetration values drop below about 1.4 cm. This drop in values coincides with the zone of increased shear strength.

P-wave velocities were measured both through the liner and on chunk samples. The velocity values are extremely low ($V_p = 1.515$ km/s) and are typical of highly siliceous sediment. The velocity curve (Fig. 11) is characterized by high-frequency, low-amplitude fluctuations. The total range in values (1.495–1.570 km/s) is only slightly greater than the precision of any one measurement (5%), and we thus conclude that the velocity fluctuations are insignificant. This constant velocity may in part explain the absence of sub-bottom reflections on the 3.5 kHz profiles. The velocity baseline appears to increase to 1.54 km/s below 210 meters sub-bottom. This increase coincides with the increase in shear strength and clay content discussed earlier.

Density, water content, and porosity were determined by gravimetric analyses and continuous and 2-minute GRAPE counts. Low densities (Fig. 12) and high poros-

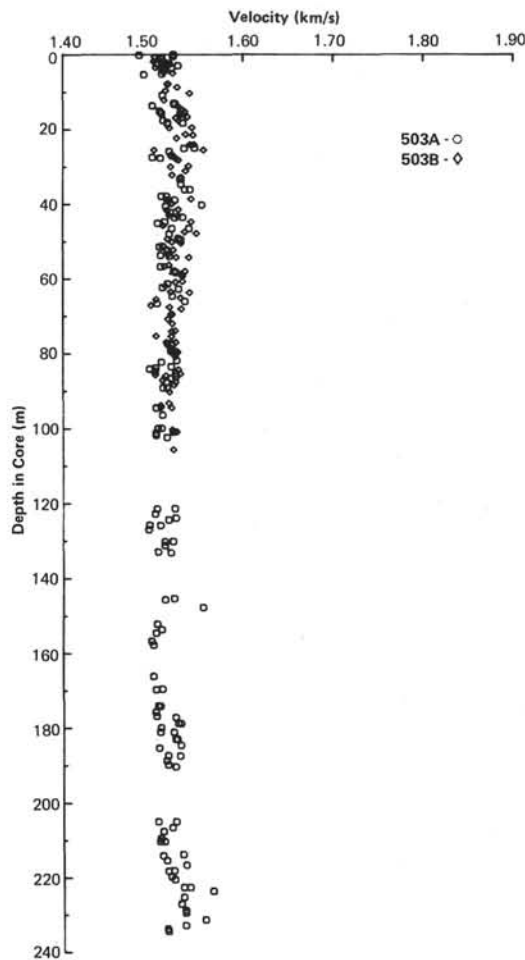


Figure 11. The variation in seismic velocity (km/s) with sub-bottom depth for Holes 503A and 503B.

ities and water contents occur throughout the section (Fig. 13). These data are also consistent with the extremely undercompacted nature of the section. Minimum densities of 1.13 g/cm³ are found between 30 and 50 meters sub-bottom, and maximum densities of 1.37 g/cm³ are found between 205 and 220 meters sub-bottom. Interestingly, the densities decrease in the deepest samples, where shear strength and velocity increase. The lack of a coincident increase in density in the bottom ten meters of the section may imply that the shear strength and velocity increases are due to a small increase in clay content or a thermal effect.

SEISMIC CORRELATION

On the approach to Site 503, the *Glomar Challenger*'s seismic array consisted of a 40 in.³ and a 5 in.³ airgun that were fired at 10-s intervals. Records were made at 10-s sweep filtered at 80/160 Hz and at 5-s delayed sweep filtered at 80/640 Hz. The 3.5-kHz profiler was in operation, but the record is of such low quality that it cannot be used for high-resolution studies of the section.

P-wave velocities on individual samples from Site 503 give an average velocity of 1.510 km/s. No intervals of high velocity or even a gradual increase in velocity occur

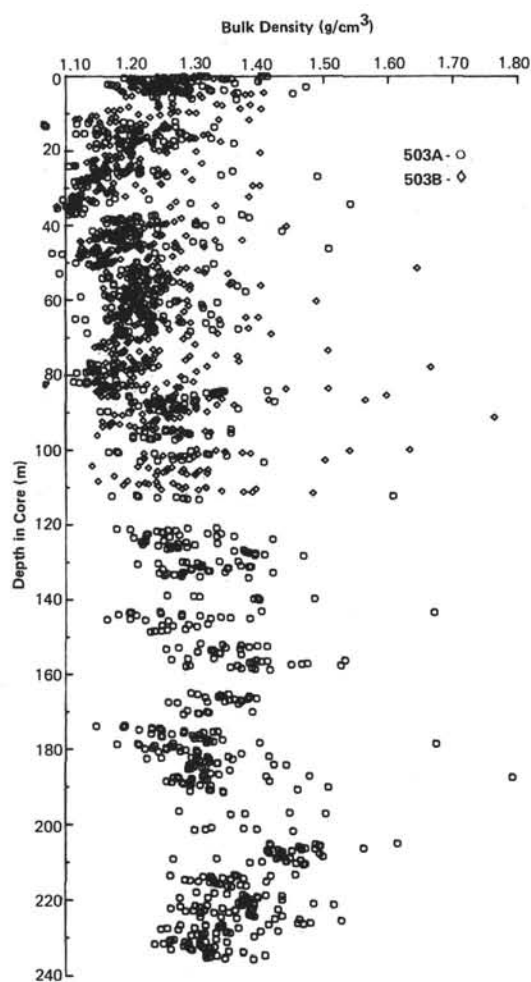


Figure 12. The variation in saturated bulk density (g/cm^3) with sub-bottom depth for Holes 503A and 503B.

with depth in the section (Fig. 11). Therefore, we use a constant 1.510 km/s to convert the time record to a depth section (Fig. 14).

Four acoustic units can be defined on the seismic profiles. Acoustic Unit 1, from 0 to 16 meters, is an acoustically transparent section that contains one reflector. Acoustic Unit 2, from 16 to 178 meters, is uniformly stratified with almost no variation in the distances between internal reflectors. Acoustic Unit 3, from 178 to 240 meters, differs from Acoustic Unit 2 in that the interval reflectors are not so uniformly spaced. Acoustic Unit 4 is basaltic basement, based on the results from Site 83 (Hays et al., 1972).

A rough correlation is observed between the acoustic units and the lithostratigraphic units (Fig. 14). However, the boundary between Acoustic Units 2 and 3 does not coincide with the boundary between Lithostratigraphic Units B and C.

BIOSTRATIGRAPHY

Sediment recovered at Site 503 represents a relatively complete section from the Quaternary through the upper part of the upper Miocene. The sediment contains both calcareous and siliceous microfossils that are suffi-

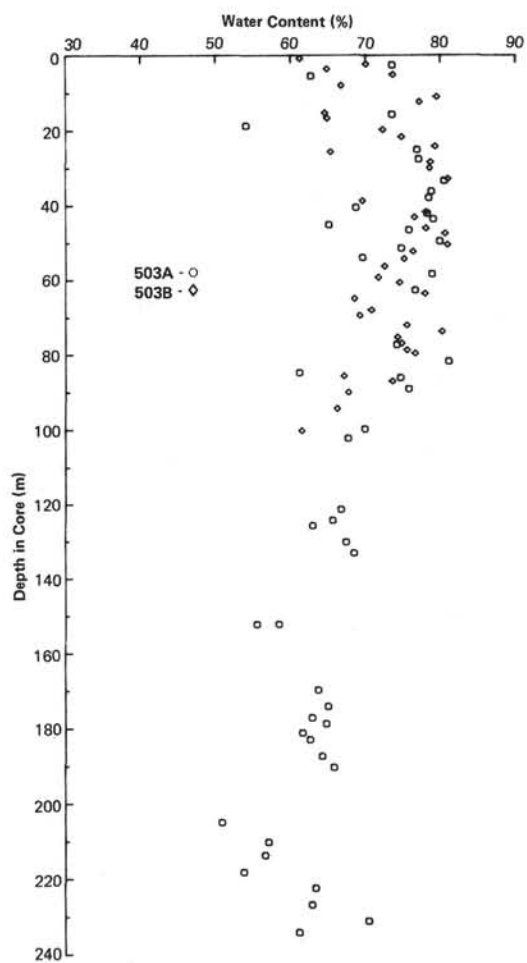


Figure 13. The variation of water content (%) with sub-bottom depth in Holes 503A and 503B.

ciently numerous and well preserved to permit us to compare the biostratigraphy of all major planktonic groups. However, several problems became apparent. Nannofossils are affected by dissolution in the Quaternary section. Reworking obscures some of the stratigraphically significant events near the Pliocene/Pleistocene boundary, in the lower Pliocene, and throughout the Miocene. Foraminifers are rarely well preserved or abundant and require the treatment of large samples to obtain sufficient number of specimens. Diatoms are rare and poorly preserved in the Quaternary section but are somewhat better preserved in the Pliocene and become abundant and very well preserved in the Miocene section. This good preservation and an assemblage dominated by forms characteristic of the present Peru-Chile Current implies high silica productivity during the Miocene. Radiolarians are somewhat corroded and sparse in several cores near the Pliocene/Pleistocene boundary and show some reworking of Miocene species into the entire section.

The Pliocene/Pleistocene boundary occurs in the upper part of Core 503A-9 and the upper part of Core 503B-10 if it is defined by the extinction of *Discoaster brouweri*. But the boundary is higher (Cores 503A-7 and 503B-7) if it is defined by foraminiferal, radiolarian, or

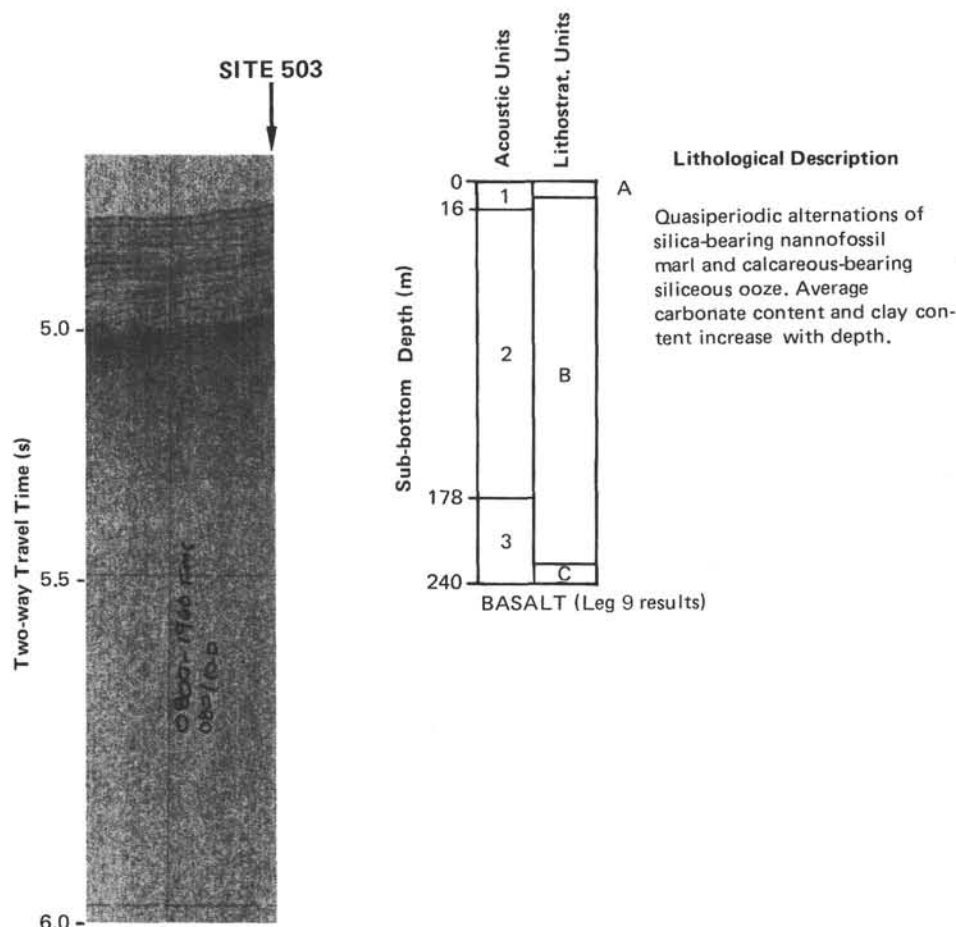


Figure 14. Seismic profile (GC68) was filtered at 80/640 Hz. The correlation with acoustic and lithostratigraphic units at Site 503.

diatom datums. Poor sediment recovery and scarcity of various marker species combine with reworking to make the precise determination of the Pliocene/Pleistocene boundary difficult. We subdivided the Pliocene into early and late intervals at the last appearance of the planktonic foraminiferal genus *Sphaeroidinellopsis* (Samples 503A-20-2, 50 cm and 503B-19-2, 75 cm). The Miocene/Pliocene boundary at Site 503 is defined by the first appearance of *Globorotalia tumida* in Sample 503-37, CC. Details of the diatom, radiolarian, calcareous nannofossil, and foraminiferal zonations are given in the following and are summarized in Figures 15 and 18.

Calcareous Nannofossils

The section at Site 503 contains most of the nannofossil zones from early late Miocene to Quaternary age. Marked variations in abundance and preservation of nannofossils occur throughout the section, so that several datums cannot be precisely determined. Reworking of Miocene and Pliocene forms was noted throughout the section. A detailed discussion of the distribution of Plio-Pleistocene calcareous nannofossils at Site 503 is found in Rio (this volume). Here, we summarize the shipboard biostratigraphy of the calcareous nannofossils, with emphasis on epoch boundaries (Figs. 15 and 18).

Biostratigraphic subdivision of the Quaternary section is hampered by poor preservation of nannofossils. However, all zones except the *Emiliania huxleyi* Acme and the small *Gephyrocapsa* Zones (Gartner, 1977) are recognized at Site 503. A short interval just above the uppermost occurrence of *Helicopontosphaera sellii* (Samples 503A-5-2, 108 cm to 503A-5-3, 48 cm; Cores 503B-2, 40 cm to 503B-3, 40 cm) in which no large *G. oceanica* were found may represent the small *Gephyrocapsa* Zone. A few reworked discoasters of Miocene and Pliocene age are found near the base of the Quaternary.

The Pliocene/Pleistocene boundary as defined by the last occurrence of the nannofossil *Discoaster brouweri* is somewhat difficult to determine in this section because of reworking. Therefore we defined the boundary by the first consistent downcore occurrence of *D. brouweri*, which is located between Samples 503A-9-1, 108 cm and 503A-9-2, 48 cm and between Samples 503B-10-1, 40 cm and 503B-10-2, 40 cm. The succession of discoaster extinctions in the upper Pliocene was easily determined (see Fig. 15). However, in the lower Pliocene, the top of the *D. tamalis* Zone (Samples 503A-13-3, 48-108 cm; 503B-13-2, 40 cm to 503B-13-3, 40 cm) is difficult to determine because of the sparsity of this species at the top of its range. The *Reticulofenestra pseudoumbilica* and *D. asymmetricus* zones could not

be differentiated in this section because of the rarity of *Amaurolithus tricorniculatus*, which is used to define the top of the *D. asymmetricus* Zone. However, the base of the *D. asymmetricus* Zone occurs between Samples 503A-26,CC and 503A-27,CC in Hole 503A and between 503B-21,CC and 503B-22,CC in Hole 503B.

The Miocene/Pliocene boundary is placed at the last consistent occurrence of *D. quinqueramus* (Core 503A-33) at a sub-bottom depth of approximately 138 meters. Considerable reworking of nannofossils is apparent at this boundary, as shown by specimens of *D. quinqueramus* that occur as high as Core 503A-31.

Almost all of the Miocene sequence falls into the *D. quinqueramus* Zone (see Fig. 15). *A. primus* is found intermittently to Core 503A-49, at a depth of approximately 208 meters. We found a moderately well-preserved flora at the base of Hole 503A that includes *D. neorectus*. *D. neorectus* was also found at about 185–190 meters sub-bottom but is probably reworked. A downward decrease in abundance and preservation also characterizes this interval.

Planktonic Foraminifers

Planktonic foraminifers are present in nearly all samples but are rarely abundant because of carbonate dissolution and dilution by siliceous microfossils. For these reasons, examination of large samples (about 30 cc) of core catcher material was often necessary. Despite this difficulty, important zonal marker species are sufficiently abundant and well preserved to use a modified version of the foraminiferal zonation developed for the eastern equatorial Pacific (Jenkins and Orr, 1972). A summary of the foraminiferal biostratigraphy is shown in Figures 15 and 18. A detailed discussion of the Neogene biostratigraphy, including the precise location of specific datums and zonal boundaries and the biogeography of planktonic foraminifers, is given in Keigwin (this volume).

The Pliocene/Pleistocene boundary at Site 503, as placed by the first appearance of *Globorotalia truncatulinoides*, is found between Samples 503A-7,CC and 503A-9,CC in Hole 503A and in Sample 503B-8,CC in Hole 503B. Jenkins and Orr (1972) defined the Pliocene/Pleistocene boundary by the last occurrence of *Globigerinoides fistulosus*, but we found this datum to be inconsistent and difficult to locate precisely. We place the early/late Pliocene boundary at the last appearance of genus *Sphaeroidinellopsis* at Core Sample 503A-20-2, 50 cm in Hole 503A and at 503B-19-2, 75 cm in Hole 503B. Jenkins and Orr (1972), however, appear to define their early/late Pliocene boundary by the last occurrence of *Sphaeroidinellopsis subdehiscens* (several meters lower than the last appearance of *S. seminulina*). The last appearance of *Sphaeroidinellopsis* at Site 503 is close to the first appearance of *G. fistulosus* (Samples 503A-20-1, 100 cm; and 503B-19-1, 75 cm). Consequently, the early/late Pliocene boundary is actually marked by two datums.

The Miocene/Pliocene boundary at Site 503 is based on the first appearance of *Globorotalia tumida* (Sample 503A-37,CC), which has been shown to be a reliable

marker (Saito et al., 1975). The Miocene/Pliocene boundary at Site 83 is based on the boundary between the nannofossil zones *Ceratolithus rugosus* and *C. tricorniculatus* (Hays et al., 1972) and is about 30 meters shallower than the Miocene/Pliocene boundary defined by planktonic foraminifers at Site 503.

Several planktonic foraminiferal datums that may be useful for subdividing the upper Miocene occur at Site 503 (see Keigwin, this volume). The last appearance of *Globoquadrina dehiscens* (Sample 503A-33,CC), which is rare at Site 503, occurs near the Miocene/Pliocene boundary and is a useful marker for that boundary. The genus *Pulleniatina* first appears in Hole 503A, Sample 503A-38,CC, preceded by an interval of sinistral *Neogloboquadrina acostaensis* between about 187–191 meters. These datums appear more distinct and stratigraphically useful in the Pacific than they are in the Caribbean. The last occurrence of *Globigerinoides bulloideus* found in Panama Basin DSDP Sites 84 and 158 (Keigwin, 1976) occurs in Hole 503A in Sample 503A-40,CC at 169.90 meters sub-bottom. This extinction may provide an important horizon for correlating Caribbean and eastern equatorial Pacific sequences. The age of basal sediments is estimated to be about 8 m.y.

Silicoflagellates

Neogene silicoflagellates at Site 503 are especially abundant and well preserved in Miocene Cores 503A-30 to 54, but Pliocene assemblages in Cores 503A-12 to 30 are less abundant and contain increased numbers of dissolution-thinned specimens. A full description of the silicoflagellate Neogene zonation, evolution, and systematics appears in Bukry (this volume). Here, we summarize the biostratigraphy, with emphasis on epoch and zonal boundaries.

The base of the *Dictyocha stapedia* Zone occurs in the upper lower Pliocene at Sample 503A-19-2, 124–125 cm. The base of the late Miocene–early Pliocene *D. fibula* Zone is defined by the Asperoid/Fibuloid reversal of *Dictyocha*. Unfortunately, the detailed counts made possible by the HPC sediments reveal six reversals of the Asperoid/Fibuloid ratio through the previously described interval of the *D. fibula* Zone. Hence the ratio is not a consistent criterion for the zonal boundary. Likewise, the top of the *D. brevispina* Zone cannot be established because reversals of the Asperoid/Fibuloid ratio indicate that the *D. fibula* Zone occurs as deep as Core 503A-54. The assemblages are diverse, and several new species are found (Bukry, this volume). The increased detail of the HPC record suggests that the upper Miocene zonation is not unique and that the Asperoid/Fibuloid ratio is quite variable.

Diatoms

Diatoms are rare and poorly preserved throughout the Quaternary section at Site 503 (Cores 503A-1 through 503A-8 and 503B-1 through 503B-8), common and well preserved in the Pliocene section (Cores 503A-9 through 503A-32 and 503B-9 through 503B-26), and abundant and very well preserved in the upper Miocene section (Cores 503A-32 through 503A-54). The upper Miocene

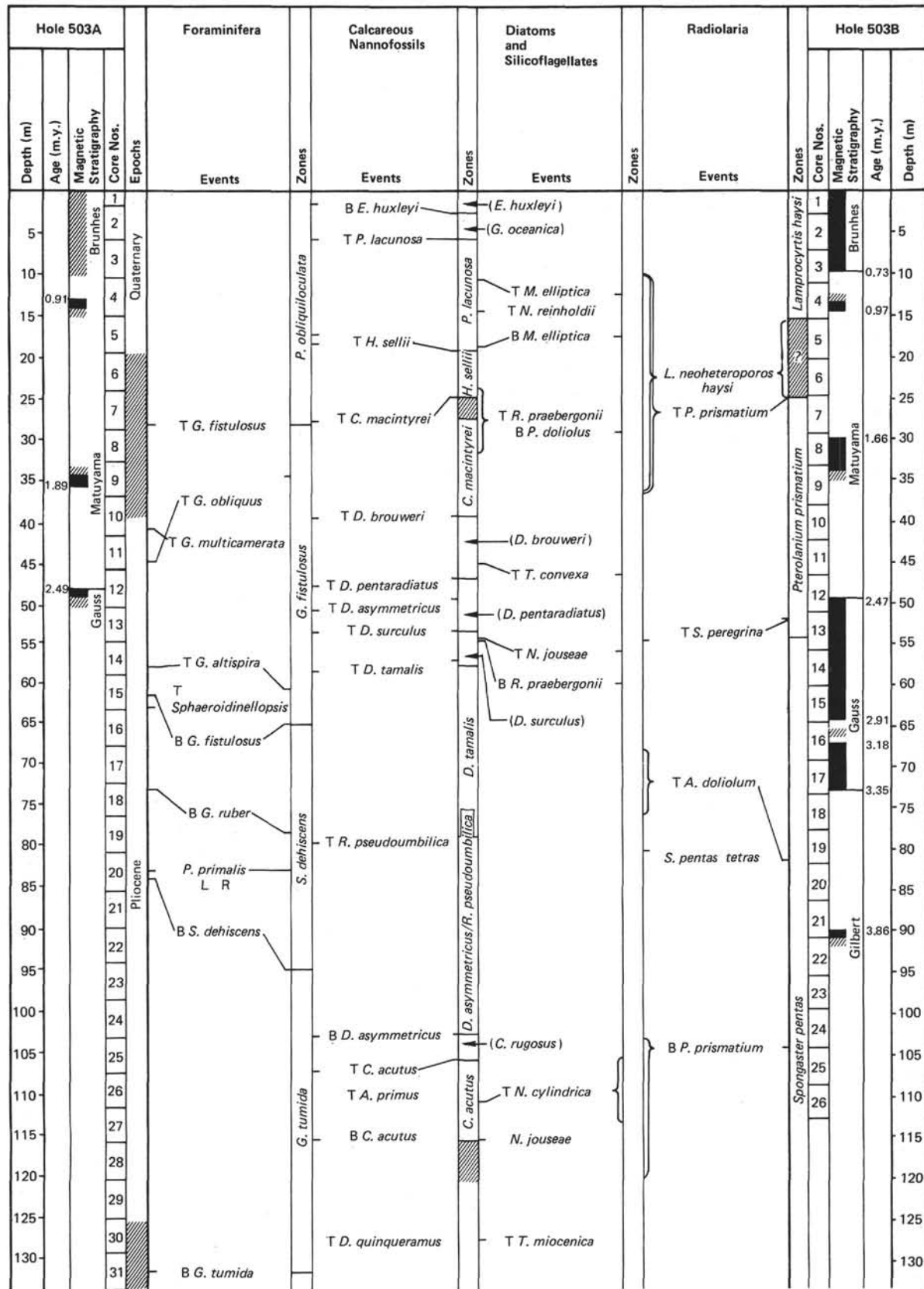
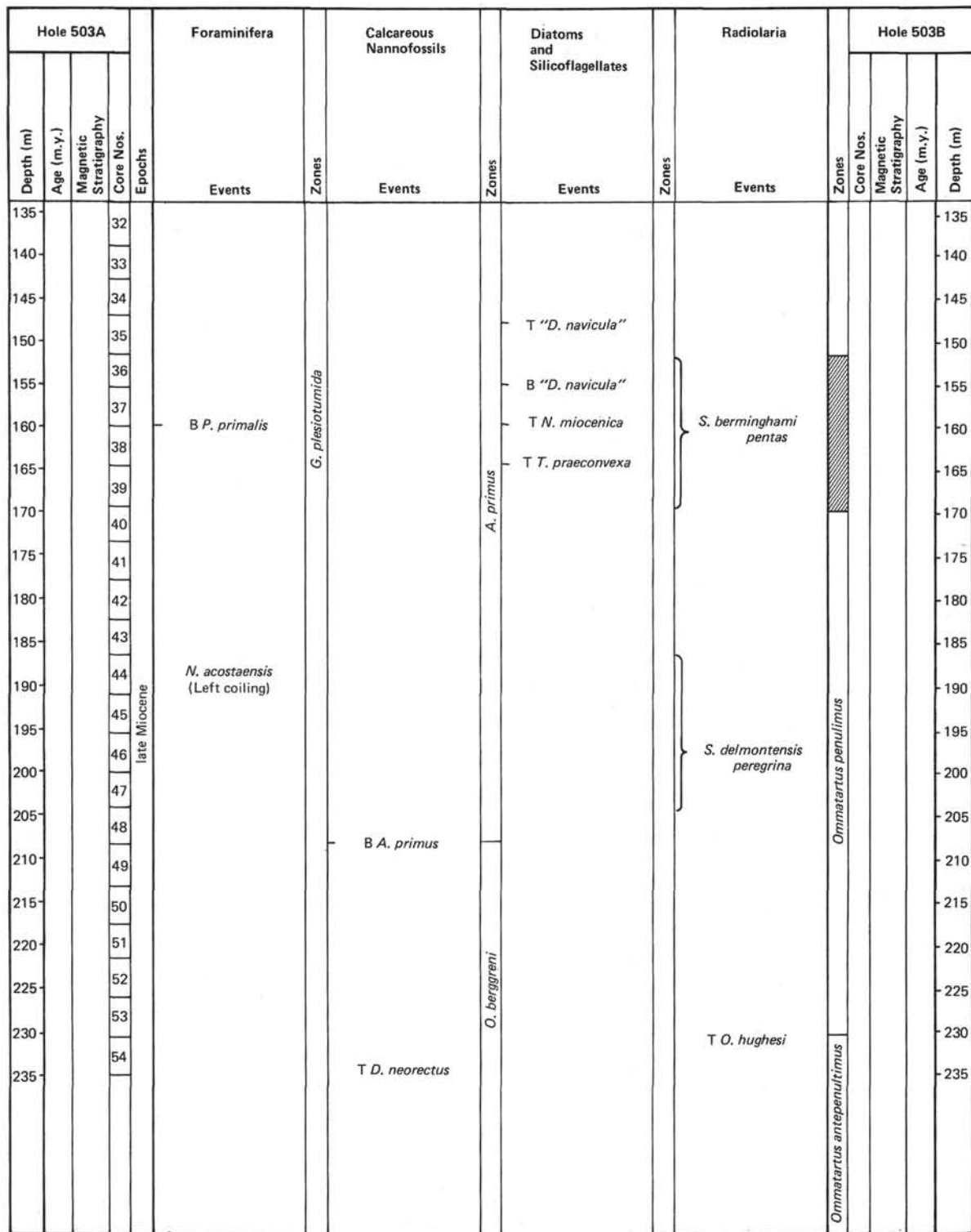


Figure 15. Biostratigraphic summary of Site 503.



T (for "top") indicates upper limits of ranges, and B (for "bottom") lower limits. Substantial ranges of uncertainty (longer than the length of one core) are indicated in the "Events" columns by braces ({ }), and elsewhere by hachuring. Positions indicated on the left side of each "Event" column refer to Hole 503A, and indications on the right side refer to Hole 503B.

Figure 15. (Continued).

interval is dominated by the genera *Thalassionema* and *Thalassiothrix*. This group is the major diatom component in Holocene sediment that underlies the Peru-Chile Current (Burckle, personal communication). The abundance of this group in upper Miocene sediment may imply significant upwelling and productivity during the late Miocene. A summary of the diatom biostratigraphy is shown in Figures 15 and 18. Here, we define only the epoch boundaries at Site 503. A detailed study of the diatom biostratigraphy, including the location of species datums and zonal boundaries in Holes 503A and 503B, is given in Sancetta (this volume).

The Pliocene/Pleistocene boundary as defined by Burckle (1977) occurs between the last appearance of *Rhizosolenia praebergonii* Samples (503A-7-3, 48 cm and 503B-7-2, 40 cm) and the first occurrence of *Pseudoeunotia doliolus* (503A-9-2, 102 cm and 503B-10-1, 40 cm). The Miocene/Pliocene boundary as defined by Burckle (1978) coincides with the last appearance of *Thalassiosira miocenica* (Sample 503A-33, CC). Slight but consistent reworking (10% of stratigraphically useful species) appears in the lower Pleistocene, and significant reworking (up to 80% of stratigraphic markers) appears in the lowermost Pliocene (Cores 503A-30 and 503A-31). The reworked flora in both intervals is composed of late Miocene species.

Radiolarians

Radiolarians are well preserved and common throughout the sediment from Holes 503A and 503B but are less common and somewhat corroded in some samples from Cores 503A-4 to 503A-9 and 503B-6 to 503B-10. Reworking of Miocene radiolarians occurs in Cores 503A-1 through 503A-29 and 503B-1 through 503B-13. The amount of reworking is generally small but approaches 20% in samples from Cores 503A-4, 5, 7, 10, and 11 and 503B-3, 6, and 7. Reworked faunas represent more than 50% of the assemblage in Cores 503A-7, 9, and 503B-8.

A summary of the radiolarian biostratigraphy is shown in Figures 15 and 18. Here, we present only the epoch boundaries at Site 503. A detailed summary of the Neogene radiolarian biostratigraphy, including the specific location of radiolarian events and zones, is given in Riedel and Westberg (this volume).

The top of the *Pterocanium prismatum* Zone, which is considered to be approximately the Pliocene/Pleistocene boundary, is placed between Core Samples 503A-7-2, 50-54 cm, and 503A-7-3, 50-54 cm. This boundary occurs in the same interval in Hole 503B. The Pliocene *P. prismatum* Zone occurs between Samples 503A-13-3, 50-54 cm and 503A-7-3, 50-54 cm in Hole 503A and between 503B-14-2, 50-54 cm and 503B-7-3, 50-54 cm in Hole 503B. The Pliocene *Spongaster pentas* Zone occurs between Samples 503A-31-2, 50-54 cm and 15-2, 66-70 cm in Hole 503A and from the base of Hole 503B to Sample 503B-14-2, 50-54 cm.

We place the Miocene/Pliocene boundary near the evolutionary transition from *S. berminghami* to *S. pentas* that takes place between Samples 503A-31-3, 50-54 cm and 503A-34-2, 50-54 cm. Hole 503A penetrated the late Miocene *Didymocyrtis penultima* Zone (Samples

503A-44-3, 50-54 cm to 503A-34-2, 50-54 cm) and reached the top of the *D. antepenultimus* Zone (Samples 503A-54-3, 52-55 cm to 503A-48-2, 50-54 cm).

PALEOMAGNETISM

The paleomagnetic measurements at Site 503 followed the procedure described in the paleomagnetics discussion of the Site 502 chapter (this volume). Each core was measured with the long-core spinner magnetometer at 10-cm intervals, and one or more discrete samples were taken from each 1.5-meter section for measurement on the small-sample spinner magnetometer.

We encountered several problems at Site 503 that degraded the quality of the magnetic data. The most serious problem is the presence of rust scale from the drill pipe. The dark scales of rust are concentrated at the top of each core but also are smeared inside the liner to several meters depth even in otherwise undisturbed portions of the core. The rust scale is highly magnetic and consequently, when present, obscures the magnetic properties of the sediment.

The rust scale is a serious problem in Hole 503A but less so in Hole 503B. Site 503 was deeper than 502, and drill pipe was deployed that had not been used for several months. The relative contribution of the rust contamination to the magnetic measurements is accentuated at Site 503 because of remanent intensities of about 40 (10^{-5}) emu. Generally, long-core magnetic data from at least the topmost 1.5-meter section of most cores could not be used because of the high noise level.

In contrast to these difficulties, various modifications to the corer between Sites 502 and 503 greatly improved core-to-core orientation. There was also greater attention to handling cores on deck to minimize relative rotation between core sections as well as disturbance of this less cohesive sediment. These improvements in part offset the problem of the rust scale, particularly in Hole 503B. The combination of long-core and discrete sample measurements allows us to recognize the gross features of magnetostratigraphy to the middle of the Gilbert Chron, approximately the top 100 meters of the section. Sediment magnetism below approximately 130 meters sub-bottom (near the Miocene/Pliocene boundary) becomes very weak and difficult to measure.

The depths of the magnetic reversals in the two holes are given in Table 5 and plotted with respect to the geomagnetic polarity reversal timescale (modified from Mankinen and Dalrymple, 1979) in Figure 16. We tentatively identify most of the recognized paleomagnetic chrons and subchrons to the Gauss Chron. We emphasize that many of the boundaries are based on discrete samples spaced 0.5 meter or more apart. Core recovery is poor in the Gilbert Chron, and we have not been able to refine the level of reversal boundaries in this interval. Magnetization of sediment below about 130 meters is so weak as to make the determination of a polarity stratigraphy for the upper Miocene section almost impossible.

ACCUMULATION RATES

We used 12 horizons to generate sedimentation rate and accumulation rate data for Site 503 (Table 6). These

Table 5. Location in each hole and the sub-bottom depths of the paleomagnetic boundaries found at Site 503.

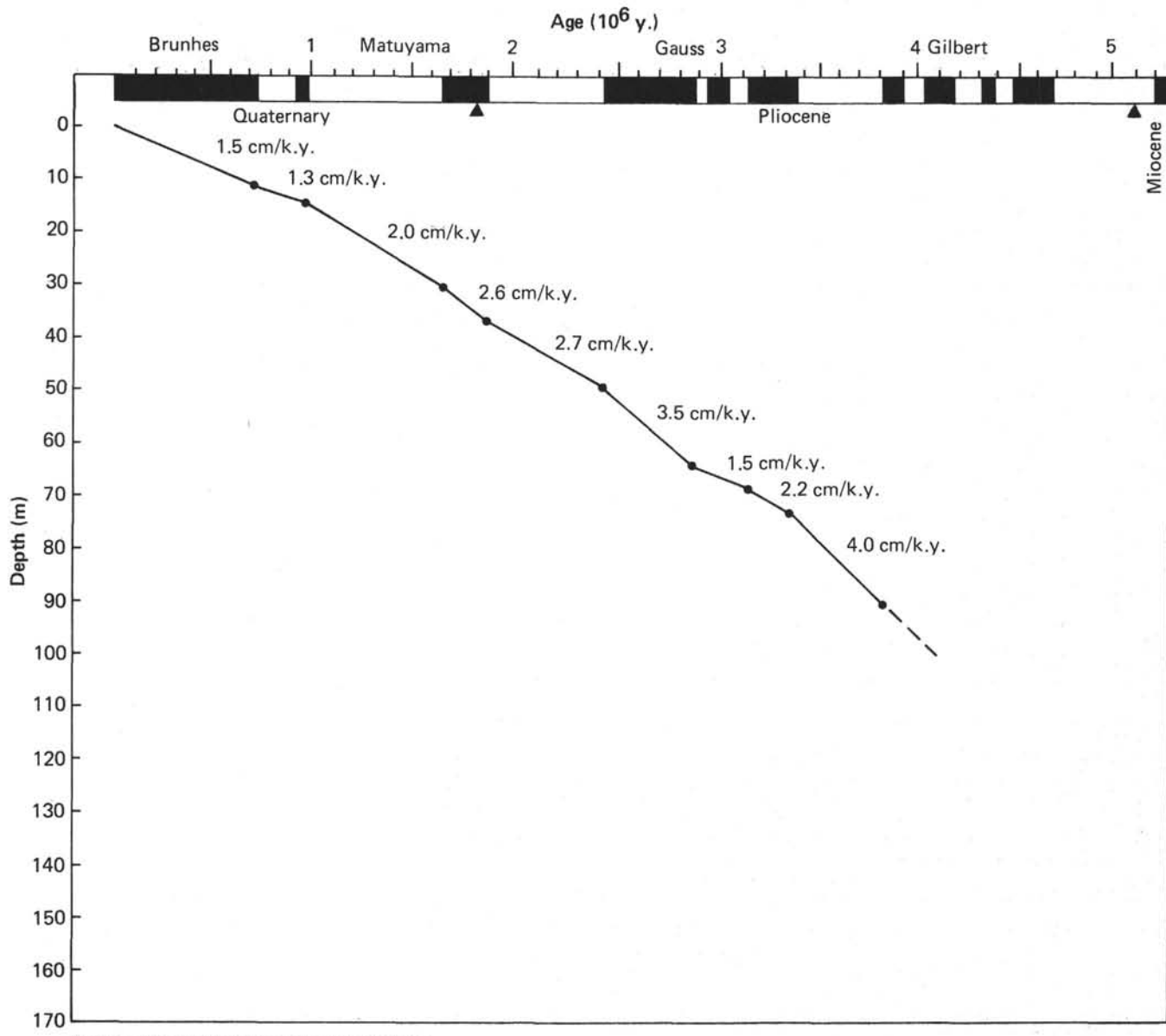
| Paleomagnetic Chrons and Subchrons | Hole 503A | | Hole 503B | |
|------------------------------------|---------------------------|-----------------------|----------------------------------|-----------------------|
| | Sample (interval in cm) | Sub-bottom Depth (cm) | Sample (interval in cm) | Sub-bottom Depth (cm) |
| Brunt/Matuyama | — | — | 3-3, 60-70 | 10.82 ± 0.05 |
| top of Jaramillo | 4-2, 100-120 | 12.17 ± 0.05 | 4-2, 30-40 ^b | — |
| bottom of Jaramillo | — | — | 7-3, 110 to 8-2, 20 ^a | 13.33 ± 0.05 |
| top of Olduvai | — | — | — | 29.9 ± 0.90 |
| bottom of Olduvai | 9-2, 100-130 ^a | 35.12 ± 0.15 | — | — |
| Matuyama/Gauss | 12-2, 60-90 | 47.95 ± 0.15 | 12-2, 60-100 | 49.20 ± 0.10 |
| top of Kaena | 14-3, 30-40 | 57.15 ± 0.05 | — | — |
| bottom of Kaena | — | — | — | — |
| top of Mammoth | — | — | 15-3, 80-100 | 63.55 ± 0.10 |
| bottom of Mammoth | — | — | 16-2, 75-140 | 66.84 ± 0.30 |
| Gauss/Gilbert | — | — | 17-3, 80-100 | 72.51 ± 0.10 |
| top of Cochiti | 21A-3, 10-40 ^a | 88.65 ± 1.15 | 21-3, 25-45 | 89.70 ± 0.10 |

^a The paleomagnetic record is not definitive at these levels.

^b Selection of this level assumes correct orientation between Cores 503B-7 and 503B-8.

horizons represent the eight best magnetostratigraphic boundaries, the three best-dated biostratigraphic datum levels, and an assumed zero age for the sediment/water interface. The age and thickness of the 11 time intervals bounded by these horizons is given in Table 6. The thickness of each interval was computed in holes that contain the inclusive age boundaries so that differences in sub-bottom depth between holes are eliminated.

A sedimentation rate for each interval was calculated from the age versus depth relationship. Sedimentation rate is a function of both sediment influx at the time of deposition and postdepositional compaction, so bulk accumulation rates were calculated in order to remove some of the compaction effect. The calculated accumu-



* ages corrected for latest decay constant

Figure 16. Age versus sub-bottom depth for magnetostratigraphic boundaries at Site 503.

Table 6. Measured and calculated parameters used to determine sedimentation and accumulation rates.

| Time Interval | Age (m.y.) | Depth ^a (m) | Mean Thickness ^b (m) | Sedimentation Rate (cm/k.y.) | Mean δ_{w} ^c g/cm ³ | W.C. % | Mean δ_d ^d g/cm ³ | Bulk Accumulation Rate ^e (g/cm ² /k.y.) | Mean CaCO ₃ (%) | Accumulation Rate ^f CaCO ₃ (g/cm ² /k.y.) | Accumulation Rate ^f Non-CaCO ₃ (g/cm ² /k.y.) |
|--|------------|------------------------|---------------------------------|------------------------------|---|--------|--|---|----------------------------|--|--|
| 1. 0 to Brunhes/Matuyama | 0-0.73 | 0-? | 10.8 | 1.5 | 1.4 | 71 | 0.80 | 1.20 | 54 | 0.65 | 0.55 |
| | | 0-10.8 | | | 1.4 | 72 | | | | | |
| 2. Brunhes/Matuyama to bottom of Jaramillo | 0.73-0.98 | 7-13.5 | 2.5 | 1.0 | 1.35 | — | 0.70 | 0.70 | 35 | 0.24 | 0.46 |
| 3. Bottom of Jaramillo to top of Olduvai | 0.98-1.66 | 13.5-? | 16.6 | 2.4 | 1.3 | 73 | 0.75 | 1.80 | 43 | 0.77 | 1.03 |
| 4. Top of Olduvai to Gauss/Matuyama | 1.66-2.48 | 7-48.0 | 19.2 | 2.3 | 1.3 | 79 | 0.70 | 1.60 | 33 | 0.53 | 1.07 |
| | | 29.9-49.1 | | | 1.3 | 80 | | | | | |
| 5. Gauss/Matuyama to top of Kaena | 2.48-2.92 | 48.0-57.1 | 11.8 | 2.7 | 1.3 | 78 | 0.70 | 1.90 | 34 | 0.65 | 1.25 |
| | | 49.1-63.6 | | | 1.35 | 78 | | | | | |
| 6. Top of Kaena to bottom of Mammoth | 2.92-3.18 | 57.1-? | 3.2 | 1.2 | 1.3 | — | 0.80 | 1.00 | 44 | 0.44 | 0.56 |
| 7. Bottom of Mammoth to Gauss/Gilbert | 3.18-3.40 | 63.6-66.8 | 5.7 | 2.6 | 1.4 | 72 | | | | | |
| | | 66.8-72.5 | | | 1.3 | — | 0.70 | 1.80 | | 0.63 | 1.17 |
| 8. Gauss/Gilbert to top of Cochiti | 3.40-3.86 | 7-88.6 | 16.9 | 3.7 | 1.3 | 75 | 0.75 | 2.80 | 35 | 0.98 | 1.82 |
| | | 72.5-89.8 | | | 1.35 | 76 | | | | | |
| 9. Top of Cochiti to LAD <i>T. miocenica</i> | 3.86-5.0 | 88.6-127.0 | 38.4 | 3.4 | 1.4 | 71 | 0.80 | 2.70 | 46 | 1.24 | 1.46 |
| | | 89.8-? | | | — | — | | | | | |
| 10. LAD <i>T. miocenica</i> to LAD <i>T. praecanvexa</i> | 5.0-5.7 | 127-160 | 33 | 4.7 | 1.4 | 65 | 0.85 | 4.00 | 53 | 2.10 | 1.90 |
| | | ? | | | — | — | | | | | |
| 11. LAD <i>T. praecanvexa</i> to FAD <i>A. primus</i> | 5.7-6.5 | 160-208 | 48 | 6.0 | 1.3 | 66 | 0.80 | 4.80 | 53 | 2.54 | 2.26 |
| | | ? | | | — | — | | | | | |

^a Depths for each time interval for Holes 503A and 503B.^b Mean thickness computed using boundaries of a time interval recovered in either hole.^c Wet bulk density from GRAPE data.^d Calculated dry bulk density: $\delta_d = \delta_w/(1 + wc)$.^e Bulk accumulation rate = sedimentation rate $\times \delta_d$.^f Accumulation rate of carbonate = bulk accumulation rate $\times \%$ carbonate; non-carbonate rate = bulk - carbonate rate.

LAD = last occurrence datum

FAD = first occurrence datum

lation rate provides a better approximation of sediment influx rate, particularly in older, more compacted sediment (van Andel and others, 1975).

Sedimentation rates at Site 503 range from 1.0 to 6.0 cm/k.y., with an average of 2.9 cm/k.y. We found the highest sedimentation rates in the upper Miocene and lower Pliocene sections and the lowest rates in the Pleistocene sequence. A short interval in the mid-Pliocene is characterized by low sedimentation rates. Because only slight changes in age or thickness will result in variations of the same order of magnitude, fluctuations about this trend may be due to the resolution of the time scale.

The wet-bulk density (GRAPE) and water content data were used to calculate bulk accumulation rates for each time interval used in the sedimentation rate curve (Table 6). Trends in bulk accumulation rates (Fig. 17) decrease throughout the section, with highest values in the upper Miocene and a sharp decrease in the mid-Pliocene similar to the trend of sedimentation rates. The decrease in rates is consistent with the trends for the equatorial Pacific (van Andel and others, 1975) and may be due to several factors, including reduction of sediment influx from terrigenous sources, decreased biogenic productivity, and reduced carbonate preservation. In order to distinguish among these components the carbonate and noncarbonate accumulation rates were calculated from bulk density and average carbonate content (Table 6 and Fig. 16). Carbonate accumulation rates decrease through the section, with highest rates in the upper Miocene and lower Pliocene interval (>4 m.y.) and lowest in the Pleistocene sequence. The trend is consistent with the equatorial Pacific pattern shown by van Andel and others (1975). The mid-Pliocene and Quaternary (4 Ma to Holocene) are characterized by a uniformly low car-

bonate accumulation rate, with values less than 1.0 g/cm²/k.y. The decrease in carbonate accumulation rates in this interval may reflect the deepening of the site as the plate moved from the spreading center.

Noncarbonate accumulation rates also decrease throughout the section. The decrease in noncarbonate rates throughout the equatorial Pacific (van Andel and others, 1975) may be due to a reduction in the siliceous biogenic component (see Sancetta, this volume) rather than to a reduction in the influx of terrigenous material (see Rea, this volume).

SUMMARY AND CONCLUSIONS

Our objective at Site 503 was to recover an undisturbed, complete upper Neogene and Quaternary section using the Hydraulic Piston Corer (HPC). Our major objective was met by coring two holes to a total depth of 235.0 meters sub-bottom, and we recovered a reasonably complete section that represents approximately the past 8 m.y. We recovered 58.8% of the cored interval in Hole 503A and 83.5% in Hole 503B, with about 81% and 86%, respectively, of the sediment undisturbed. After modifications to the core catcher and shear pins, the HPC performed well. The value of the HPC in obtaining undisturbed sediment can be appreciated when Site 503 is compared to Site 83 (see Frontispiece, this volume). A summary of recovery, lithology, paleomagnetism, biostratigraphy, and bulk accumulation rate is given in Figure 18.

Hays et al. (1972) indicated that Site 83 was on the east flank of the East Pacific Rise. However, total field magnetometer data recorded on our approach to and departure from Site 503 indicate that both Site 503 and 83 are actually located on the north flank of Galapagos

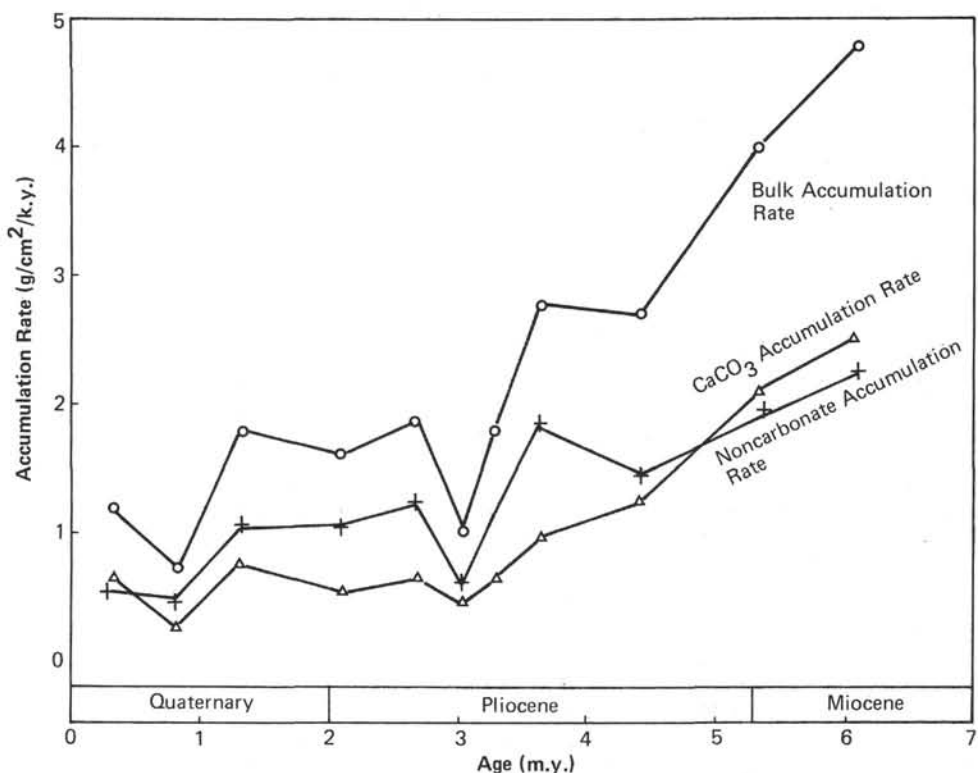


Figure 17. Plots of bulk, carbonate, and noncarbonate accumulation rates ($\text{g}/\text{cm}^2/10^3\text{y.}$) versus time for Site 503. The data points are midpoints of each time interval from Table 6.

Ridge, not the east flank of East Pacific Rise (see Gardner's Underway Geophysics, this volume).

The section at Site 503 is rather uniform and is composed of pelagic sediment with only minor compositional changes. Cycles of carbonate and color changes are apparent throughout the entire section, with periodicities on the order of 40 k.y. per cycle. Curiously, very little volcanic glass and no zeolites were found. The sediment changes from an oxidized to a reduced oxidation state at 8.45 meters and is reduced throughout the remainder of the section. The lack of sediment disturbance is illustrated by open burrows that occur from 9.3 to 64.0 meters sub-bottom. Nodules formed of rhodochrosite around burrows occur from 13.5 to 235 meters and are common from 13.5 to 50 meters. Clay content remains fairly constant at low percentages from 0 to 226 meters but then abruptly increases to greater than 25%. This increase occurs within 10 meters of the oceanic basement and may be caused by an increase of clay produced by seafloor weathering of the basement.

Detailed measurements of shear strength, sonic velocity, bulk density, water content, porosity, and cohesion show that the entire section is undercompacted. Shear strengths average about $400 \text{ g}/\text{cm}^2$ from 15 to about 210 meters. Although similar values were obtained at 25 meters depth at Site 502, they increased with depth. The maximum value of shear strength at Site 503 is only $1686 \text{ g}/\text{cm}^2$ and occurred below 210 meters. Porosities are approximately 90%, and water contents are about 80% down to a depth of 210 meters. Sonic

velocities average 1.510 km/s down to a depth of 210 meters. The change in all physical properties at about 210 meters may indicate a "collapse" of the section at this level. One explanation may be that the siliceous microfossils, especially radiolarians, hold the sediment in a highly porous state until some threshold lithostatic load is applied. The section collapsed at loads above the threshold and became less porous, which results in higher velocities and shear strengths and lower water contents.

The sediment contains microfossil assemblages that range in age from Quaternary through the latter part of the late Miocene. Calcareous and siliceous microfossils are sufficiently numerous and well preserved for detailed stratigraphic interpretation. Cyclic zones of carbonate dissolution appear to occur throughout the sequence. Reworked assemblages of nannofossils and a monospecific diatom assemblage appears in the late Miocene. Radiolarians and diatoms are poorly preserved in Quaternary sediment, but preservation is good in the Tertiary section.

We were able to identify most magnetostratigraphic chronos and subchrons above the Gauss/Gilbert boundary, even though rust contamination was a serious problem, especially in Hole 503A. Most magnetostratigraphic datums are located to the nearest meter, because discrete sample measurements were needed to avoid rust contamination. We observed distinct cycles of NRM intensity with wavelengths comparable to the carbonate cycles. This covariance implies a direct correlation of intensity with lithology. Unfortunately, the rust problem

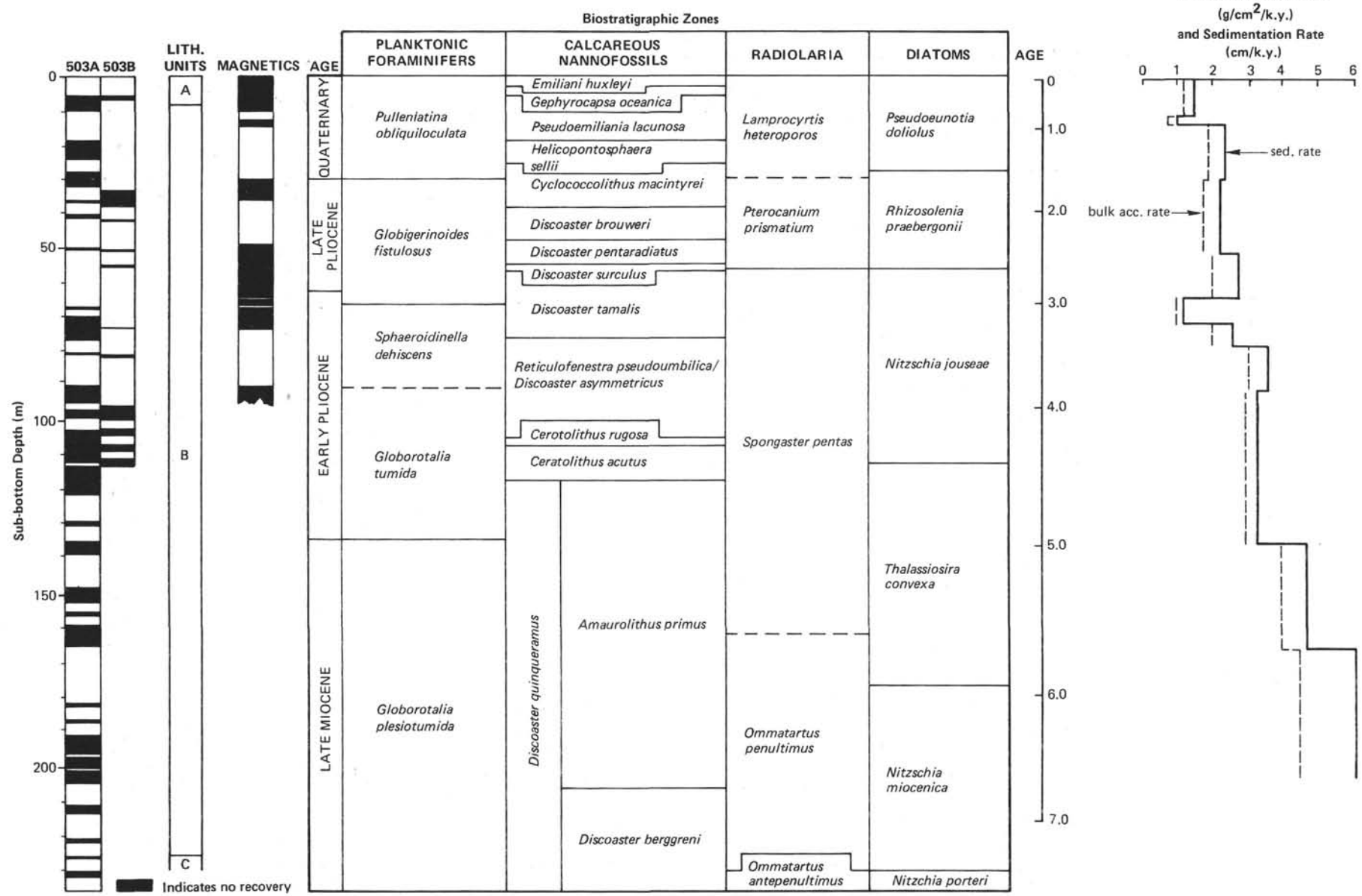


Figure 18. Summary of the recovery, lithostratigraphy, magnetostratigraphy, biostratigraphy, and sediment accumulation rates for Site 503.

obscures many of paleomagnetic trends, but a decrease in the NRM intensity does occur during the lower Gilbert Chron.

Bulk accumulation rates at Site 503 steadily decrease from late Miocene ($4.0 \text{ g/cm}^2/\text{k.y.}$) to late Quaternary ($1.2 \text{ g/cm}^2/\text{k.y.}$) with a distinct interval of low accumulation rates ($1.2\text{--}1.6 \text{ g/cm}^2/\text{k.y.}$) in the mid-Pliocene. The rate of both carbonate and noncarbonate accumulation mimics the trend of bulk accumulation, and noncarbonate components (silica and clay) generally reflect the carbonate pattern.

REFERENCES

- Boyce, R. E., 1976. Definitions and laboratory techniques of compressional sound velocity parameters and wet-water content, wet-bulk density, and porosity parameters by gravimetric and gamma ray attenuation techniques. In Schlanger, S. O., Jackson, E. D., et al., *Init. Repts. DSDP*, 33: Washington (U.S. Govt. Printing Office), 931-958.
- , 1977. Deep Sea Drilling Project procedures for shear strength measurement of clayey sediment using modified Wykeham and Farrance laboratory vane apparatus. In Barker, P. F., Dalziel, I. W. D., et al., *Init. Repts. DSDP*, 36: Washington (U.S. Govt. Printing Office), 1059-1068.
- Burk, L. H., 1977. Pliocene and Pleistocene diatom datum levels from the equatorial Pacific. *Quat. Res.*, 7:330-340.
- , 1978. Early Miocene to Pliocene diatom datum levels for the equatorial Pacific. *Spec. Publ. Geol. Res. and Develop. Centre, Republic of Indonesia*, pp. 25-44.
- Gartner, S., 1977. Calcareous nannofossil biostratigraphy and revised zonation of the Pleistocene. *Mar. Micropaleontol.*, 2:1-25.
- Hays, J. D., et al., 1972. *Init. Repts. DSDP*, 9: Washington (U.S. Govt. Printing Office).
- Jenkins, G. D., and Orr, W. N., 1972. Planktonic foraminiferal biostratigraphy of the eastern equatorial Pacific, Leg 9. In Hays et al., *Init. Repts. DSDP*, 9: Washington (U.S. Govt. Printing Office), 1059-1205.
- Keigwin, L. D., Jr., 1976. Late Cenozoic planktonic foraminiferal biostratigraphy and paleoceanography of the Panama Basin. *Micro-paleontology*, 22:419-442.
- Mankinen, E. A., and Dalrymple, G. B., 1979. Revised geomagnetic timescale for interval 0-5 m.y.B.P. *J. Geophys. Res.*, 84:615-626.
- Saito, T., Burk, L. H., and Hays, J. D., 1975. Late Miocene to Pleistocene biostratigraphy of equatorial Pacific sediments. *Late Neogene Epoch Boundaries: Micropaleontol. Spec. Publ. 1*: New York (Micropaleontology Press), 226-244.
- van Andel, Tj. H., Heath, G. R., and Moore, T. C., Jr., 1975. Cenozoic history and paleoceanography of the central equatorial Pacific Ocean. *Geol. Soc. Am. Mem.*, 143.

APPENDIX

Table 3. Smear slide summary of major and minor lithologies for Site 503. The estimates are qualitative, using < 5% estimate = rare, 5-25% = common, 25-75% = abundant, and > 75% = dominant.

SMEAR SLIDE SUMMARY: Dominant Lithology

HOLE 503



| SAMPLE INTERVAL Core Section Interval (cm) | BIOGENIC COMPONENTS | | | | | | NON-BIOGENIC COMPONENTS | | | | | | AUTHIGENIC COMPONENTS | | | | | | | | | | | |
|---|---------------------|--------------|--------------|---------|-----------------|-------------|-------------------------|--------|-----------|----------------|-------------|------------|-----------------------|---------------|-----------------|------------|----------|-----------------------|---------------------|--------|--------------------|-------------------------|------------------|-----------------|
| | Forams | Nannofossils | Radiolarians | Diatoms | Sponge Spicules | Fish Debris | Silico-flagellates | Quartz | Feldspars | Heavy Minerals | Light Glass | Dark Glass | Glauconite | Clay Minerals | Other (specify) | Palagonite | Zeolites | Amorphous Iron Oxides | Fe/Mn Micro Nodules | Pyrite | Recrystall. Silica | Carbonate (unspecified) | Carbonate Rhombs | Other (specify) |
| 1-1, 42 | | | | | | | | | | | | | | | | | | | | | | | | |
| 1-1, 80 | | | | | | | | | | | ■ | | | | | | | | | | | | | |
| 1-2, 75 | | | | | | | | | | | | | | | | | | | | | | | | |
| 1-3, 100 | | | | | | | | | | | | | | | | | | | | | | | | |

Table 3. (Continued).

SMEAR SLIDE SUMMARY: Dominant Lithology

HOLE 503A



| Core Section Interval (cm) | BIOGENIC COMPONENTS | | | | NON-BIOGENIC COMPONENTS | | | | AUTHIGENIC COMPONENTS | | | | | | | | | | | | | | | | |
|----------------------------|---------------------|--------------|--------------|---------|-------------------------|-------------|--------------------|--------|-----------------------|----------------|-------------|------------|------------|---------------|-----------------|------------|----------|-----------------------|---------------------|--------|----------|-------------------------|------------------|-----------------|--|
| | Forams | Nannofossils | Radiolarians | Diatoms | Sponge Spicules | Fish Debris | Silico-flagellates | Quartz | Feldspars | Heavy Minerals | Light Glass | Dark Glass | Glauconite | Clay Minerals | Other (specify) | Palagonite | Zeolites | Amorphous Iron Oxides | Fe/Mn Micro Nodules | Pyrite | Recryst. | Carbonate (unspecified) | Carbonate Rhombs | Other (specify) | |
| 1-1, 80 | ■ | ■ | ■ | | | | | | | | | | | | | | | | | | | | | | |
| 1-1, 145 | ■ | ■ | ■ | | | | | | | | | | | | | | | | | | | | | | |
| 2-1, 80 | ■ | ■ | | | | | | | | | ■ | | | | | | | | | | | | | | |
| 2-1, 130 | ■ | ■ | | | | | | | | | | | | | | | | | | | | | | | |
| 2, CC-10 | | | | | | | | | | | | | | | | | | | | | | | | | |
| 4-1, 60 | | | | | | | | | | | | | | | | | | | | | | | | | |
| 4-3, 20 | | | | | | | | | | | | | | | | | | | | | | | | | |
| 5-1, 55 | | | | | | | | | | | | | | | | | | | | | | | | | |
| 5-2, 30 | | | | | | | | | | | | | | | | | | | | | | | | | |
| 5-3, 5 | | | | | | | | | | | | | | | | | | | | | | | | | |
| 7-2, 113 | | | | | | | | | | | | | | | | | | | | | | | | | |
| 7-3, 40 | | | | | | | | | | | | | | | | | | | | | | | | | |
| 7-3, 85 | | | | | | | | | | | | | | | | | | | | | | | | | |
| 9-1, 90 | | | | | | | | | | | | | | | | | | | | | | | | | |
| 9-2, 75 | | | | | | | | | | | | | | | | | | | | | | | | | |
| 10-1, 20 | | | | | | | | | | | | | | | | | | | | | | | | | |
| 10-2, 90 | | | | | | | | | | | | | | | | | | | | | | | | | |
| 11-2, 2 | | | | | | | | | | | | | | | | | | | | | | | | | |
| 11-2, 140 | | | | | | | | | | | | | | | | | | | | | | | | | |
| 12-1, 110 | | | | | | | | | | | | | | | | | | | | | | | | | |
| 12-3, 10 | | | | | | | | | | | | | | | | | | | | | | | | | |
| 13-1, 98 | | | | | | | | | | | | | | | | | | | | | | | | | |
| 13-2, 10 | | | | | | | | | | | | | | | | | | | | | | | | | |
| 13-3, 100 | | | | | | | | | | | | | | | | | | | | | | | | | |
| 14-2, 100 | | | | | | | | | | | | | | | | | | | | | | | | | |
| 14-3, 40 | | | | | | | | | | | | | | | | | | | | | | | | | |
| 14-2, 90 | | | | | | | | | | | | | | | | | | | | | | | | | |
| 15-2, 140 | | | | | | | | | | | | | | | | | | | | | | | | | |
| 16-2, 100 | | | | | | | | | | | | | | | | | | | | | | | | | |
| 17-2, 10 | | | | | | | | | | | | | | | | | | | | | | | | | |
| 18, CC-10 | | | | | | | | | | | | | | | | | | | | | | | | | |
| 19-1, 110 | | | | | | | | | | | | | | | | | | | | | | | | | |
| 19-2, 130 | | | | | | | | | | | | | | | | | | | | | | | | | |
| 20-2, 110 | | | | | | | | | | | | | | | | | | | | | | | | | |
| 20-3, 50 | | | | | | | | | | | | | | | | | | | | | | | | | |
| 21-2, 60 | | | | | | | | | | | | | | | | | | | | | | | | | |
| 21-3, 95 | | | | | | | | | | | | | | | | | | | | | | | | | |
| 23-2, 107 | | | | | | | | | | | | | | | | | | | | | | | | | |
| 24-2, 40 | | | | | | | | | | | | | | | | | | | | | | | | | |
| 24-2, 110 | | | | | | | | | | | | | | | | | | | | | | | | | |
| 27-1, 113 | | | | | | | | | | | | | | | | | | | | | | | | | |
| 29-1, 45 | | | | | | | | | | | | | | | | | | | | | | | | | |
| 29-2, 70 | | | | | | | | | | | | | | | | | | | | | | | | | |
| 30-2, 80 | | | | | | | | | | | | | | | | | | | | | | | | | |
| 31-2, 30 | | | | | | | | | | | | | | | | | | | | | | | | | |
| 31-2, 85 | | | | | | | | | | | | | | | | | | | | | | | | | |
| 31-2, 120 | | | | | | | | | | | | | | | | | | | | | | | | | |
| 32-1, 60 | | | | | | | | | | | | | | | | | | | | | | | | | |
| 34-2, 110 | | | | | | | | | | | | | | | | | | | | | | | | | |
| 34-3, 55 | | | | | | | | | | | | | | | | | | | | | | | | | |
| 35-1, 70 | | | | | | | | | | | | | | | | | | | | | | | | | |
| 36-1, 140 | | | | | | | | | | | | | | | | | | | | | | | | | |
| 36-2, 80 | | | | | | | | | | | | | | | | | | | | | | | | | |
| 37-1, 105 | | | | | | | | | | | | | | | | | | | | | | | | | |
| 37-2, 25 | | | | | | | | | | | | | | | | | | | | | | | | | |
| 39-2, 45 | | | | | | | | | | | | | | | | | | | | | | | | | |
| 39-2, 135 | | | | | | | | | | | | | | | | | | | | | | | | | |
| 40-1, 60 | | | | | | | | | | | | | | | | | | | | | | | | | |
| 41-1, 35 | | | | | | | | | | | | | | | | | | | | | | | | | |

Table 3. (Continued).

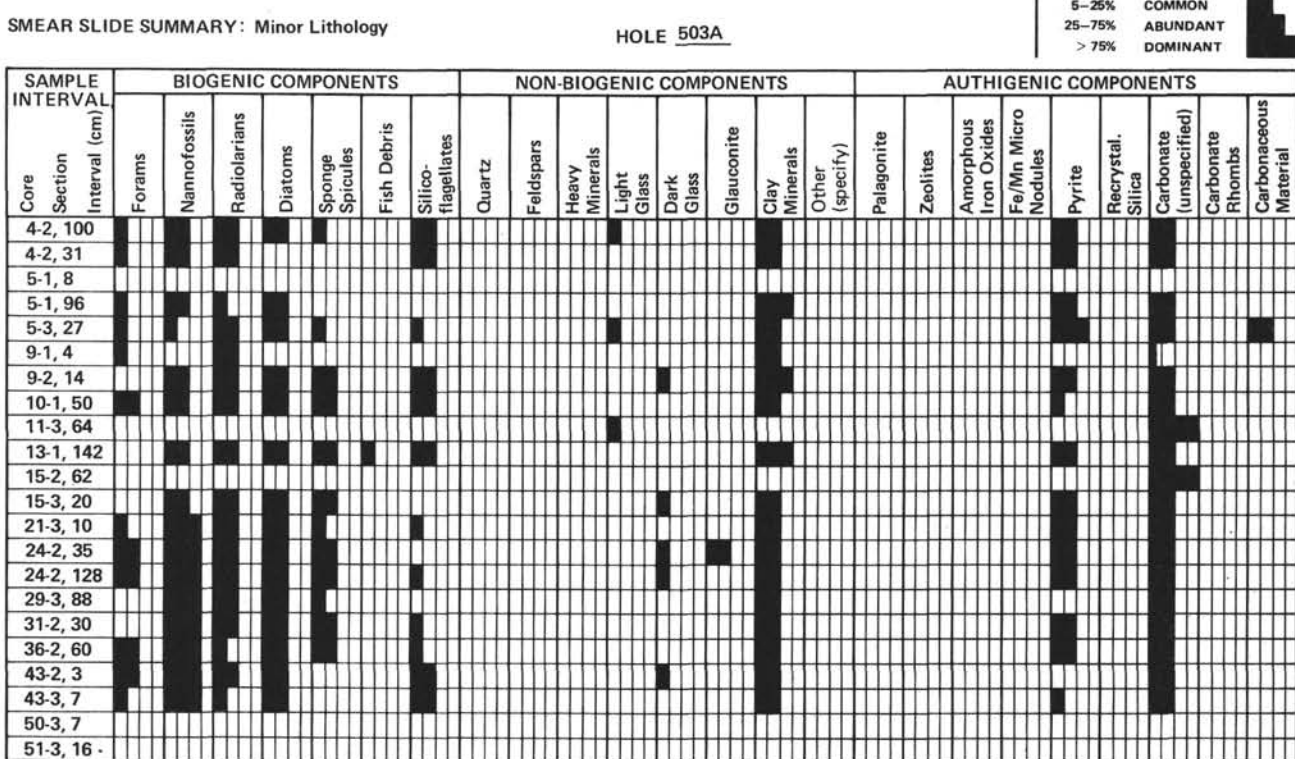
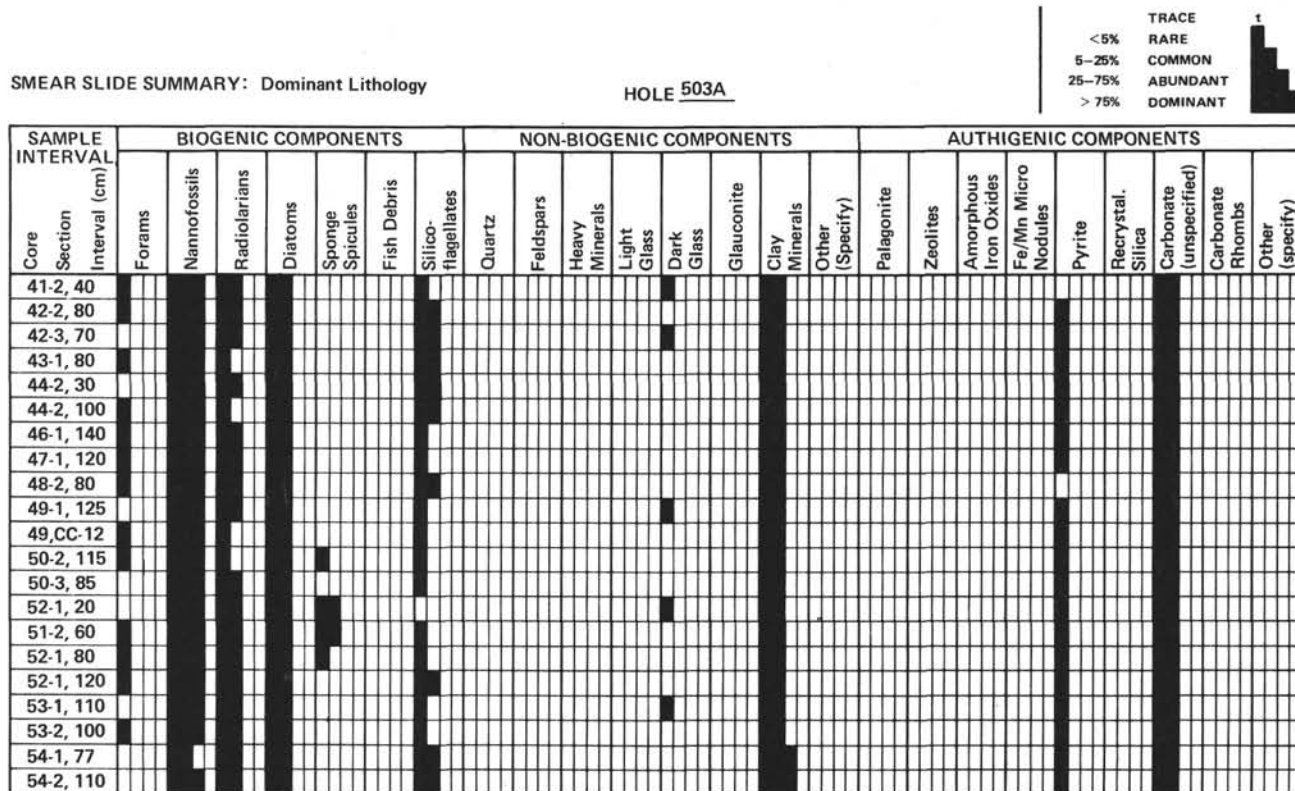


Table 3. (Continued).

SMEAR SLIDE SUMMARY: Dominant Lithology

HOLE 503B

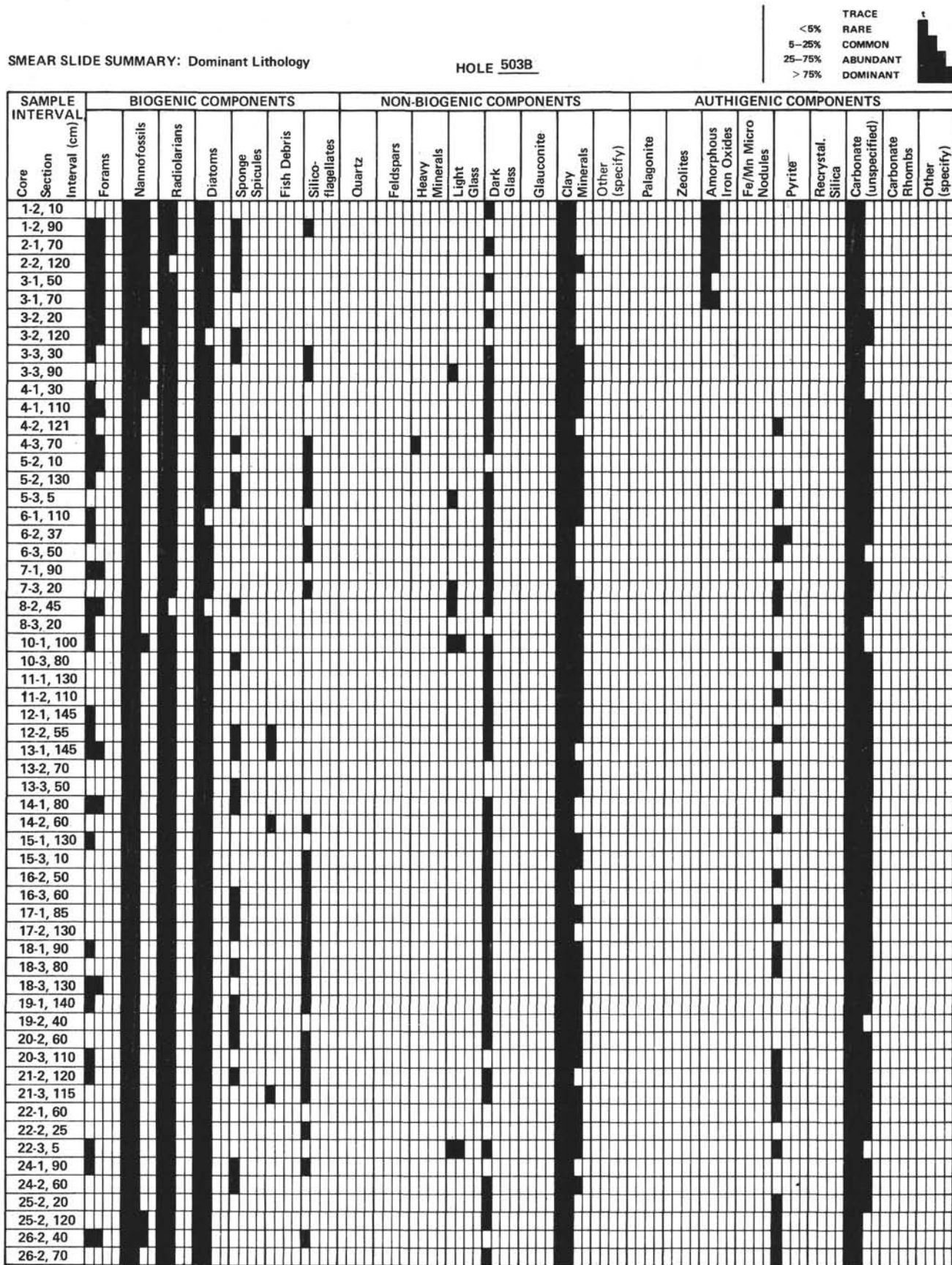


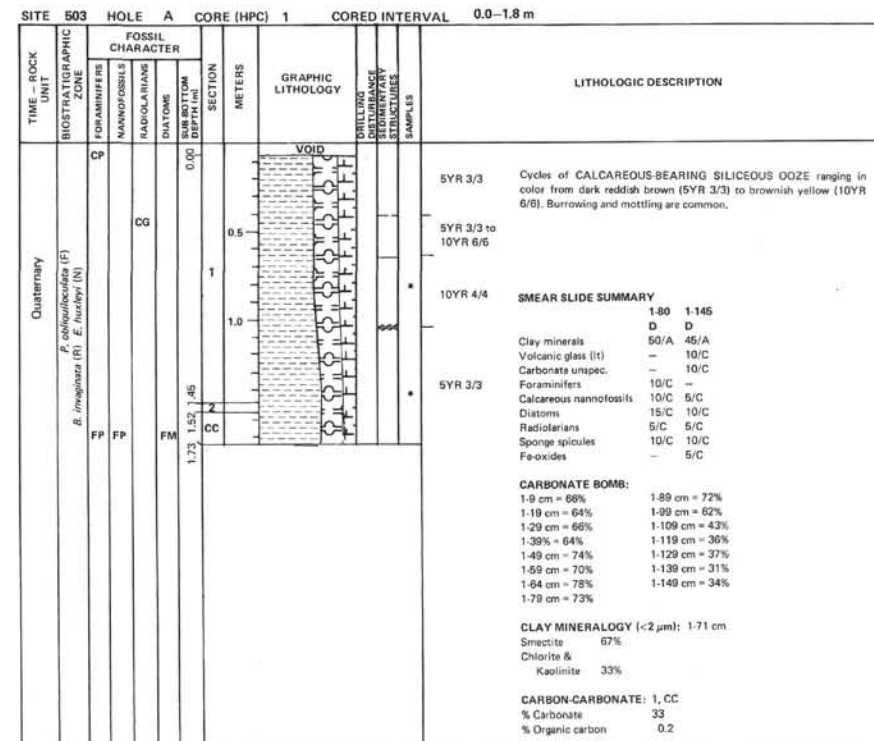
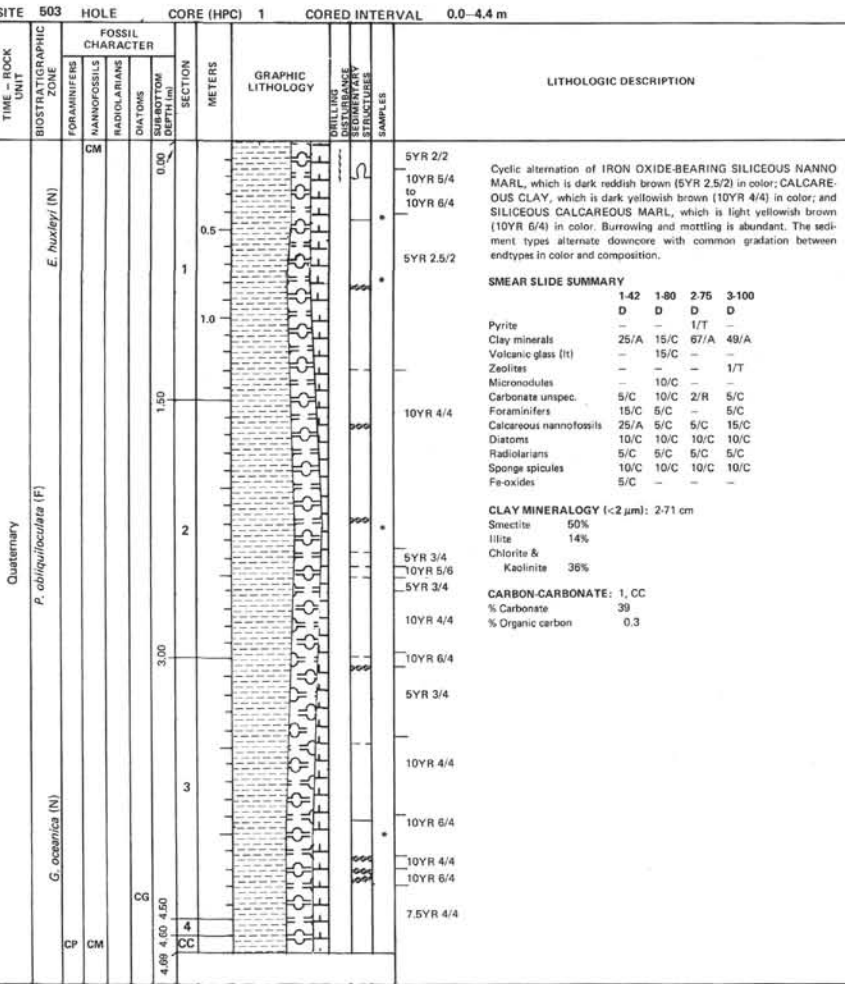
Table 3. (Continued).

SMEAR SLIDE SUMMARY : Minor Lithology

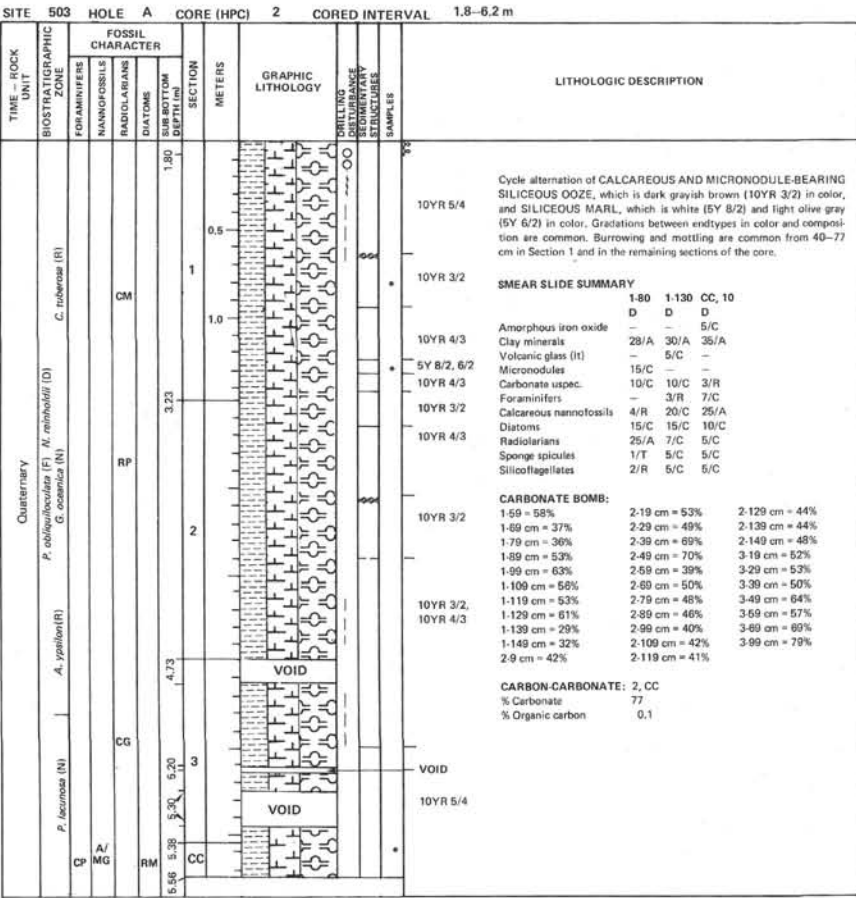
HOLE 503B

| SAMPLE INTERVAL Core Section Interval (cm) | BIOGENIC COMPONENTS | | | | | | NON-BIOGENIC COMPONENTS | | | | | | AUTHIGENIC COMPONENTS | | | | | | | | | | | |
|--|---------------------|--------------|--------------|---------|--------------------|-------------|-------------------------|--------|-----------|-------------------|----------------|---------------|-----------------------|------------------|--------------------|------------|----------|--------------------------|------------------------|--------|-----------------------|----------------------------|---------------------|--------------------|
| | Forams | Nannofossils | Radiolarians | Diatoms | Sponge Spicules | Fish Debris | Silico- flagellates | Quartz | Feldspars | Heavy Minerals | Light Glass | Dark Glass | Glauconite | Clay Minerals | Other (specify) | Palagonite | Zeolites | Amorphous Iron Oxides | Fe/Mn Micro Nodules | Pyrite | Recrystall. Silica | Carbonate (unspecified) | Carbonate Rhombs | Other (specify) |
| 1-1, 118 | █ | █ | █ | █ | █ | █ | █ | █ | █ | █ | █ | █ | █ | █ | █ | █ | █ | █ | █ | █ | █ | █ | █ | █ |
| 3-2, 63 | █ | █ | █ | █ | █ | █ | █ | █ | █ | █ | █ | █ | █ | █ | █ | █ | █ | █ | █ | █ | █ | █ | █ | █ |
| 4-2, 52 | █ | █ | █ | █ | █ | █ | █ | █ | █ | █ | █ | █ | █ | █ | █ | █ | █ | █ | █ | █ | █ | █ | █ | █ |
| 7-1, 108 | █ | █ | █ | █ | █ | █ | █ | █ | █ | █ | █ | █ | █ | █ | █ | █ | █ | █ | █ | █ | █ | █ | █ | █ |
| 10-1, 30 | █ | █ | █ | █ | █ | █ | █ | █ | █ | █ | █ | █ | █ | █ | █ | █ | █ | █ | █ | █ | █ | █ | █ | █ |
| 12-1, 109 | █ | █ | █ | █ | █ | █ | █ | █ | █ | █ | █ | █ | █ | █ | █ | █ | █ | █ | █ | █ | █ | █ | █ | █ |
| 12-1, 72 | █ | █ | █ | █ | █ | █ | █ | █ | █ | █ | █ | █ | █ | █ | █ | █ | █ | █ | █ | █ | █ | █ | █ | █ |

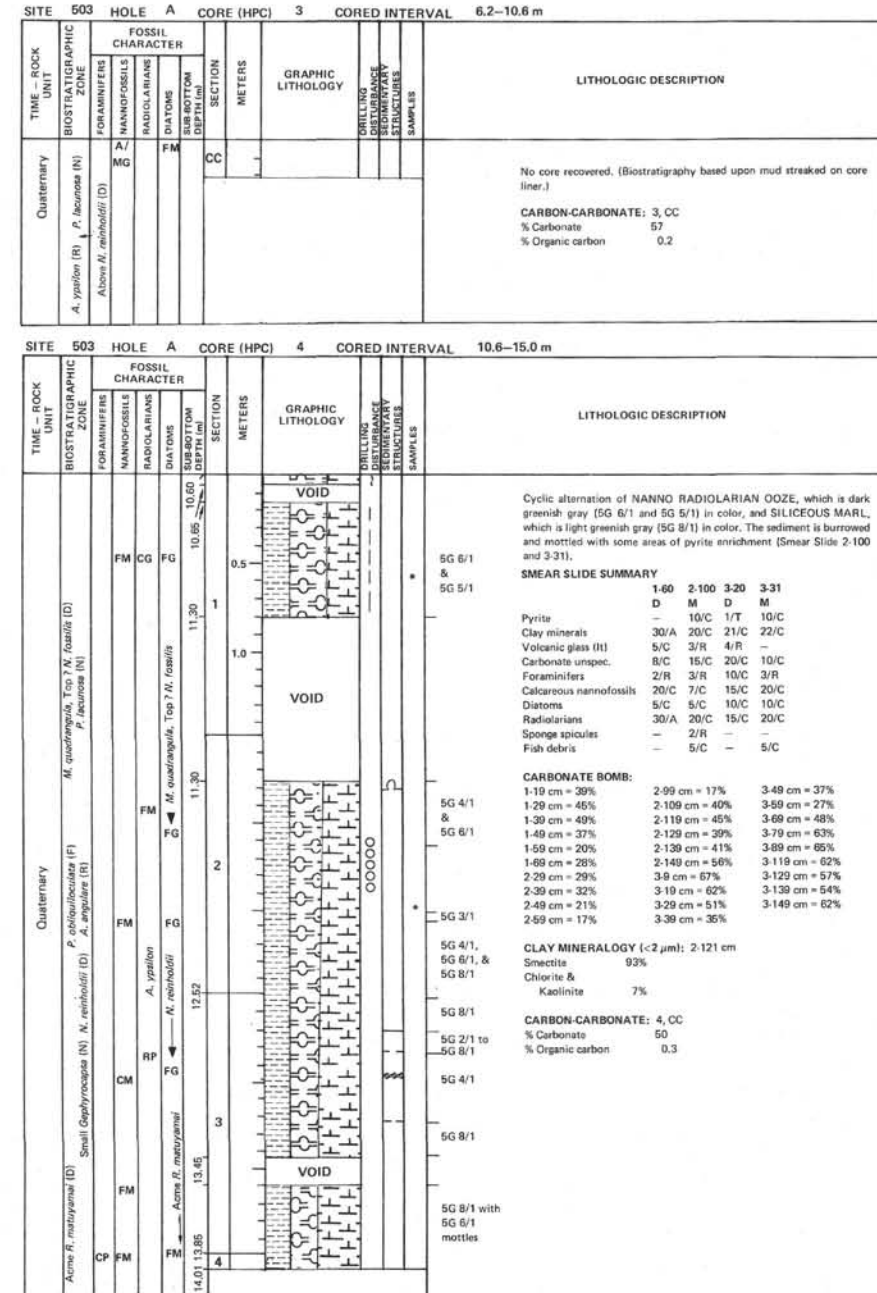


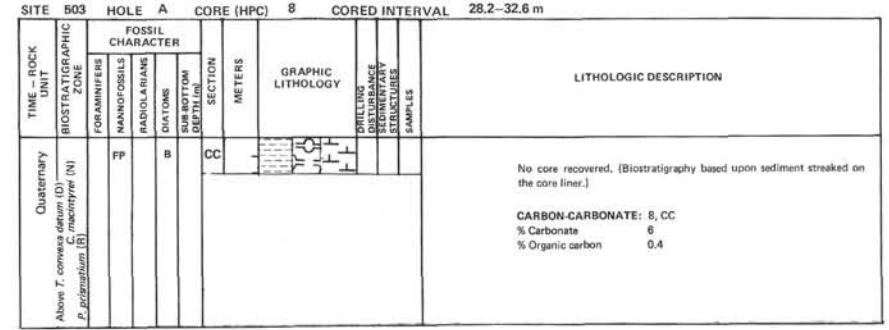
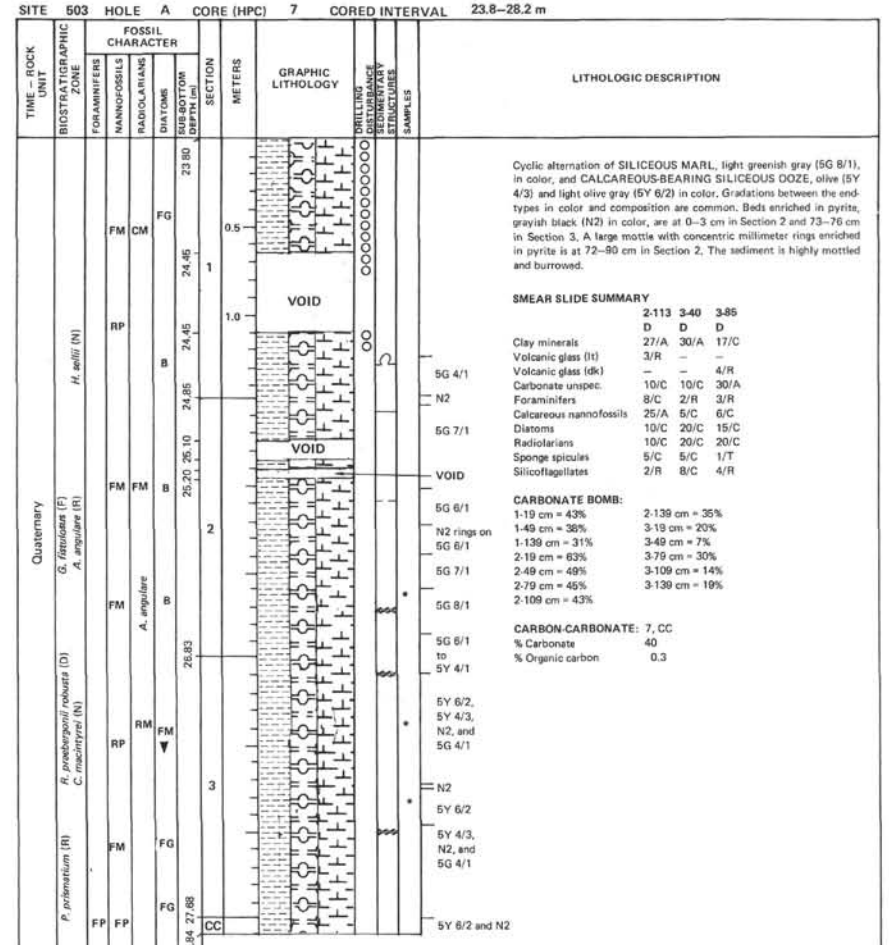
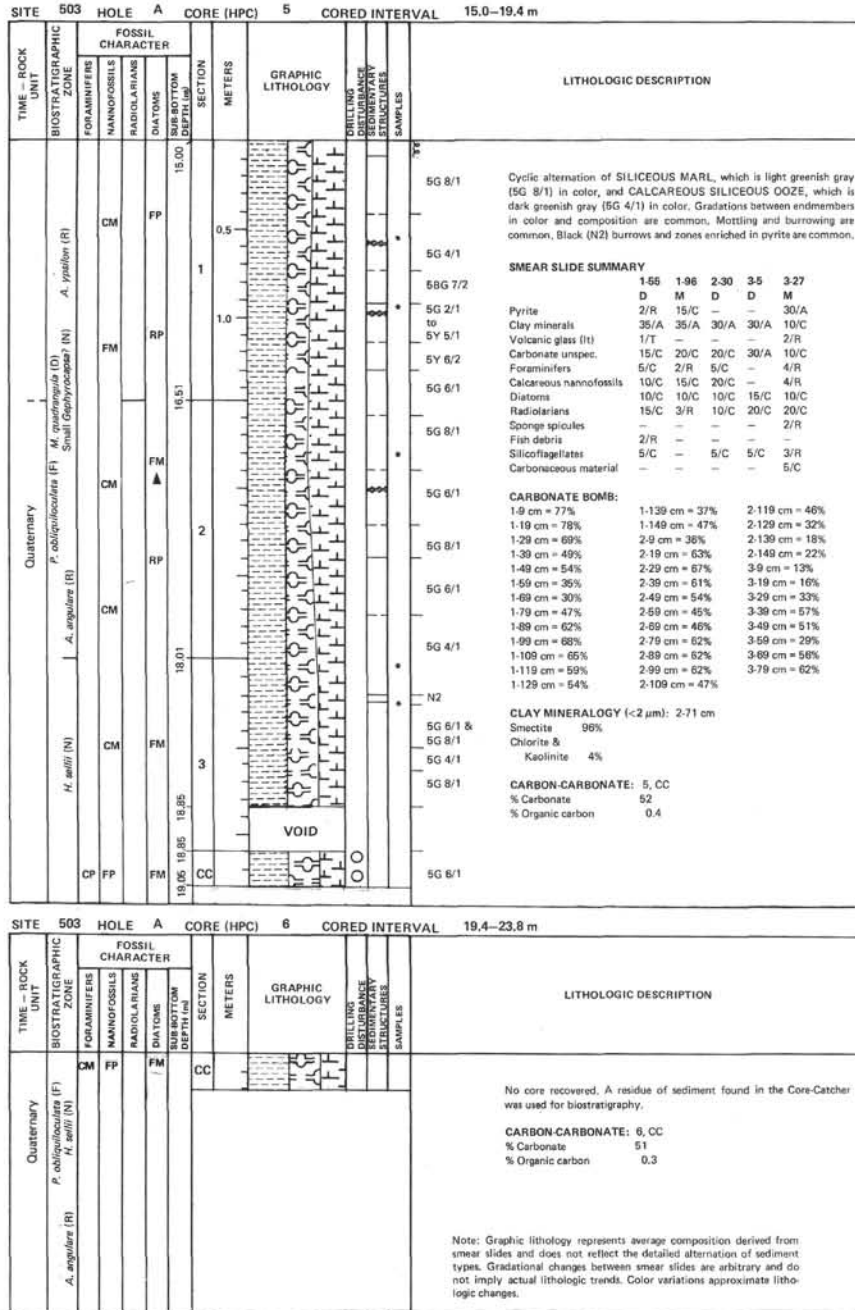


Note: Graphic lithology represents average composition derived from smear slides and does not reflect the detailed alternation of sediment types. Gradational changes between smear slides are arbitrary and do not imply actual lithologic trends. Color variations approximate lithologic changes.



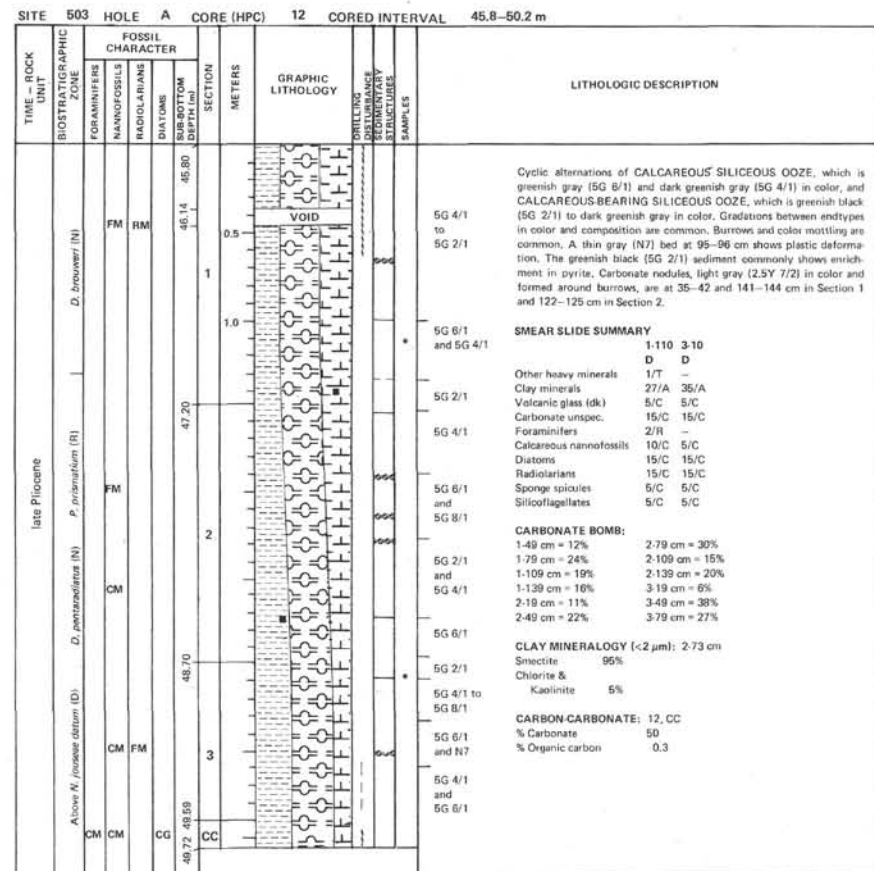
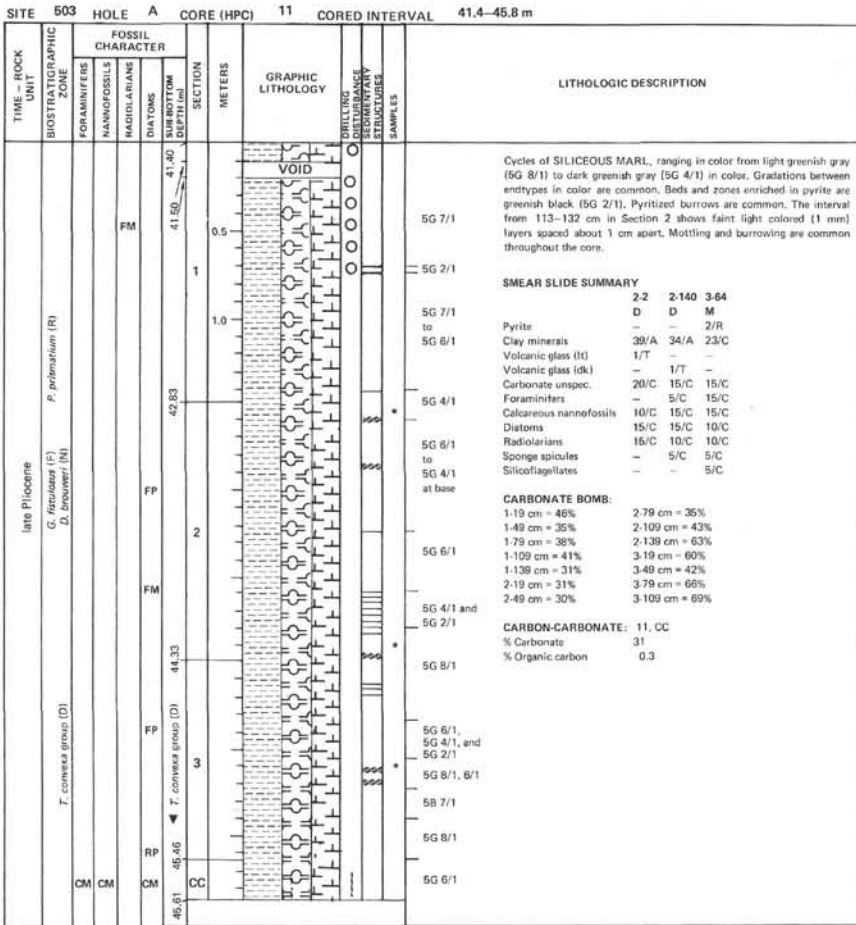
Note: Graphic lithology represents average composition derived from smear slides and does not reflect the detailed alternation of sediment types. Gradational changes between smear slides are arbitrary and do not imply actual lithologic trends. Color variations approximate lithologic changes.



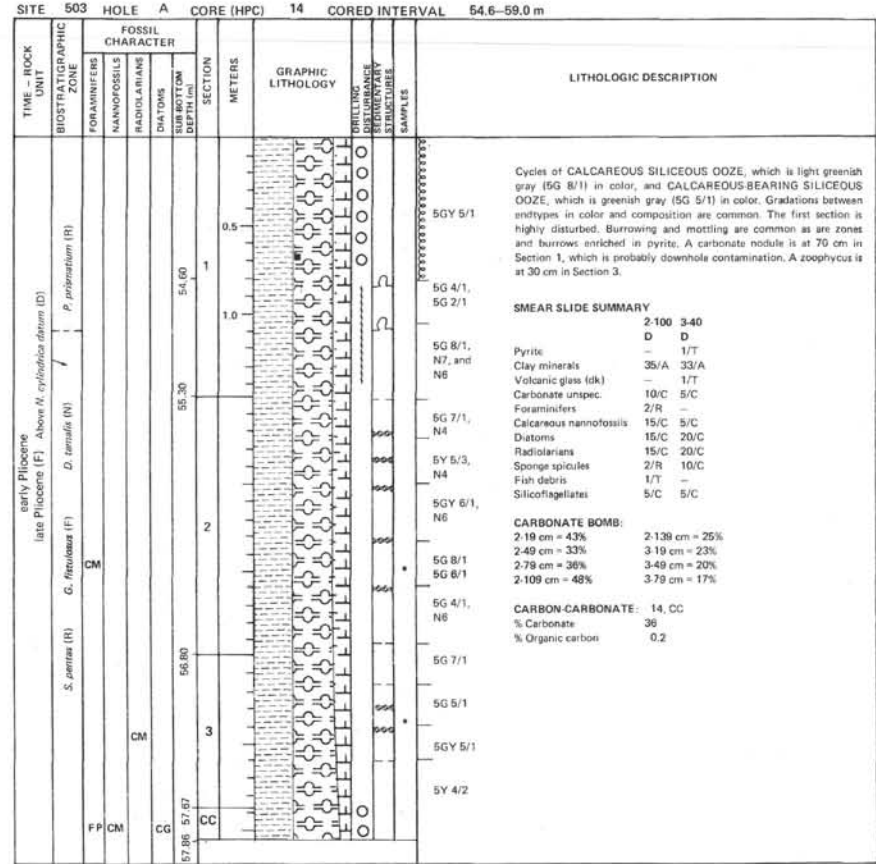
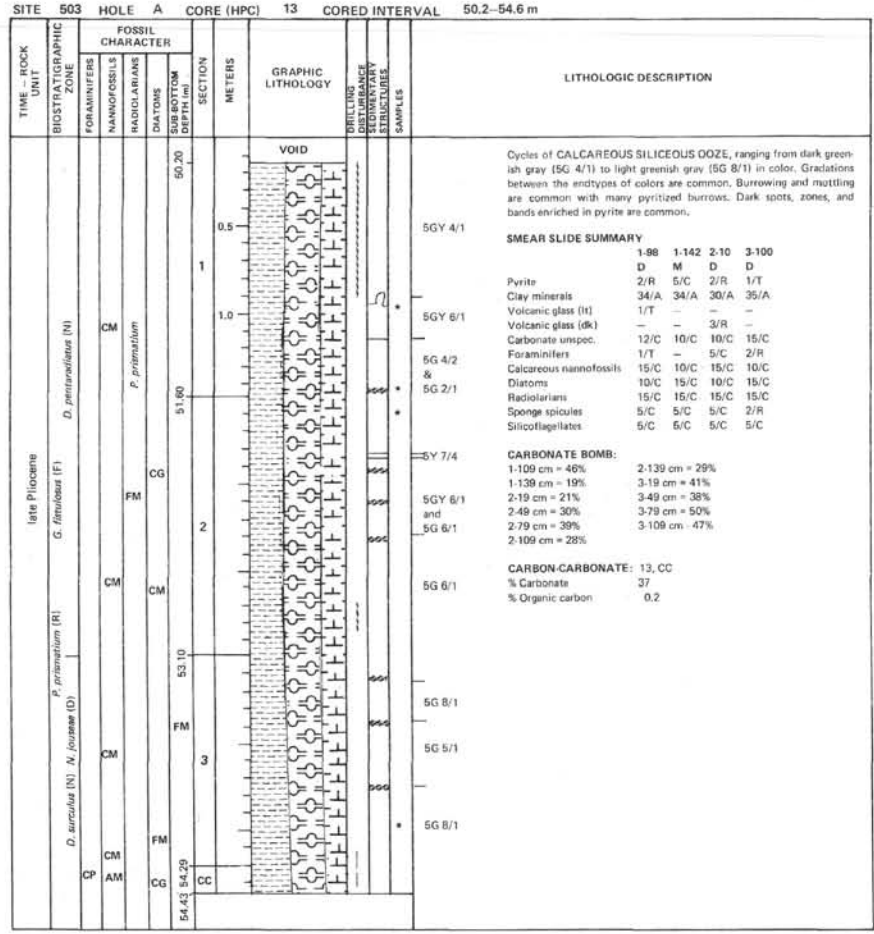


| SITE 503 | | | | HOLE A | CORE (HPC) | 9 | CORED INTERVAL | 32.6-37.0 m | | | SITE 503 | | | | HOLE A | CORE (HPC) | 10 | CORED INTERVAL | 37.0-41.4 m | | |
|---------------|-------------|--|--|--------------|------------|------------------|----------------|-------------|------------------------|-------------|-----------------|---|--------|------------------|--------|------------------------|--------|----------------|-------------|--------|--|
| TIME - ROCK | UNIT | BIOSTRATIGRAPHIC ZONE | | | | FOSSIL CHARACTER | | METERS | LITHOLOGIC DESCRIPTION | TIME - ROCK | UNIT | BIOSTRATIGRAPHIC ZONE | | FOSSIL CHARACTER | METERS | LITHOLOGIC DESCRIPTION | | | | | |
| | | FORAMINIFERS | | NANNOFOSSILS | | | | | | | | FORAMINIFERS | | NANNOFOSSILS | | | | | | | |
| | | FP | CM | FG | B | 32.94 | 32.60 | DEPTH(m) | SECTION | | | CP | RP | FM | 37.00 | SECTION | | | | | |
| late Pliocene | Pleistocene | G. <i>franciscana</i> (D) ▲ Above T. <i>conexa</i> datum (D) D. <i>brouweri</i> (N) P. <i>pseudopumila</i> (D) P. <i>polystoma</i> (R) | ▼ R. <i>proboscidea</i> (D) D. <i>brouweri</i> (N) | | | | | | | | | | | | | | | | | | |
| 36.08 | 35.99 | RP | RM | RP | B | 34.25 | 34.05 | | 1 | 1.0 | 5G 5/2 | 5G 2/1 | 5G 5/2 | 37.00 | 1 | 0.5 | 5G 6/2 | 5G 6/2 | 5G 6/2 | 5G 6/2 | |
| 36.08 | 35.99 | RP | FM | RP | B | 34.87 | | | 2 | 1.0 | 5G 2/1 | Cycles of CALCAREOUS-BEARING SILICEOUS DOZE ranging in color from greenish black (5G 2/1) to grayish green (5G 5/2). Gradations between the endotypes in color are common. The core is fairly uniform except for the interval from 35–72 cm in Section 2 which is highly mottled. A zoophycus is at 103–105 cm in Section 1. A carbonate nodule (light gray [2.5Y 7/2]) which is formed around a burrow is at 70 cm in Section 2. | 5G 6/2 | 5G 6/1 & 5G 4/1 | 5G 6/2 | 5G 6/2 | 5G 6/2 | 5G 6/2 | | | |
| 36.08 | 35.99 | RP | CP | CP | B | 35.35 | | | 3 | 1.0 | 5G 6/2 & 5G 4/1 | Pyrite Other heavy minerals Clay minerals Volcanic glass (dk) Carbonate unspec. Foraminifers Calcareous nannofossils Diatoms Radiolarians Sponge spicules Silicoflagellates | 5G 5/2 | 5G 2/1 | 5G 5/2 | 5G 6/2 | 5G 6/2 | 5G 6/2 | | | |
| 36.08 | 35.99 | RP | CP | CP | B | 35.98 | | | | 0.5 | 5G 3/1 | 5G 2/1 | 5G 4/1 | 5G 6/2 | 5G 6/2 | 5G 6/2 | 5G 6/2 | 5G 6/2 | 5G 6/2 | 5G 6/2 | |
| 36.08 | 35.99 | RP | CP | CP | B | | | | | 5G 4/1 | 5G 3/1 | 5G 4/1 | 5G 6/2 | 5G 6/2 | 5G 6/2 | 5G 6/2 | 5G 6/2 | 5G 6/2 | 5G 6/2 | 5G 6/2 | |
| | | | | | | | | | | | 5G 4/1 | 5G 3/1 | 5G 4/1 | 5G 6/2 | 5G 6/2 | 5G 6/2 | 5G 6/2 | 5G 6/2 | 5G 6/2 | 5G 6/2 | |
| | | | | | | | | | | | | | | | | | | | | | |
| | | | | | | | | | | | | | | | | | | | | | |

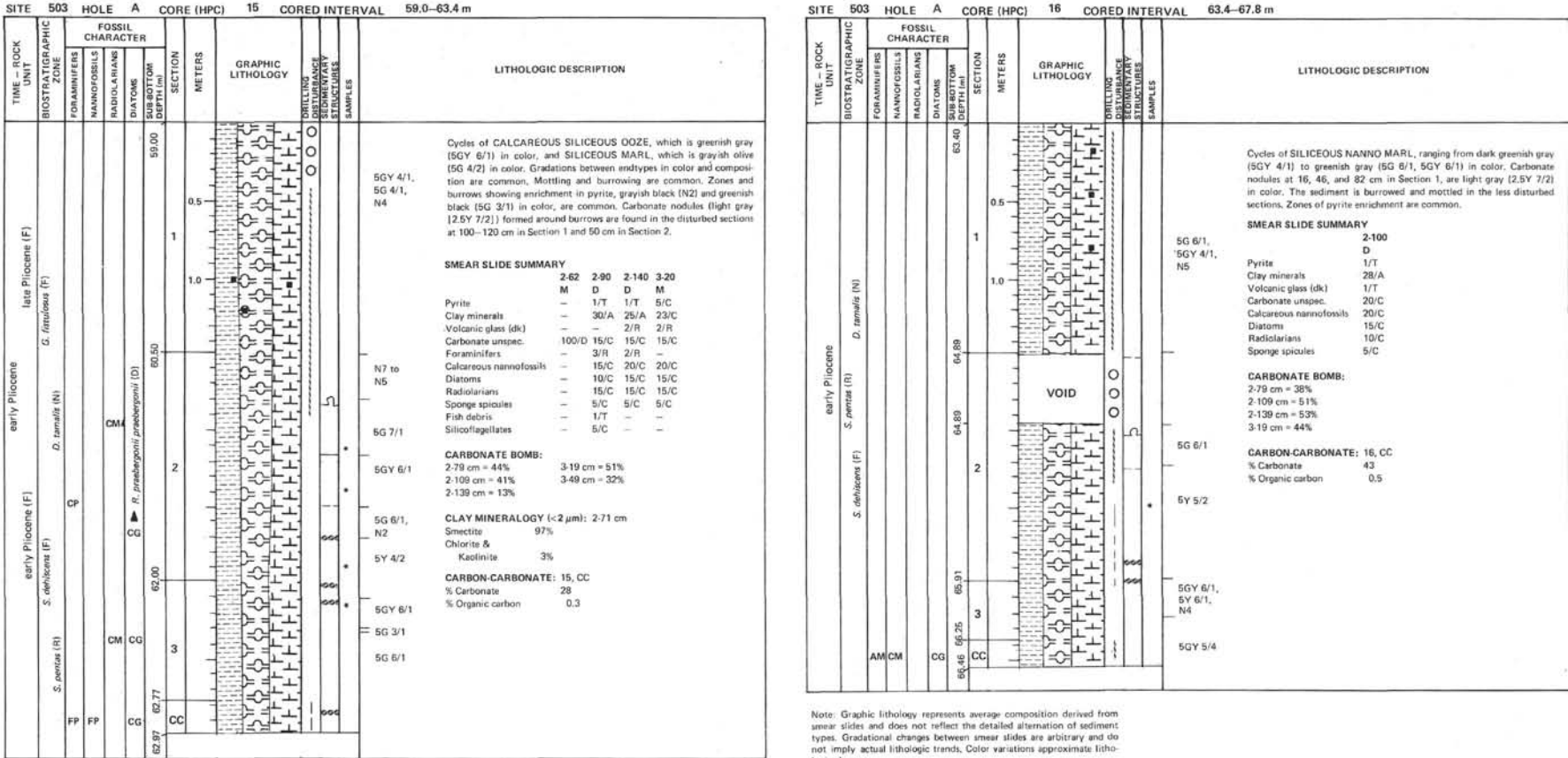
Note: Graphic lithology represents average composition derived from smear slides and does not reflect the detailed alternation of sediment types. Gradational changes between smear slides are arbitrary and do not imply actual lithologic trends. Color variations approximate lithologic changes.



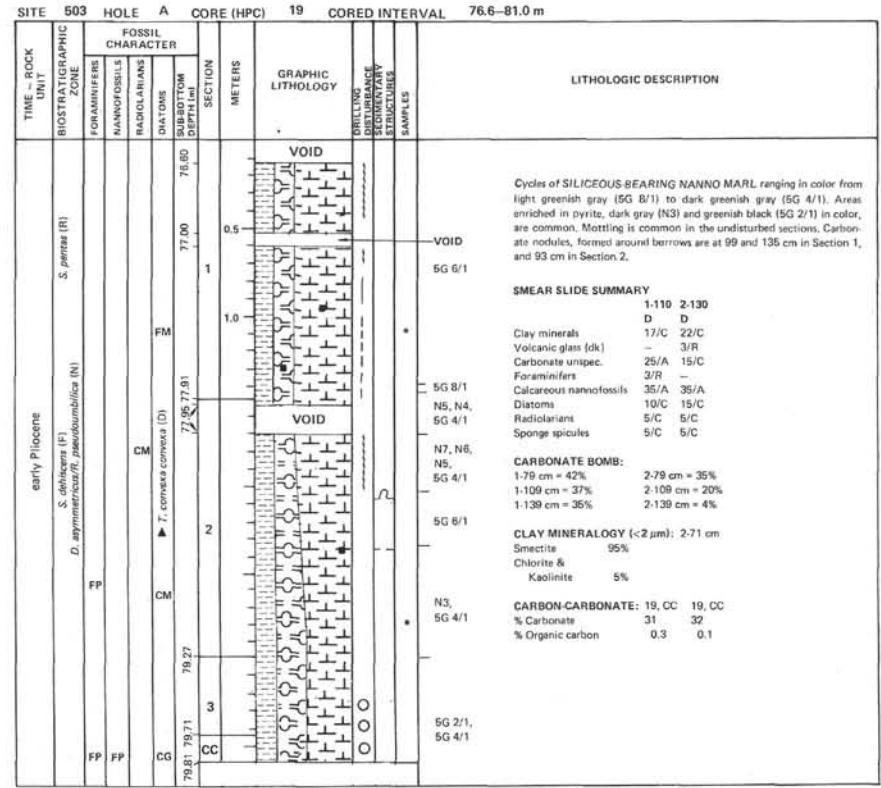
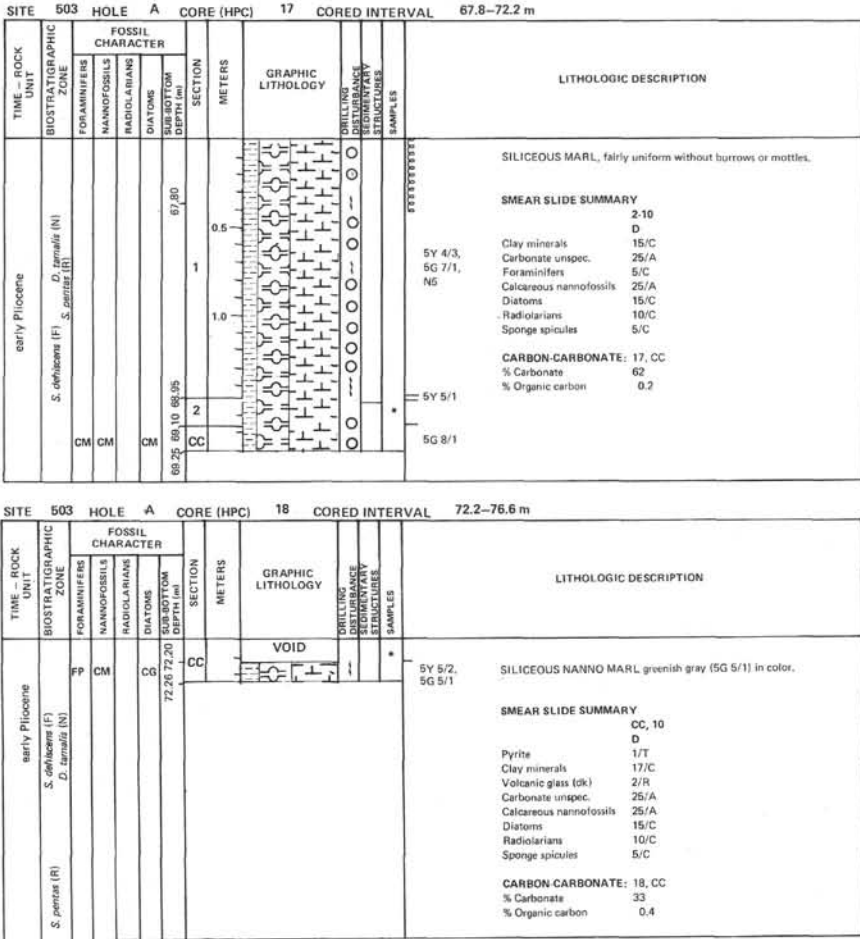
Note: Graphic lithology represents average composition derived from smear slides and does not reflect the detailed alternation of sediment types. Gradational changes between smear slides are arbitrary and do not imply actual lithologic trends. Color variations approximate lithologic changes.



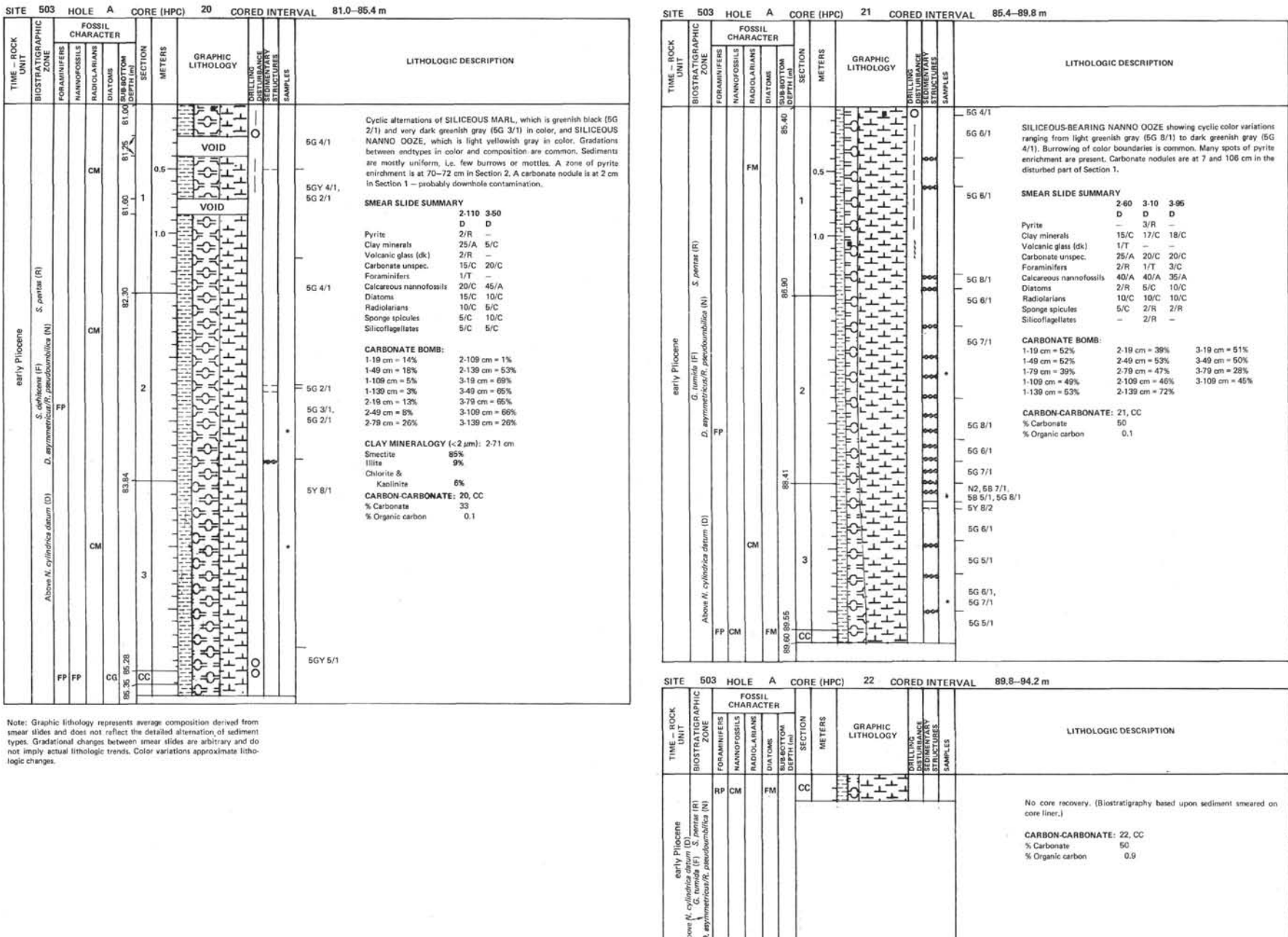
Note: Graphic lithology represents average composition derived from smear slides and does not reflect the detailed alternation of sediment types. Gradational changes between smear slides are arbitrary and do not imply actual lithologic trends. Color variations approximate lithologic change.



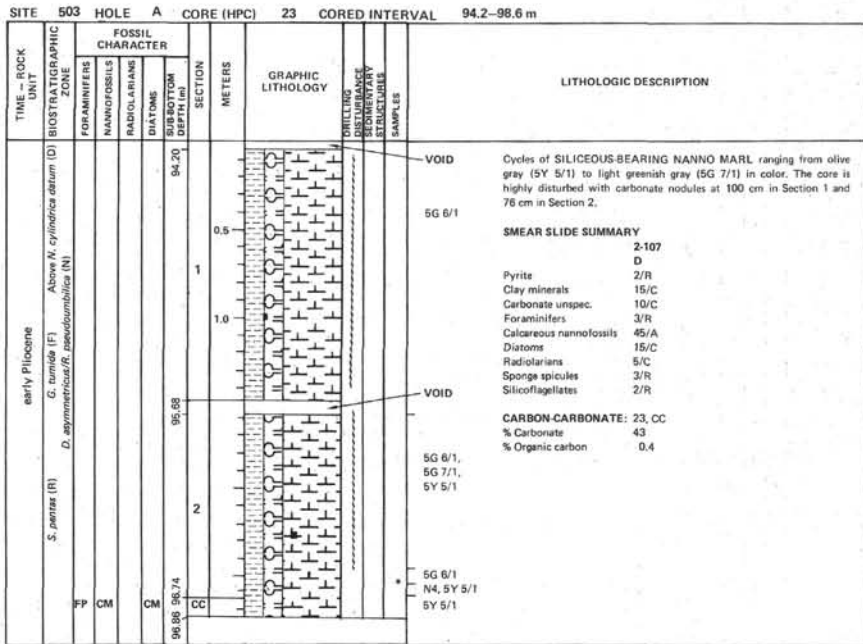
Note: Graphic lithology represents average composition derived from smear slides and does not reflect the detailed alternation of sediment types. Gradational changes between smear slides are arbitrary and do not imply actual lithologic trends. Color variations approximate lithologic changes.



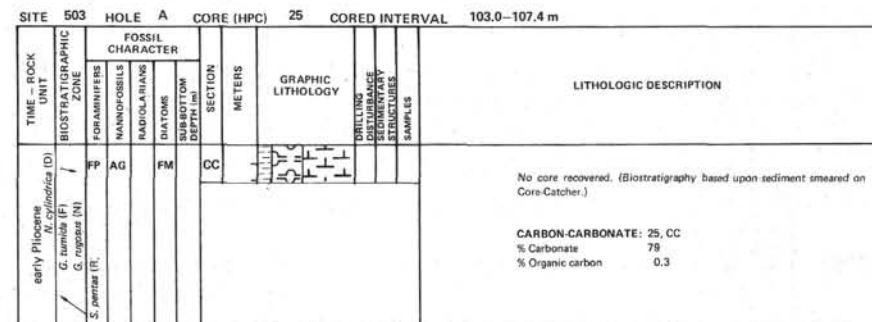
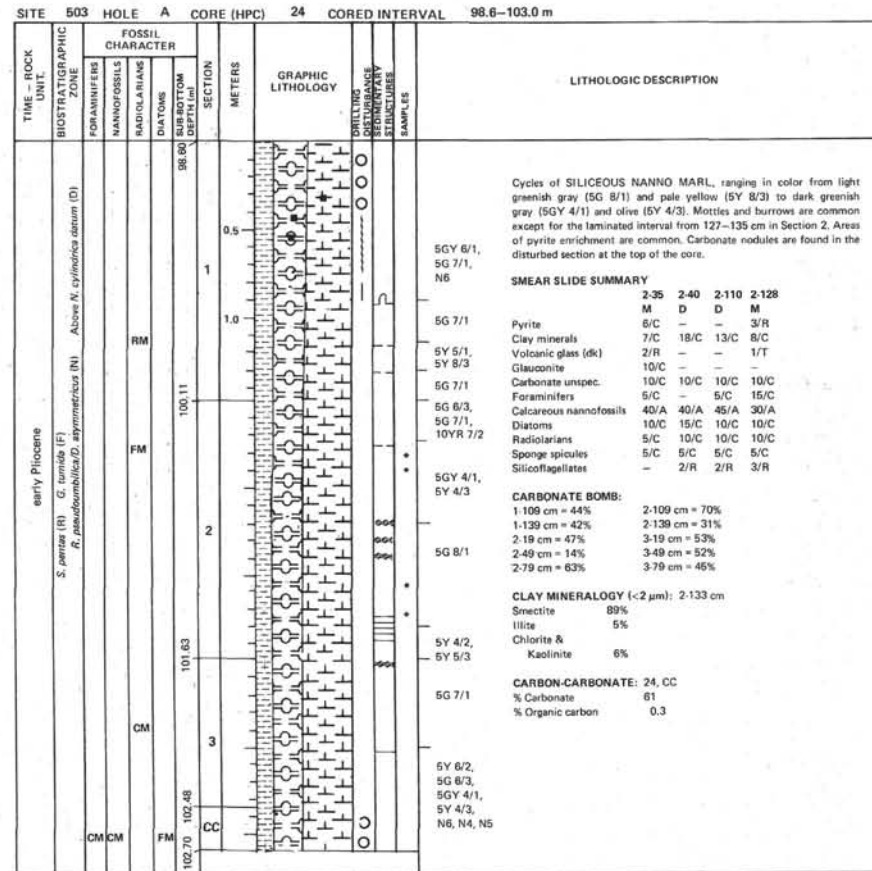
Note: Graphic lithology represents average composition derived from smear slides and does not reflect the detailed alternation of sediment types. Gradational changes between smear slides are arbitrary and do not imply actual lithologic trends. Color variations approximate lithologic changes.

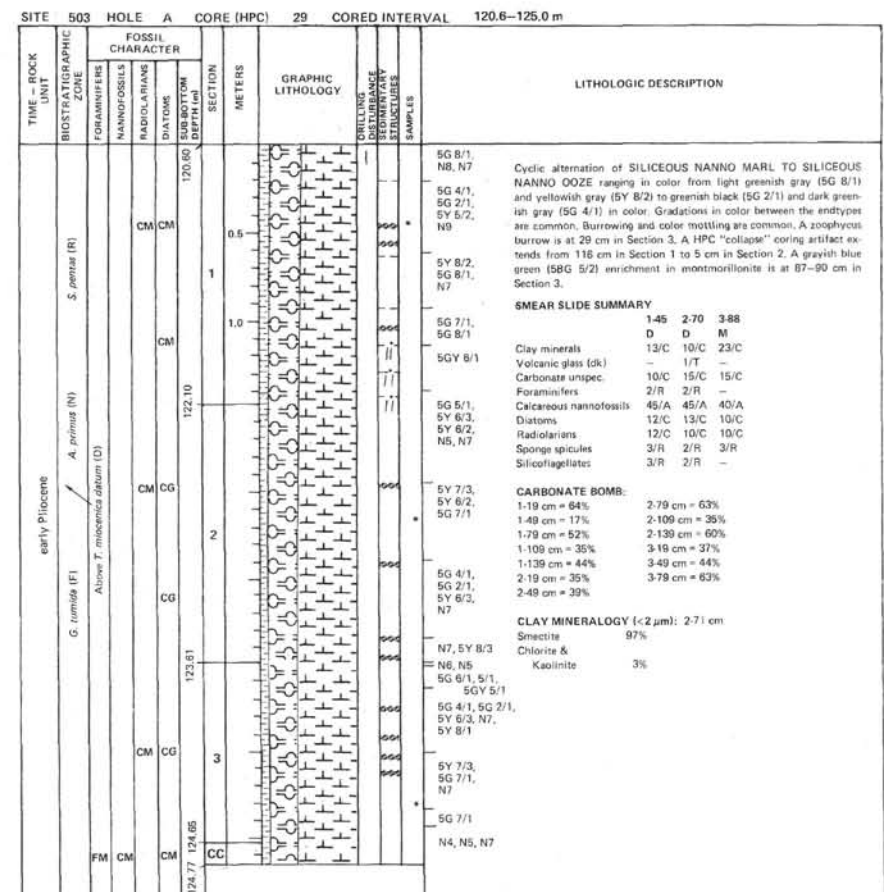
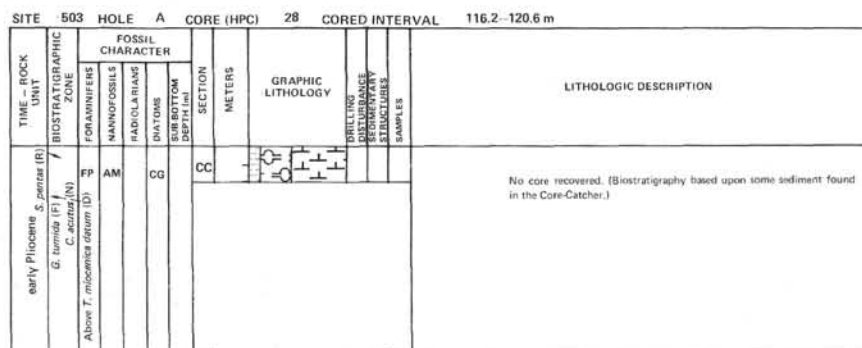
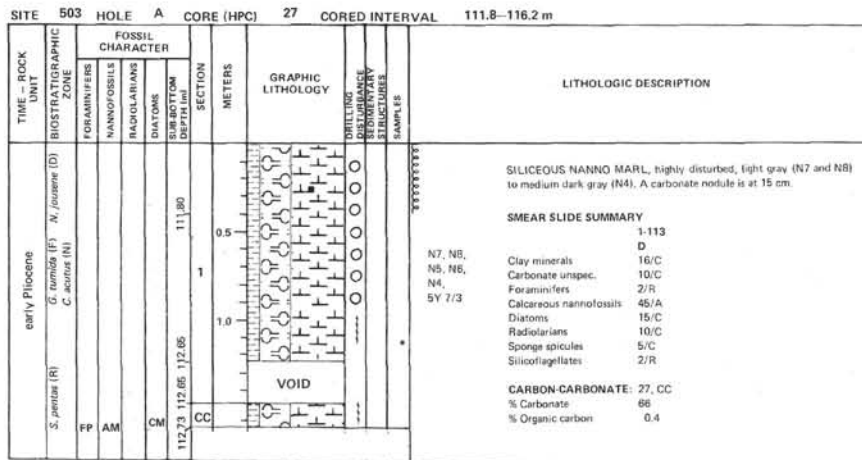
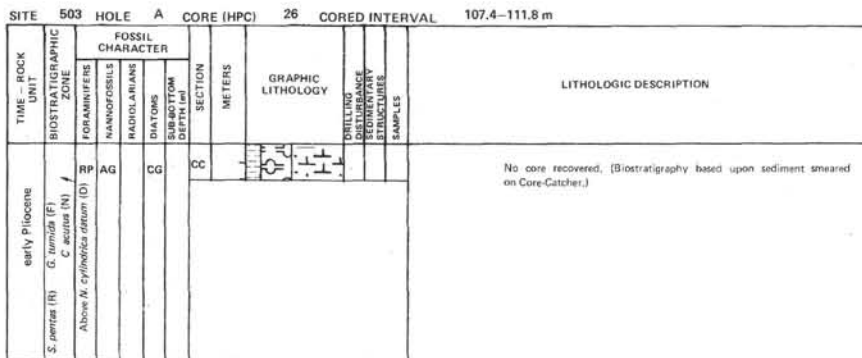


Note: Graphic lithology represents average composition derived from smear slides and does not reflect the detailed alternation of sediment types. Gradational changes between smear slides are arbitrary and do not imply actual lithologic trends. Color variations approximate lithologic changes.

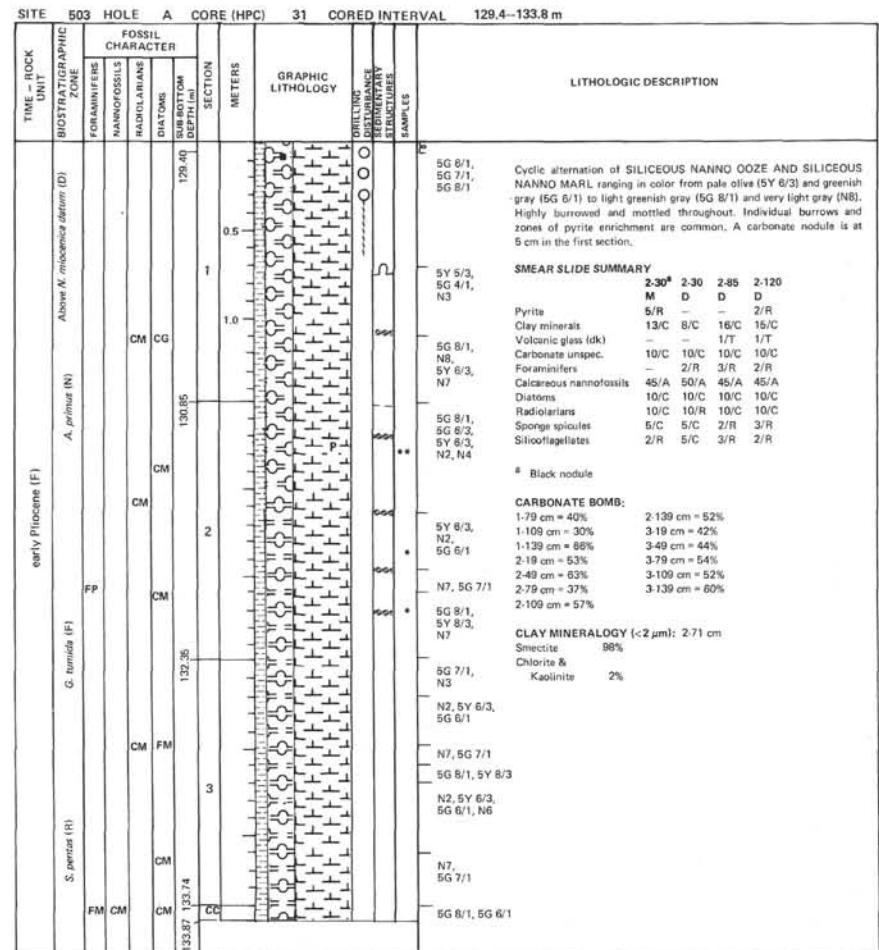
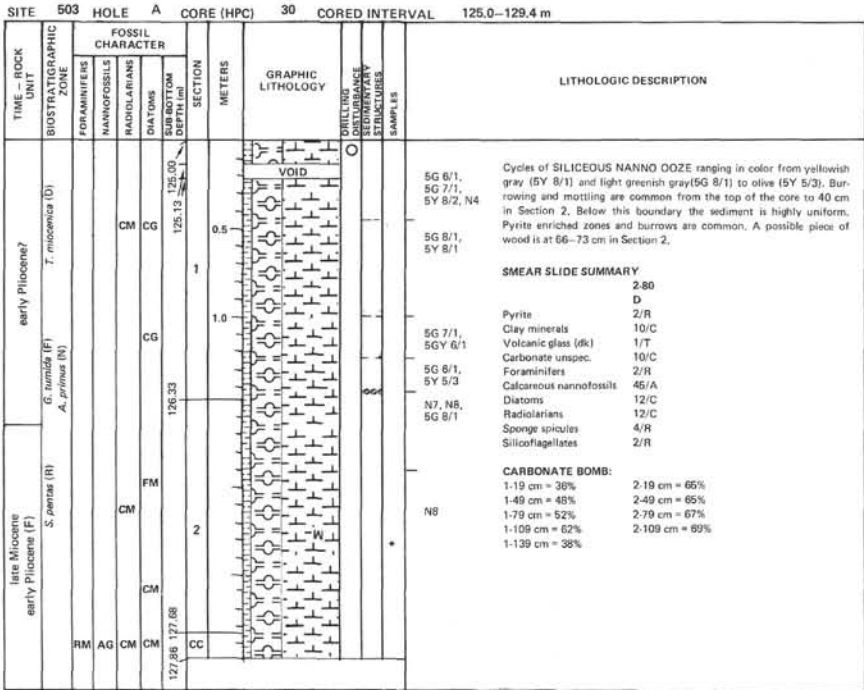


Note: Graphic lithology represents average composition derived from smear slides and does not reflect the detailed alternation of sediment types. Gradational changes between smear slides are arbitrary and do not imply actual lithologic trends. Color variations approximate lithologic changes.

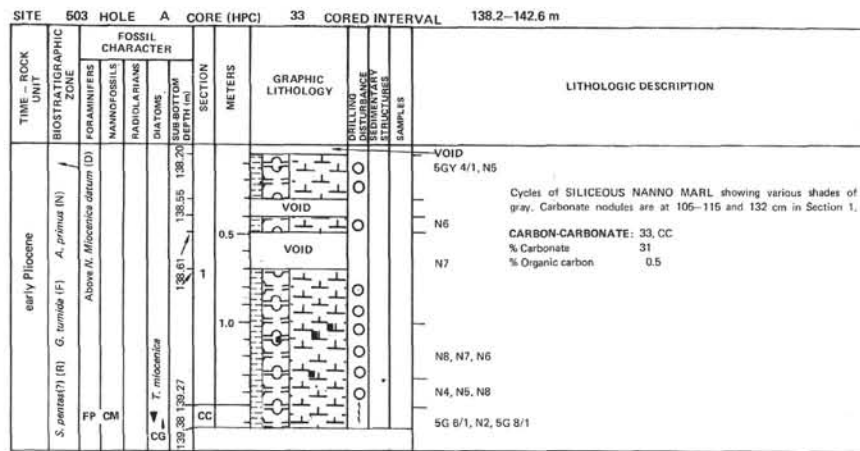
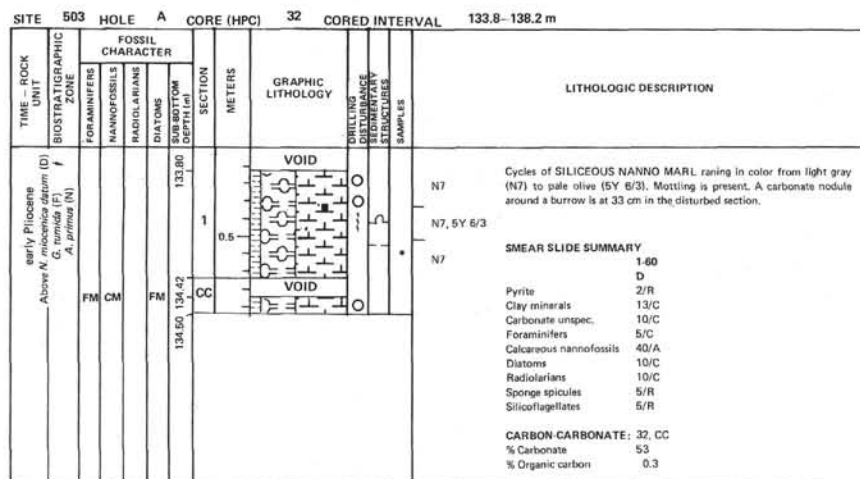




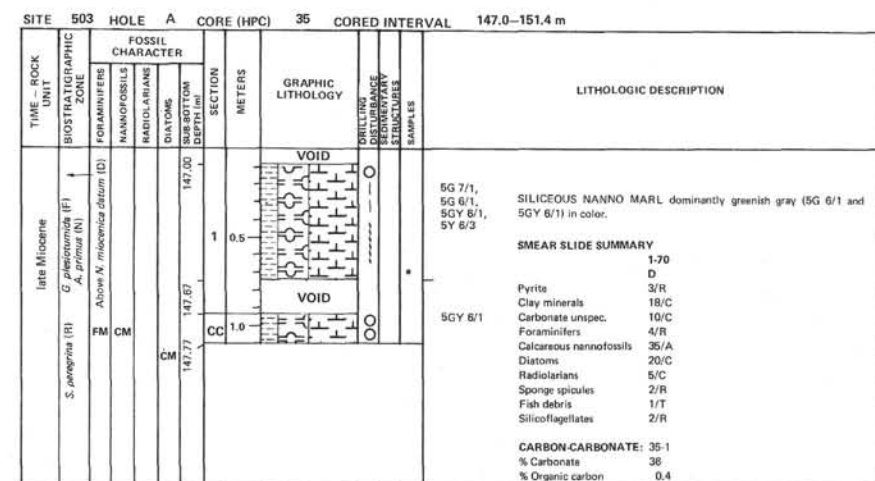
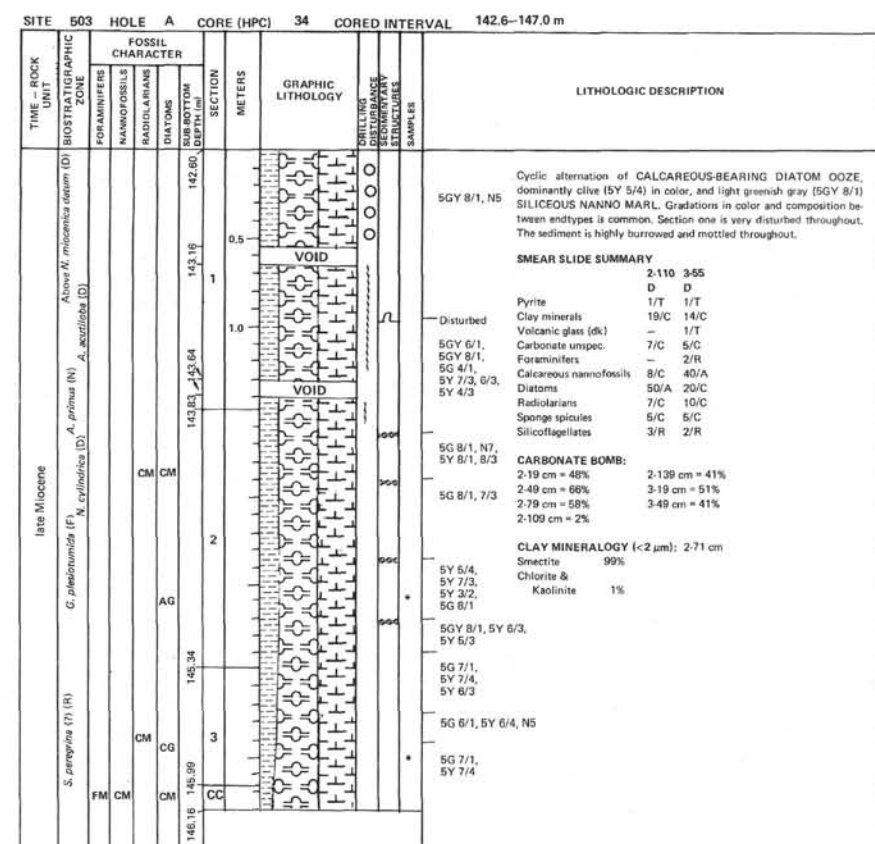
Note: Graphic lithology represents average composition derived from smear slides and does not reflect the detailed alternation of sediment types. Gradational changes between smear slides are arbitrary and do not imply actual lithologic trends. Color variations approximate lithologic changes.

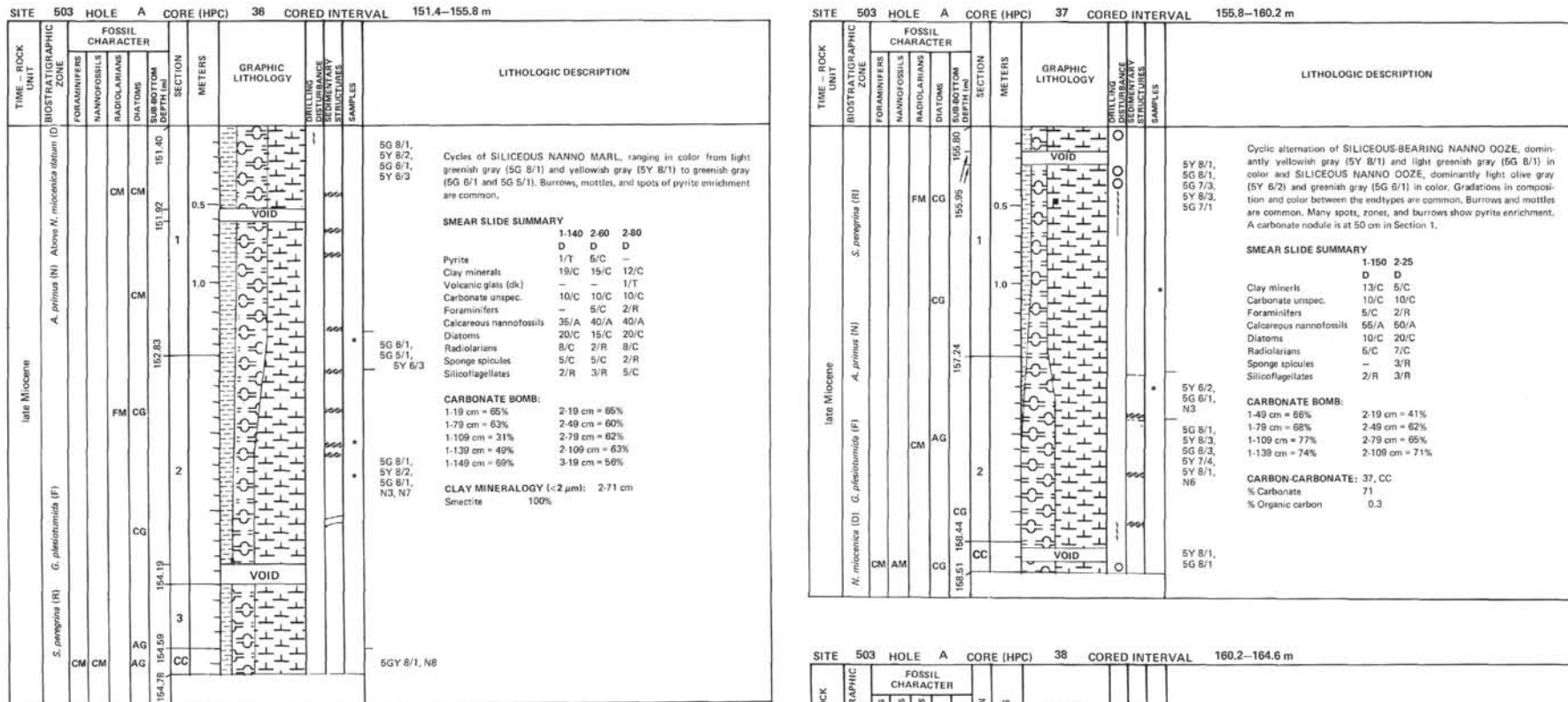


Note: Graphic lithology represents average composition derived from smear slides and does not reflect the detailed alternation of sediment types. Gradational changes between smear slides are arbitrary and do not imply actual lithologic trends. Color variations approximate lithologic changes.

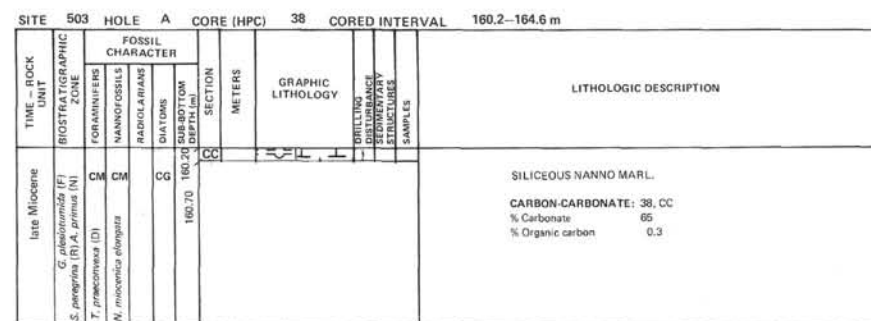


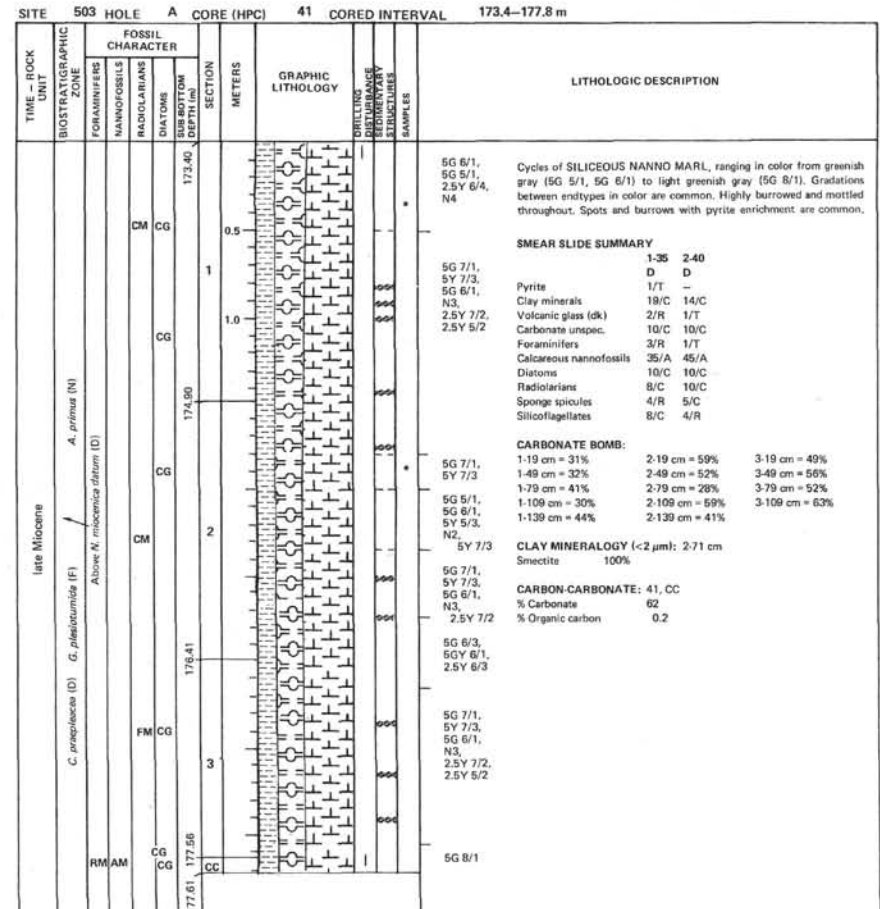
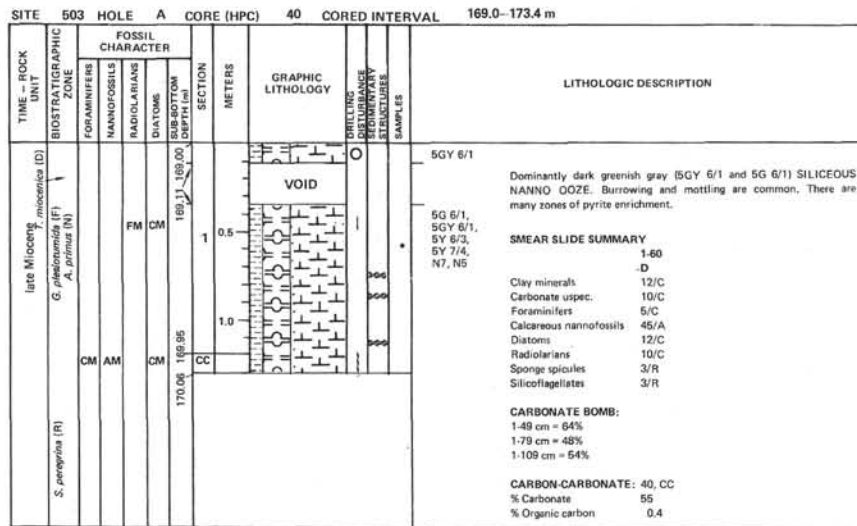
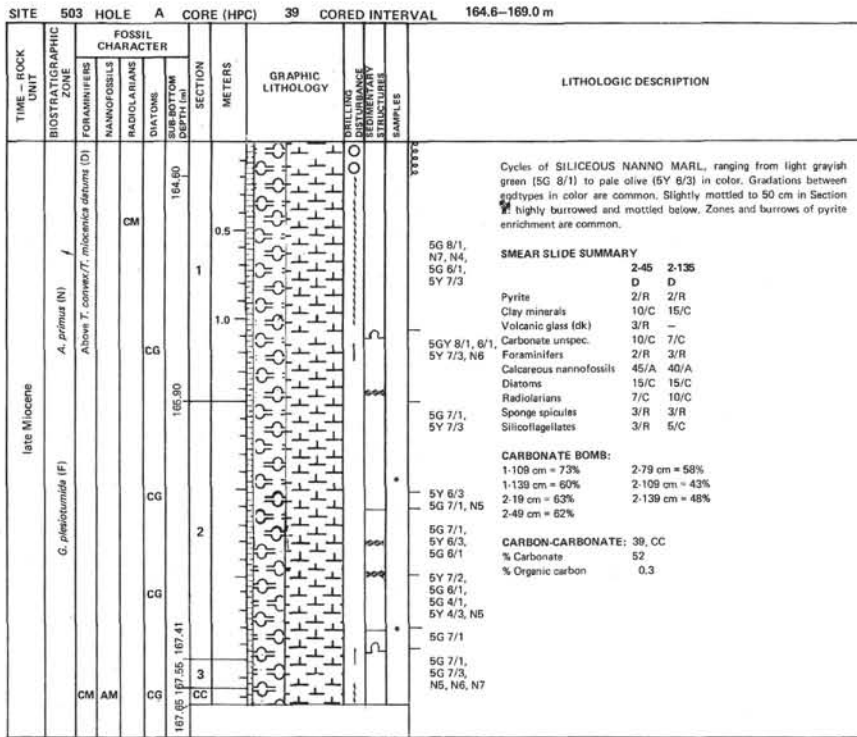
Note: Graphic lithology represents average composition derived from smear slides and does not reflect the detailed alternation of sediment types. Gradational changes between smear slides are arbitrary and do not imply actual lithologic trends. Color variations approximate lithologic changes.



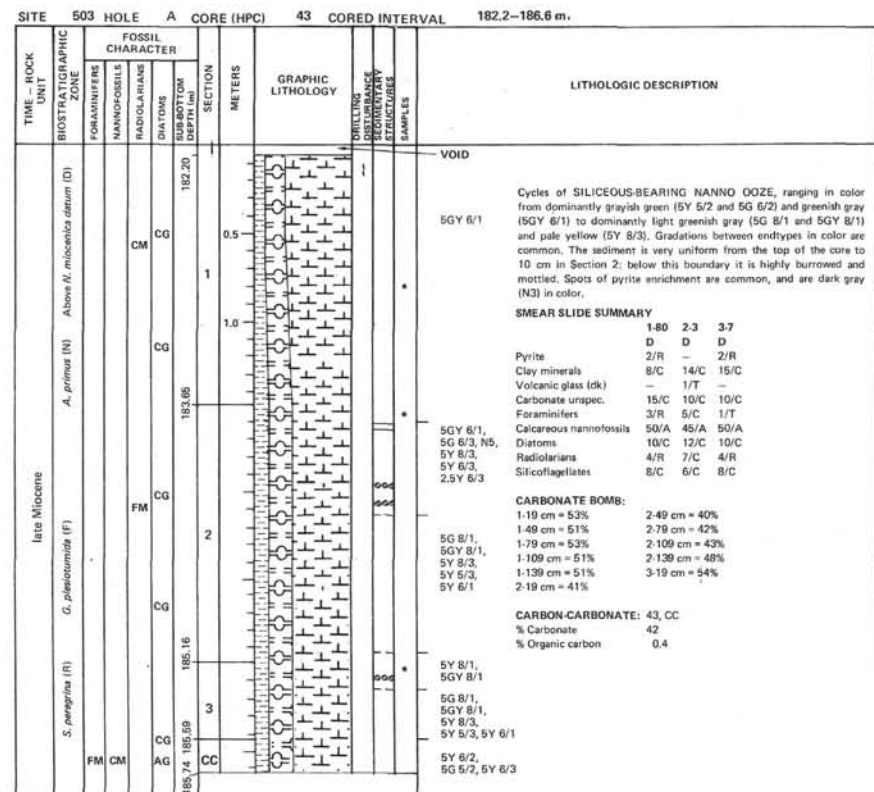
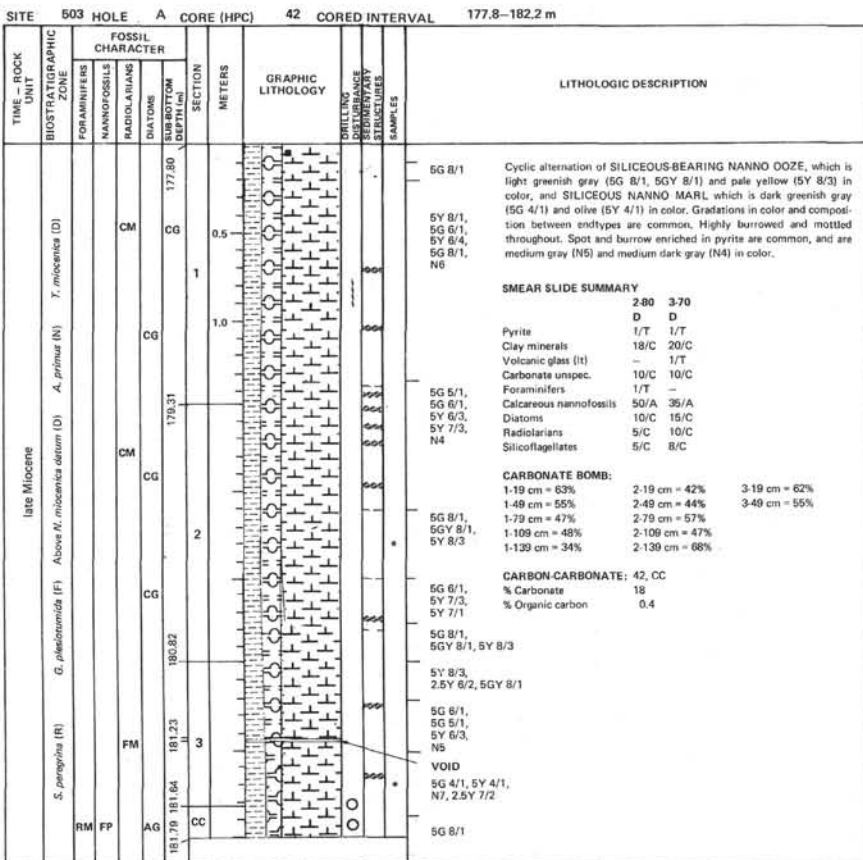


Note: Graphic lithology represents average composition derived from smear slides and does not reflect the detailed alternation of sediment types. Gradational changes between smear slides are arbitrary and do not imply actual lithologic trends. Color variations approximate lithologic changes.

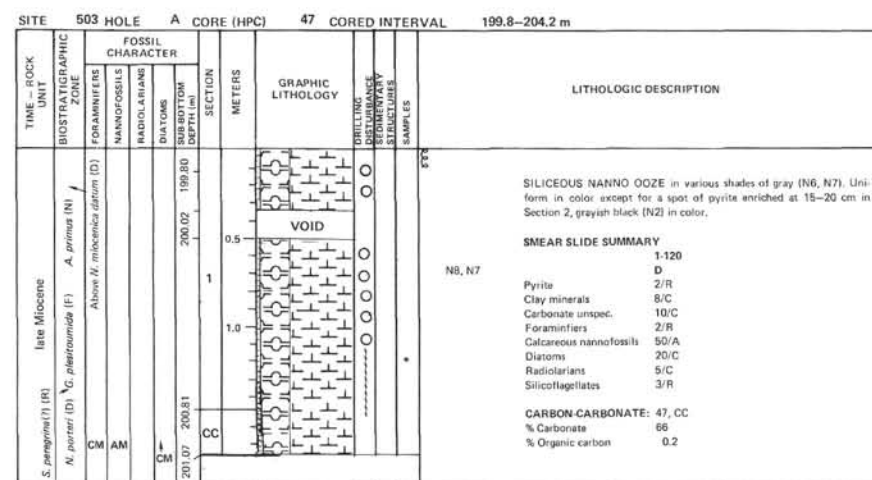
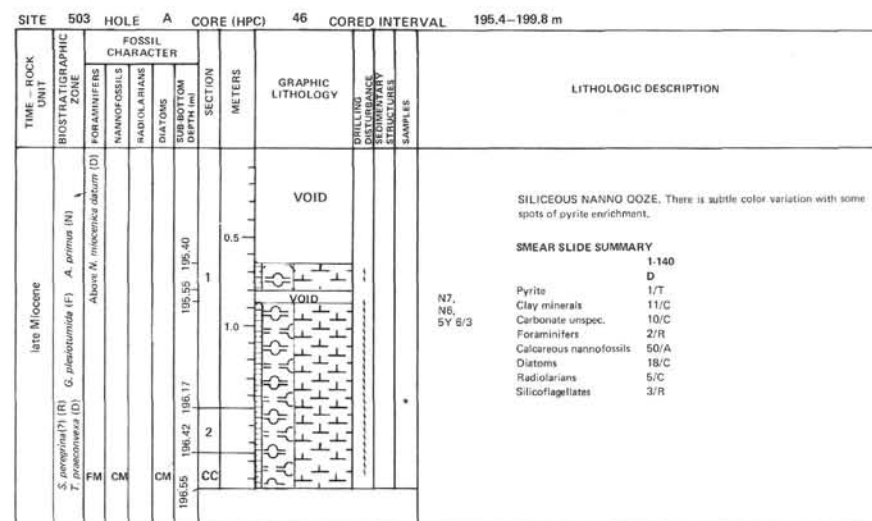
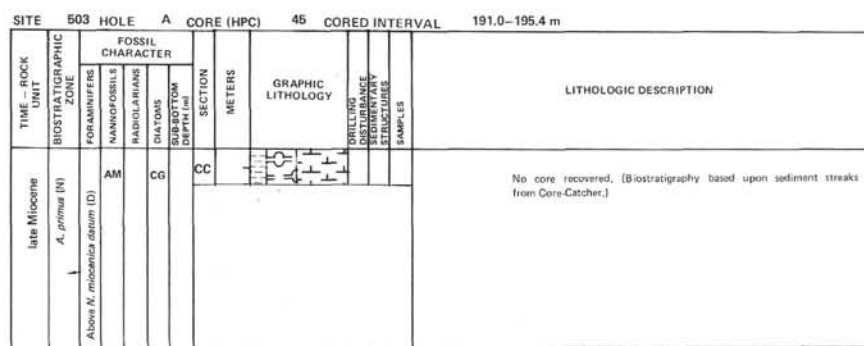
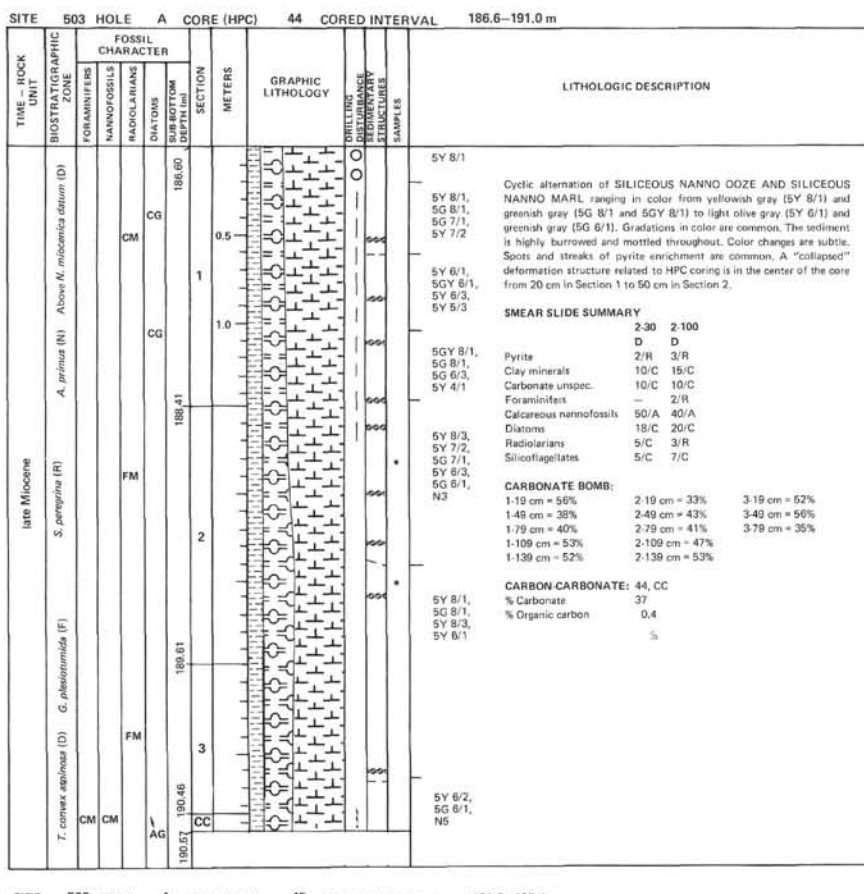




Note: Graphic lithology represents average composition derived from smear slides and does not reflect the detailed alternation of sediment types. Gradational changes between smear slides are arbitrary and do not imply actual lithologic trends. Color variations approximate lithologic changes.



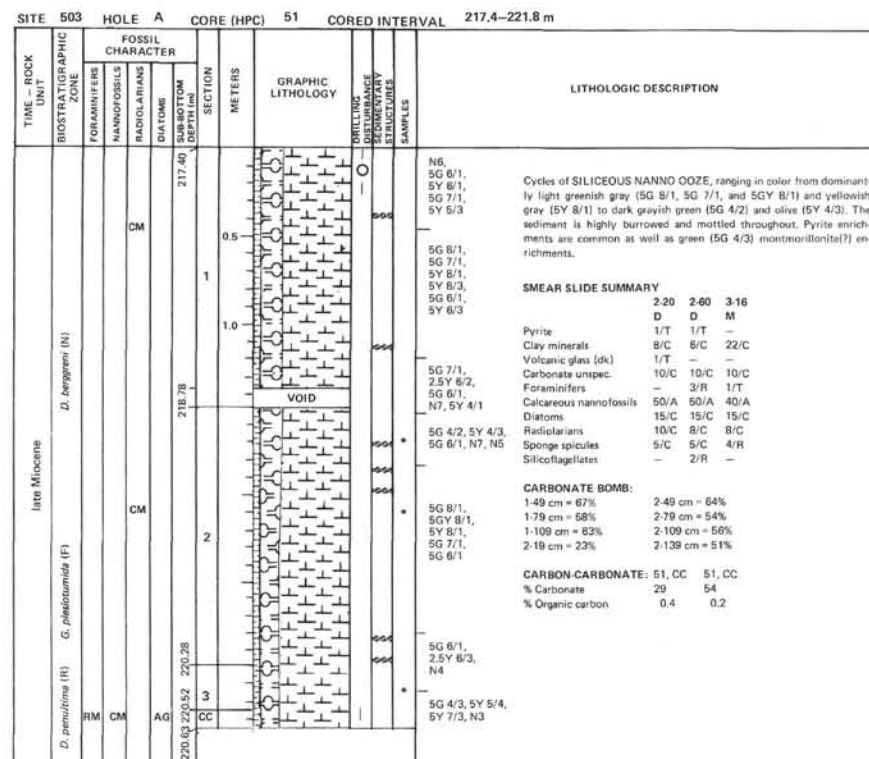
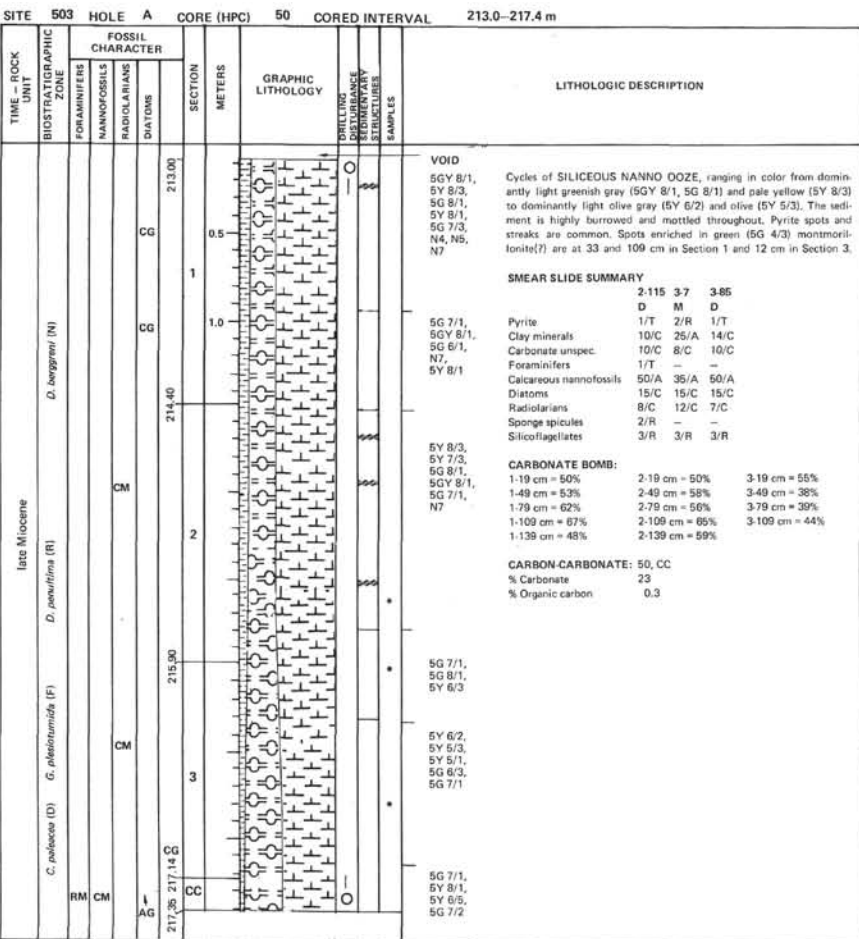
Note: Graphic lithology represents average composition derived from smear slides and does not reflect the detailed alternation of sediment types. Gradational changes between smear slides are arbitrary and do not imply actual lithologic trends. Color variations approximate lithologic changes.



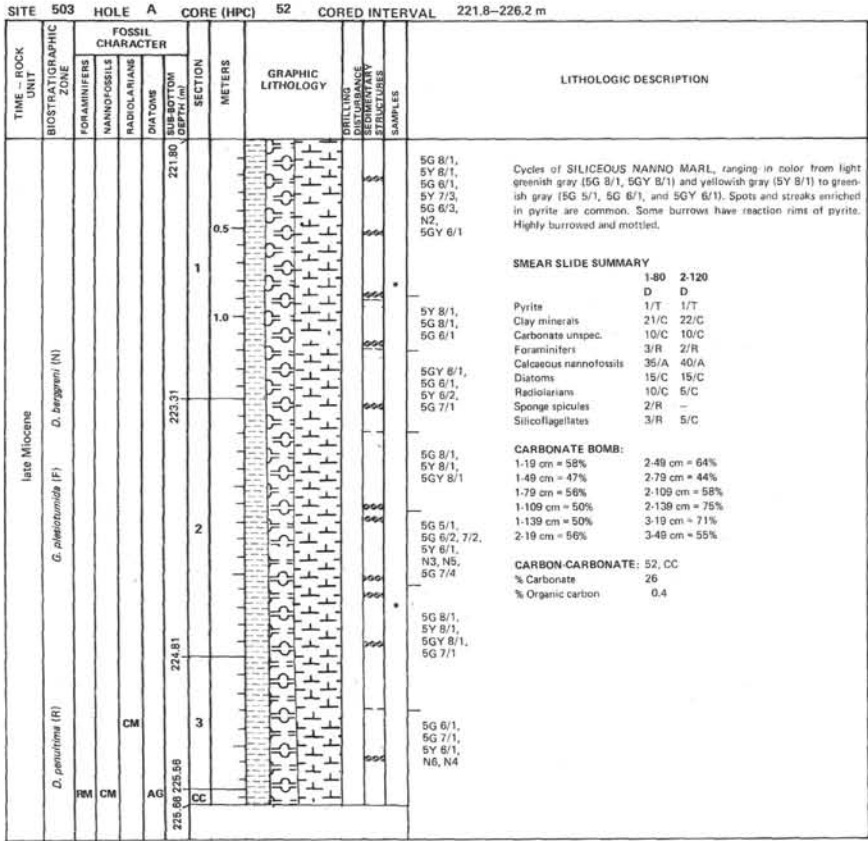
Note: Graphic lithology represents average composition derived from smear slides and does not reflect the detailed alteration of sediment types. Gradational changes between smear slides are arbitrary and do not imply actual lithologic trends. Color variations approximate lithologic changes.

| SITE | TIME - ROCK UNIT | 503 HOLE | A | CORE (HPC) | 48 | CORED INTERVAL | 204.2–208.6 m | LITHOLOGIC DESCRIPTION | | | TIME - ROCK UNIT | 503 HOLE | A | CORE (HPC) | 49 | CORED INTERVAL | 208.6–213.0 m | LITHOLOGIC DESCRIPTION | | | | | | |
|--|--|----------|----|------------|--------|----------------|---------------|---|---|--------|----------------------|--|--|--------------------------|---------------------|----------------|----------------------|--|----|--------|--------|---|----|----|
| | | | | | | | | BIOSTRATIGRAPHIC ZONE | FOSSIL CHARACTER | METERS | GRAPHIC LITHOLOGY | DRILLING DISTURBANCE STRUCTURES SAMPLES | SECTION DIATOMS SUB-BOTTOM METERS | BIOSTRATIGRAPHIC ZONE | FOSSIL CHARACTER | METERS | GRAPHIC LITHOLOGY | DRILLING DISTURBANCE STRUCTURES SAMPLES | | | | | | |
| late Miocene <i>D. pectinatula</i> (F) [D] Above <i>N. miccinica</i> (D) | G. pectinatula (F) A. prima (N) S. marginata (R) | CM | CM | CM | 205.86 | 205.40 | 204.42–204.20 | 5G 8/1, 5Y 8/1, 5GY 8/1, N5, N3, 5G 7/3 | Clay minerals Carbonate unsp. Foraminifers Calcareous nannofossils Diatoms Radiolarians Silicoflagellates | 0.5 | VOID | 1 | CM | CM | 206.60 | 206.60 | 1 | CM | CM | 210.06 | 210.06 | 1 | CM | CM |
| | | CM | CM | CM | 207.85 | 206.90 | 204.42–204.20 | 5G 8/1, 5Y 8/1, 5GY 8/1, N5, N3, 5G 7/3 | Clay minerals Carbonate unsp. Foraminifers Calcareous nannofossils Diatoms Radiolarians Silicoflagellates | 1.0 | VOID | 2 | CM | CM | 210.39 | 210.39 | 2 | CG | CG | 210.56 | 210.56 | 2 | CC | CC |
| | | CM | CM | CM | 207.85 | 207.65 | 204.42–204.20 | 5G 8/1, 5Y 8/1, 5GY 8/1, N5, N3, 5G 7/3 | Clay minerals Carbonate unsp. Foraminifers Calcareous nannofossils Diatoms Radiolarians Silicoflagellates | 1.5 | VOID | 3 | CC | CC | 210.39 | 210.39 | 3 | CC | CC | 210.39 | 210.39 | 3 | CC | CC |
| | | | | | | | | | | | | | | | | | | | | | | | | |
| | | | | | | | | | | | | | | | | | | | | | | | | |

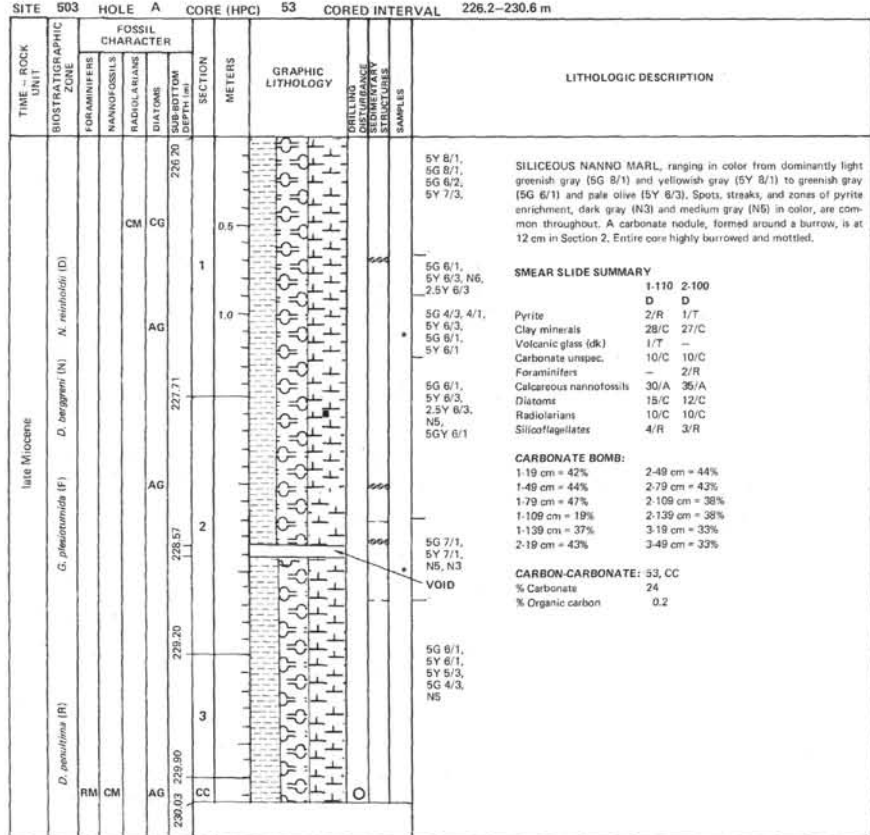
Note: Graphic lithology represents average composition derived from smear slides and does not reflect the detailed alternation of sediment types. Gradational changes between smear slides are arbitrary and do not imply actual lithologic trends. Color variations approximate lithologic changes.

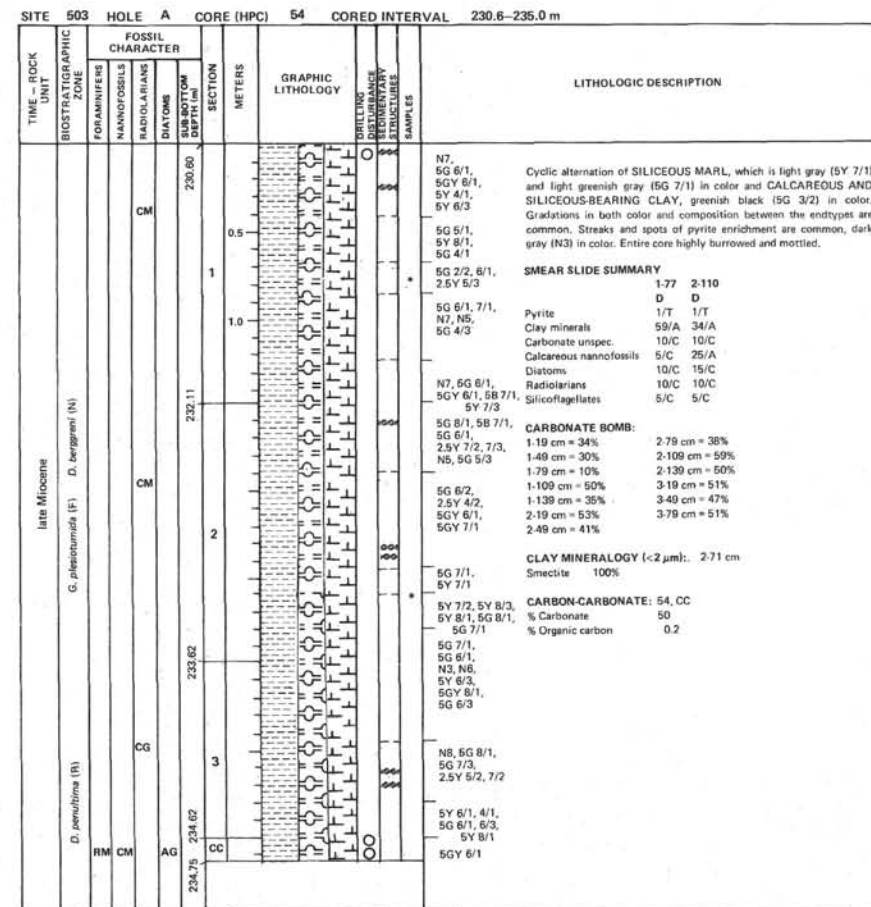


Note: Graphic lithology represents average composition derived from smear slides and does not reflect the detailed alternation of sediment types. Gradational changes between smear slides are arbitrary and do not imply actual lithologic trends. Color variations approximate lithologic changes.

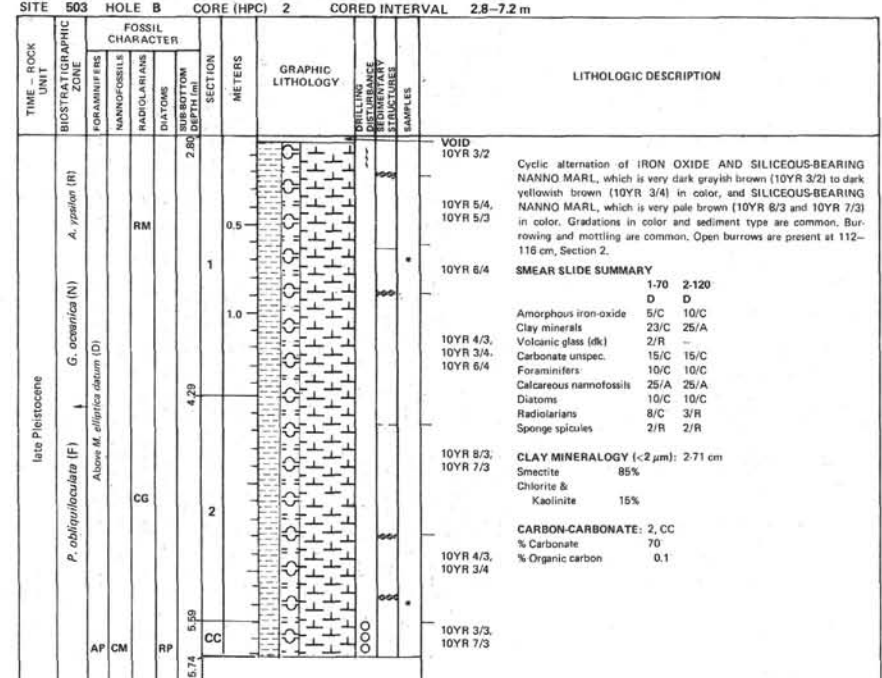
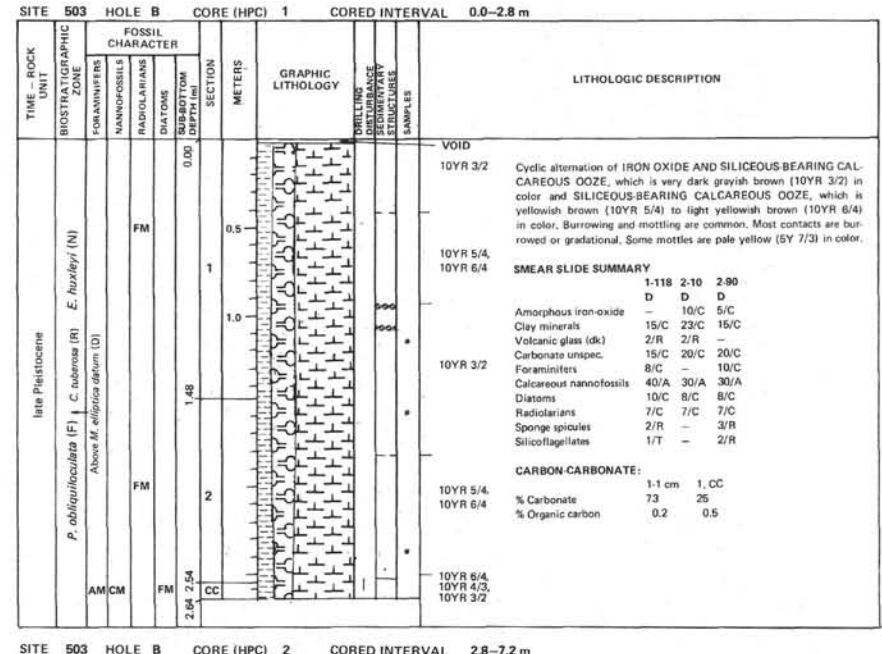


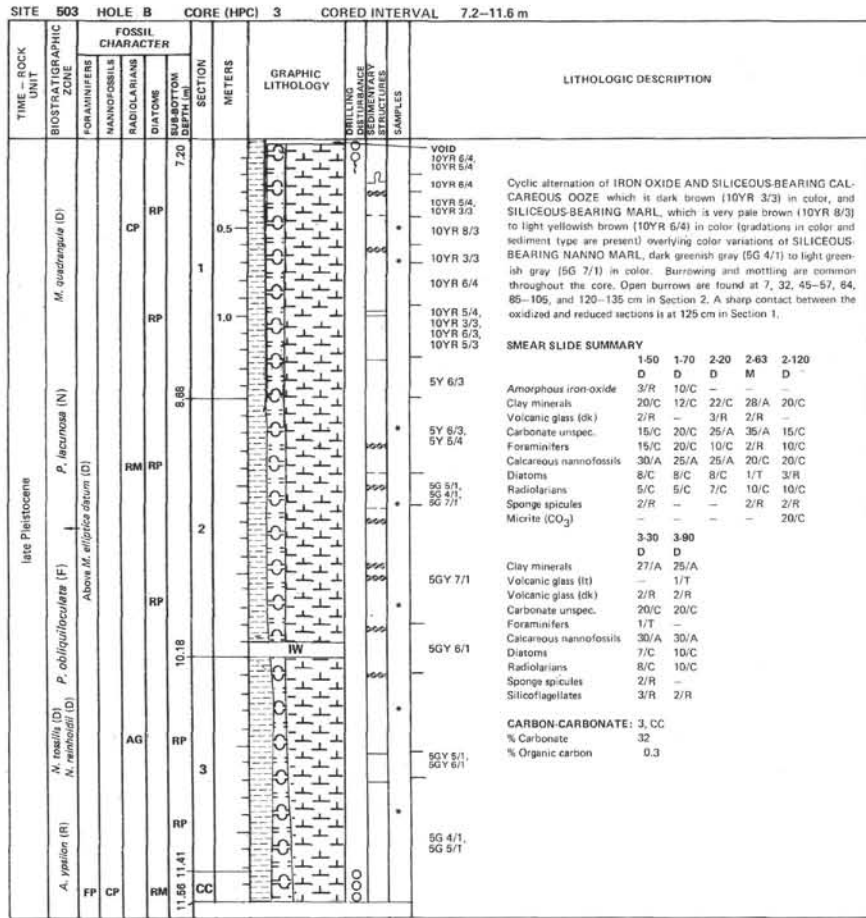
Note: Graphic lithology represents average composition derived from smear slides and does not reflect the detailed alternation of sediment types. Gradational changes between smear slides are arbitrary and do not imply actual lithologic trends. Color variations approximate lithologic changes.



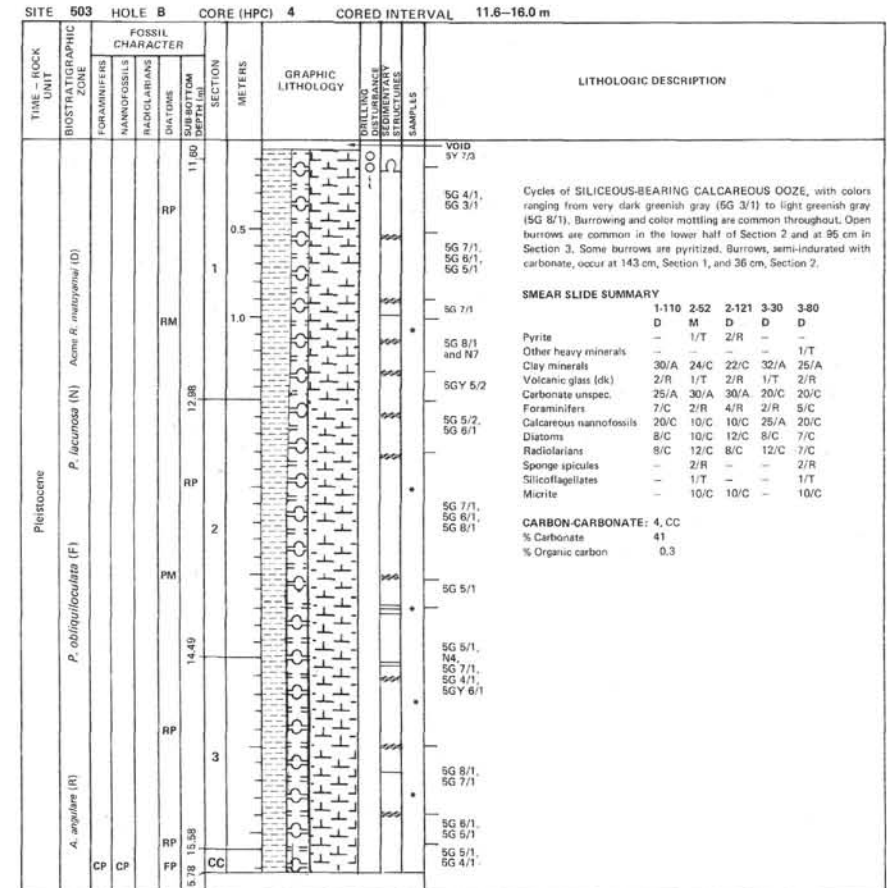


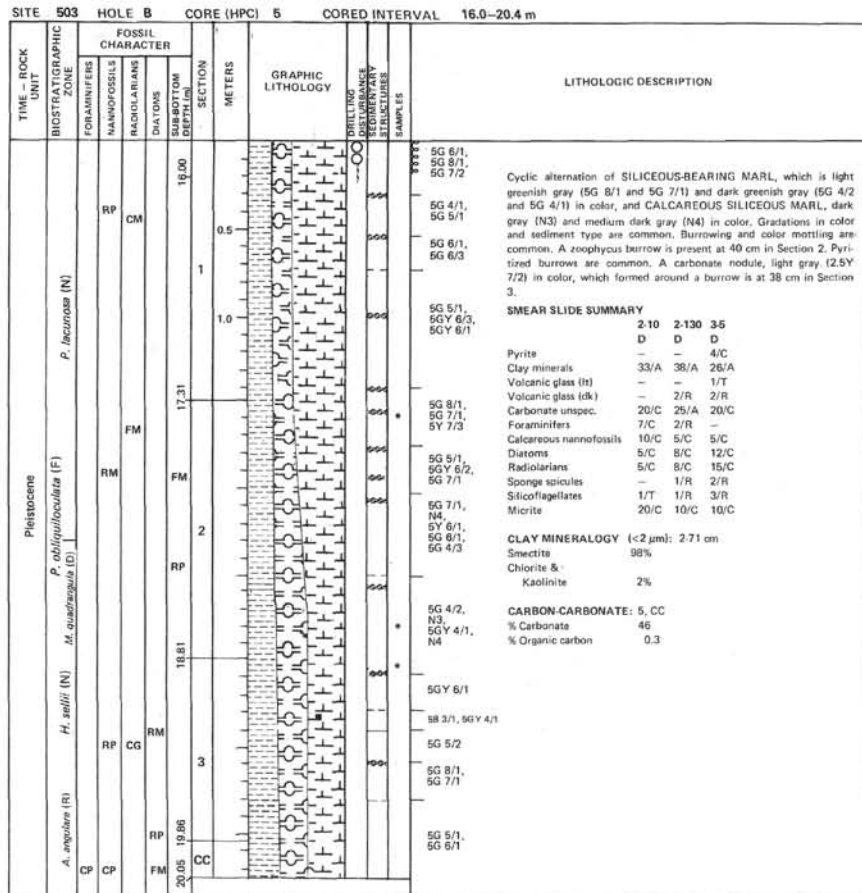
Note: Graphic lithology represents average composition derived from smear slides and does not reflect the detailed alternation of sediment types. Gradational changes between smear slides are arbitrary and do not imply actual lithologic trends. Color variations approximate lithologic changes.



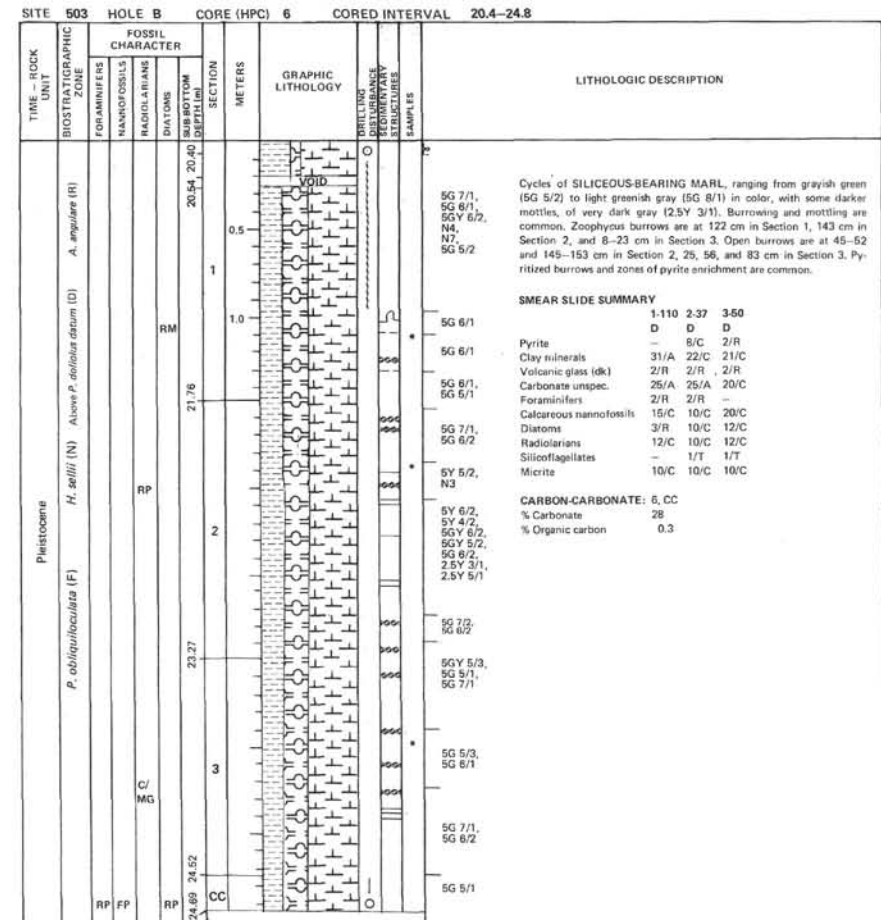


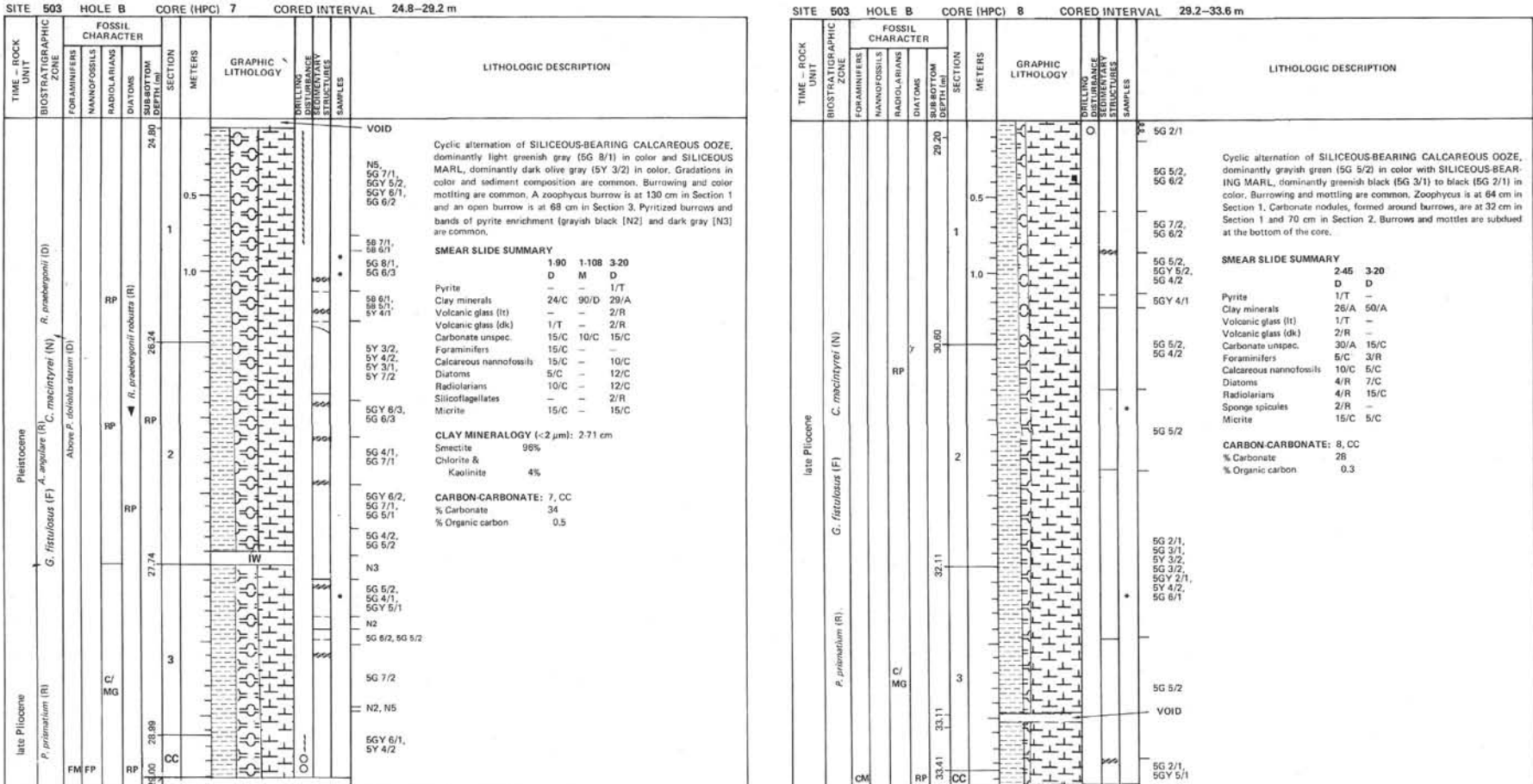
Note: Graphic lithology represents average composition derived from smear slides and does not reflect the detailed alternation of sediment types. Gradational changes between smear slides are arbitrary and do not imply actual lithologic trends. Color variations approximate lithologic changes.



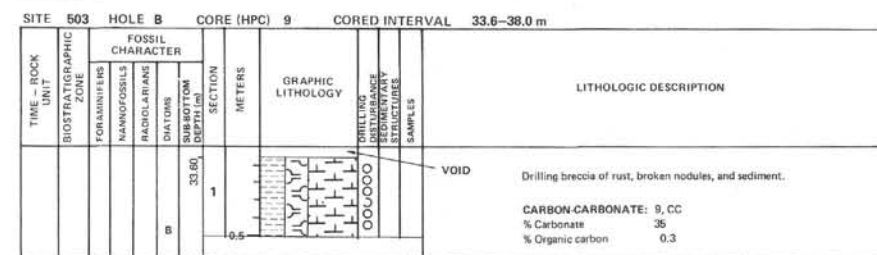
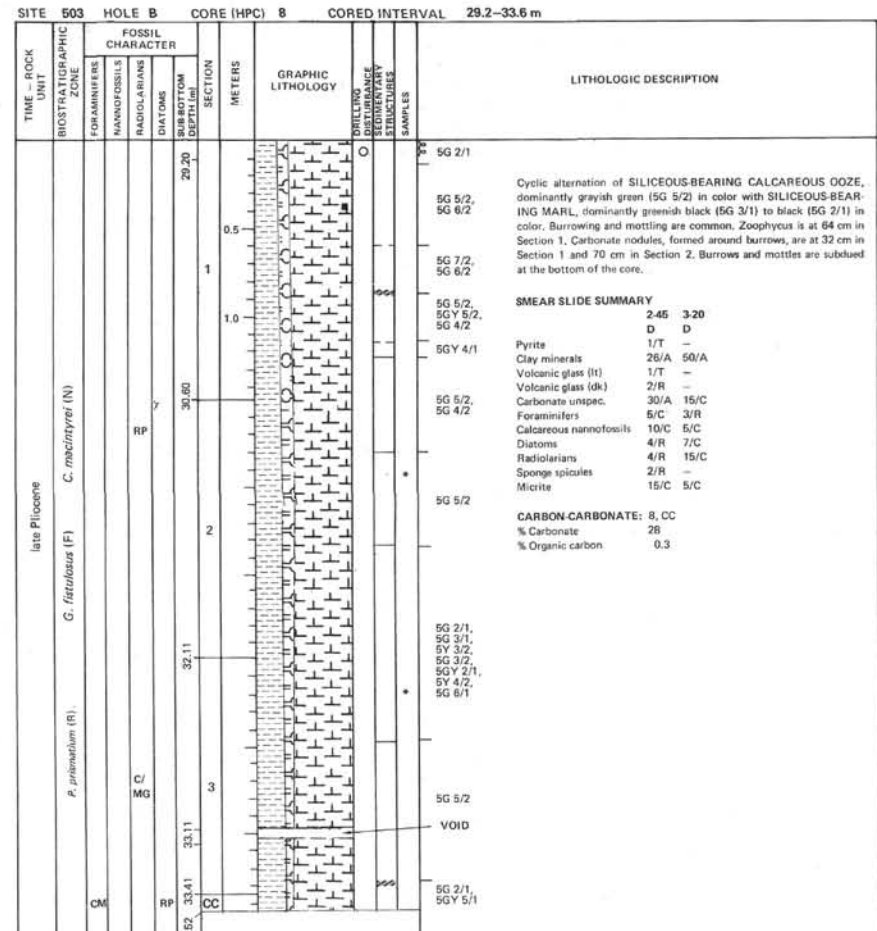


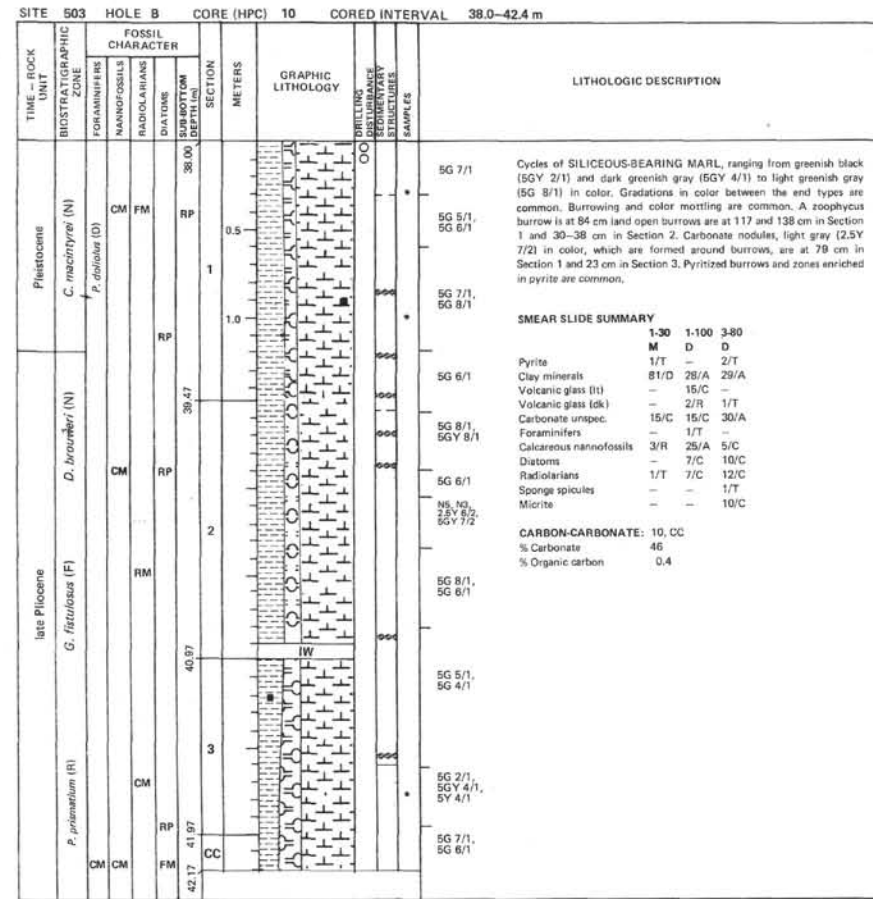
Note: Graphic lithology represents average composition derived from smear slides and does not reflect the detailed alternation of sediment types. Gradational changes between smear slides are arbitrary and do not imply actual lithologic trends. Color variations approximate lithologic changes.



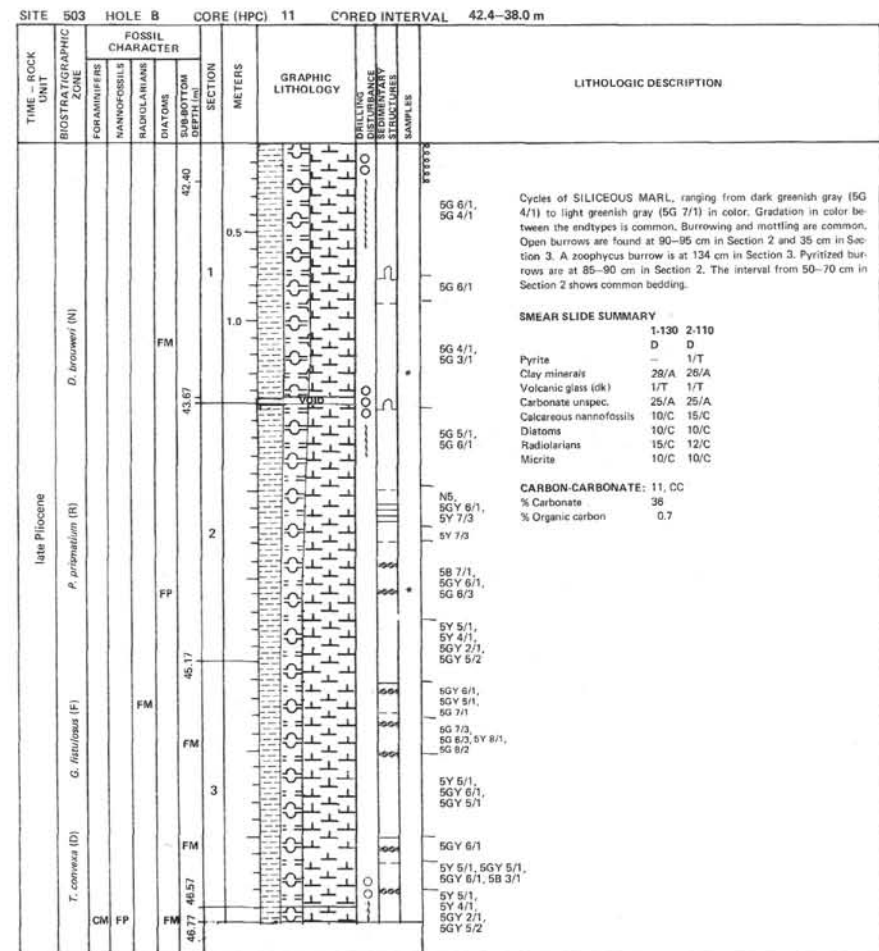


Note: Graphic lithology represents average composition derived from smear slides and does not reflect the detailed alternation of sediment types. Gradational changes between smear slides are arbitrary and do not imply actual lithologic trends. Color variations approximate lithologic changes.





Note: Graphic lithology represents average composition derived from smear slides and does not reflect the detailed alternation of sediment types. Gradational changes between smear slides are arbitrary and do not imply actual lithologic trends. Color variations approximate lithologic changes.



| TIME/ROCK UNIT | 503 | HOLE | B | CORE (HPC) | 12 | CORED INTERVAL | 46.8–51.2 m | LITHOLOGIC DESCRIPTION | | | | | | | | | | |
|------------------------------------|-------------------|--------------------|--------------|------------|--------------------|----------------|-------------|---|----------|-------------|--------|-------------------|----------|-------------|--------|-------------------|----------|-------------|
| | | | | | | | | FOSSIL CHARACTER | DRILLING | SUB-SAMPLES | METERS | GRAPHIC LITHOLOGY | DRILLING | SUB-SAMPLES | METERS | GRAPHIC LITHOLOGY | DRILLING | SUB-SAMPLES |
| BIOSTRATIGRAPHIC ZONE | FORAMINIFERS | NANNOFOSILS | RADIOLARIANS | DIATOMS | SUBBOTOM DEPTH (m) | SECTION | | 1 | 1 | 1 | 1 | 1 | 1 | 1 | 1 | 1 | 1 | 1 |
| late Pliocene | | | | | | | | | | | | | | | | | | |
| P. primatum [R] | G. reticulata [F] | D. pentodontus [N] | | | | | | | | | | | | | | | | |
| Above N. jousseaumii [D] | | | | | | | | | | | | | | | | | | |
| FP | FM | | | | | | | | | | | | | | | | | |
| | FP | FM | | | | | | | | | | | | | | | | |
| | AG | | | | | | | | | | | | | | | | | |
| FP | FM | | | | | | | | | | | | | | | | | |
| 50.82 | 50.67 | 50.44 | 3 | | 49.90 | | | | | | | | | | | | | |
| CC | CC | CC | | | | | | | | | | | | | | | | |
| 50.82 | 50.67 | 50.44 | 3 | | 49.90 | | | | | | | | | | | | | |
| 5Y 4/2, 4/3, 5Y 6/1, 5GY 6/1 | | | | | | | | 5Y 4/2, 4/3, 5Y 6/1, 5GY 6/1 | | | | | | | | | | |
| | | | | | | | | 5Y 5/1, 5Y 6/1, N3 | | | | | | | | | | |
| | | | | | | | | 5Y 6/2 | | | | | | | | | | |
| | | | | | | | | SGY 8/1, N4, 5G 7/1, N5 5Y 4/2, 5G 4/1, 5GY 6/1, 5G 5/1, 5GY 5/1, 5G 2/1 VOID | | | | | | | | | | |
| | | | | | | | | 5Y 4/1, 5Y 3/1 | | | | | | | | | | |

Note: Graphic lithology represents average composition derived from smear slides and does not reflect the detailed alternation of sediment types. Gradational changes between smear slides are arbitrary and do not imply actual lithologic trends. Color variations approximate lithologic changes.

| TIME/ROCK UNIT | 503 | HOLE | B | CORE (HPC) | 13 | CORED INTERVAL | 51.2–55.6 m | LITHOLOGIC DESCRIPTION | | | | | | | | | | |
|-----------------------|-------------------|--------------------|--------------|------------|--------------------|----------------|-------------|------------------------|----------|-------------|--------|-------------------|----------|-------------|--------|-------------------|----------|-------------|
| | | | | | | | | FOSSIL CHARACTER | DRILLING | SUB-SAMPLES | METERS | GRAPHIC LITHOLOGY | DRILLING | SUB-SAMPLES | METERS | GRAPHIC LITHOLOGY | DRILLING | SUB-SAMPLES |
| BIOSTRATIGRAPHIC ZONE | FORAMINIFERS | NANNOFOSILS | RADIOLARIANS | DIATOMS | SUBBOTOM DEPTH (m) | SECTION | | 1 | 1 | 1 | 1 | 1 | 1 | 1 | 1 | 1 | 1 | 1 |
| late Pliocene | | | | | | | | | | | | | | | | | | |
| P. carinatum [H] | G. reticulata [F] | D. pentodontus [N] | | | | | | | | | | | | | | | | |
| FP | FM | | | | | | | D. pentodontus [N] | | | | | | | | | | |
| | CM | | | | | | | FM | | | | | | | | | | |
| | CM | | | | | | | CM | | | | | | | | | | |
| | FM | | | | | | | FM | | | | | | | | | | |
| 54.90 | 54.70 | 54.5 | 3 | | 54.15 | | | | | | | | | | | | | |
| CC | CC | CC | | | | | | | | | | | | | | | | |
| 5G 7/1, 6/1, 5/1, N6 | | | | | | | | IV | | | | | | | | | | |
| | | | | | | | | | | | | | | | | | | |
| | | | | | | | | | | | | | | | | | | |
| | | | | | | | | | | | | | | | | | | |
| | | | | | | | | | | | | | | | | | | |
| | | | | | | | | | | | | | | | | | | |
| | | | | | | | | | | | | | | | | | | |
| | | | | | | | | | | | | | | | | | | |
| | | | | | | | | | | | | | | | | | | |

Cycles of SILICEOUS MARL, which is light greenish gray (5GY 8/1, 5G 8/1, and 5G 7/1), olive gray (5Y 4/2), and dark olive gray (5Y 3/2) in color. Graftations in color are common. Burrowing and color mottling are common. Carbonate nodules, light gray (2.5Y 7/2) in color, formed around burrows, are at 80–90 and 106 cm in Section 2. A zoophytes burrow is at 105–111 cm in Section 2. Areas of pyrite enrichment are common.

SMEAR SLIDE SUMMARY

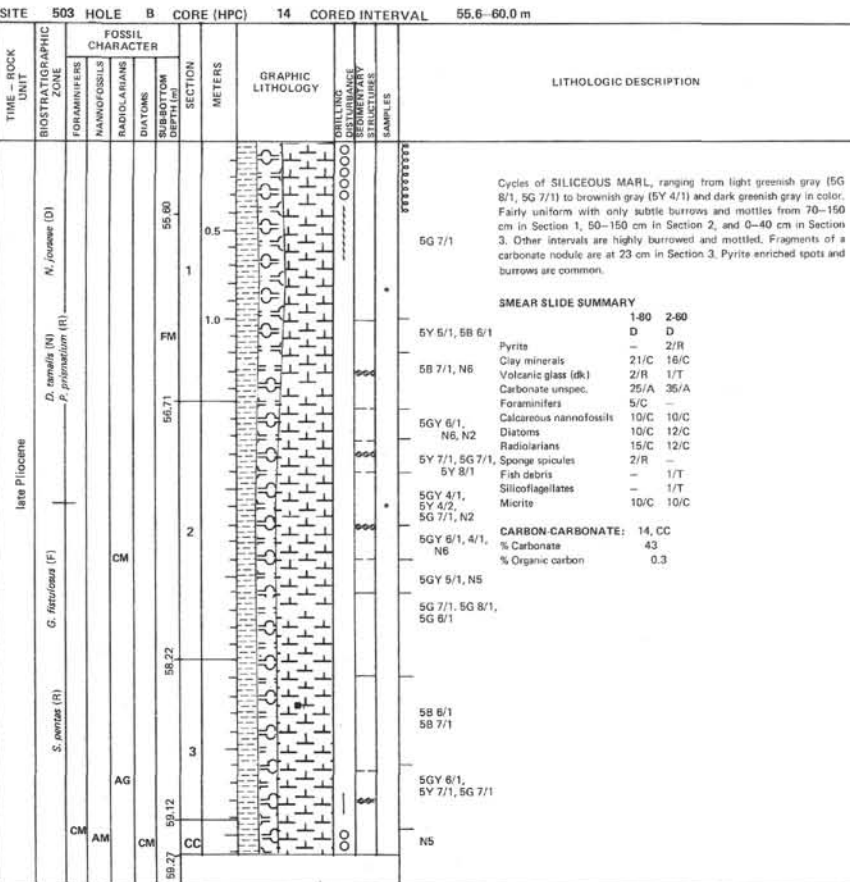
| | | | |
|-------------------------|-------|-------|------|
| 1-72 | 1-109 | 1-145 | 2-56 |
| M | M | D | D |
| 2/R | 2/R | — | 1/T |
| Clay minerals | 26/A | 16/C | 30/A |
| Volcanic glass (dk) | 2/R | 2/R | 1/T |
| Carbonate unspc. | 20/C | 25/A | 30/A |
| Foraminifers | — | 5/C | 1/T |
| Calcareous nannofossils | 10/C | 15/C | 9/C |
| Diatoms | 15/C | 5/C | 12/C |
| Radiolarians | 15/C | 15/C | 12/C |
| Sponge spicules | 1/T | — | 1/T |
| Fish debris | — | — | 1/T |
| Micrite | 10/C | 15/C | 10/C |

CLAY MINERALOGY (<2 µm): 2.71 cm

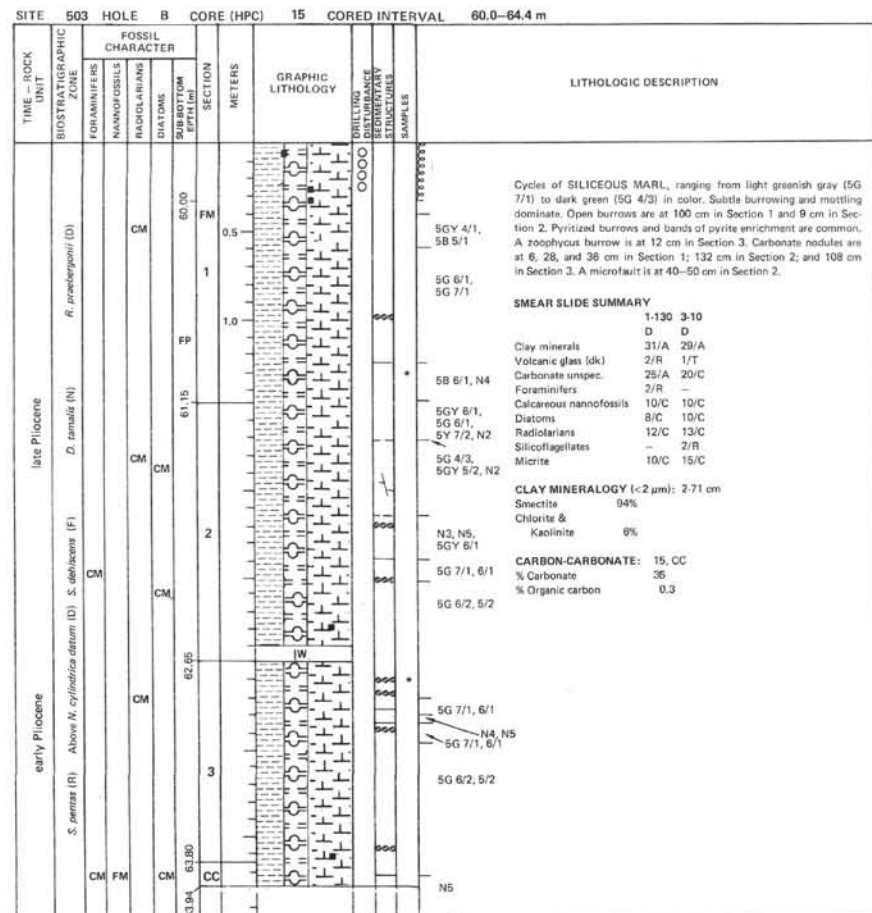
| | |
|-------------------------|-----|
| Smectite | 95% |
| Chlorite & Kaolinite | 5% |

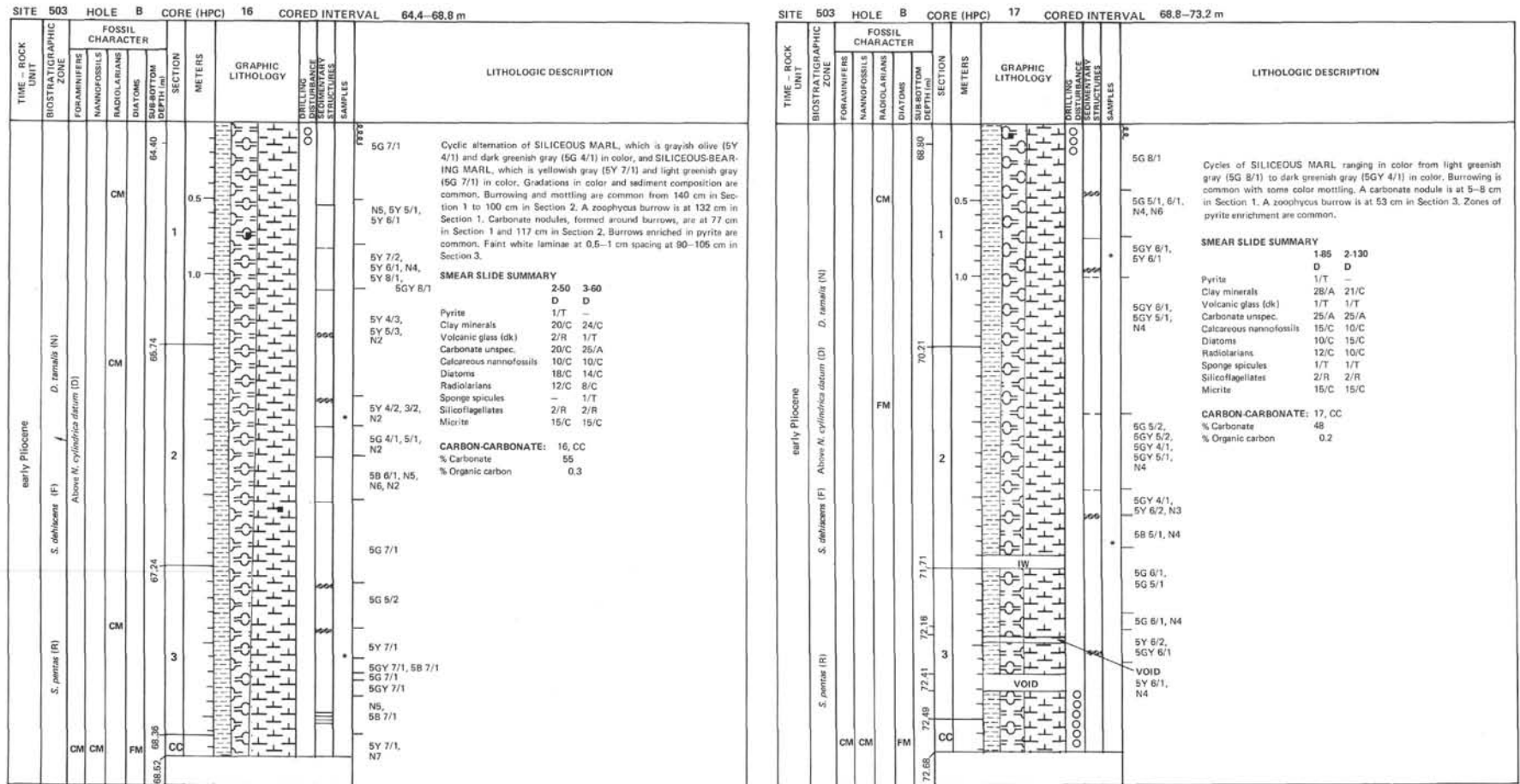
CARBON-CARBONATE: 13, CC
% Carbonate 46
% Organic carbon 0.3

N4, N5
5GY 5/1
5GY 6/1
5G 7/1, 6/1, 8/1, N6

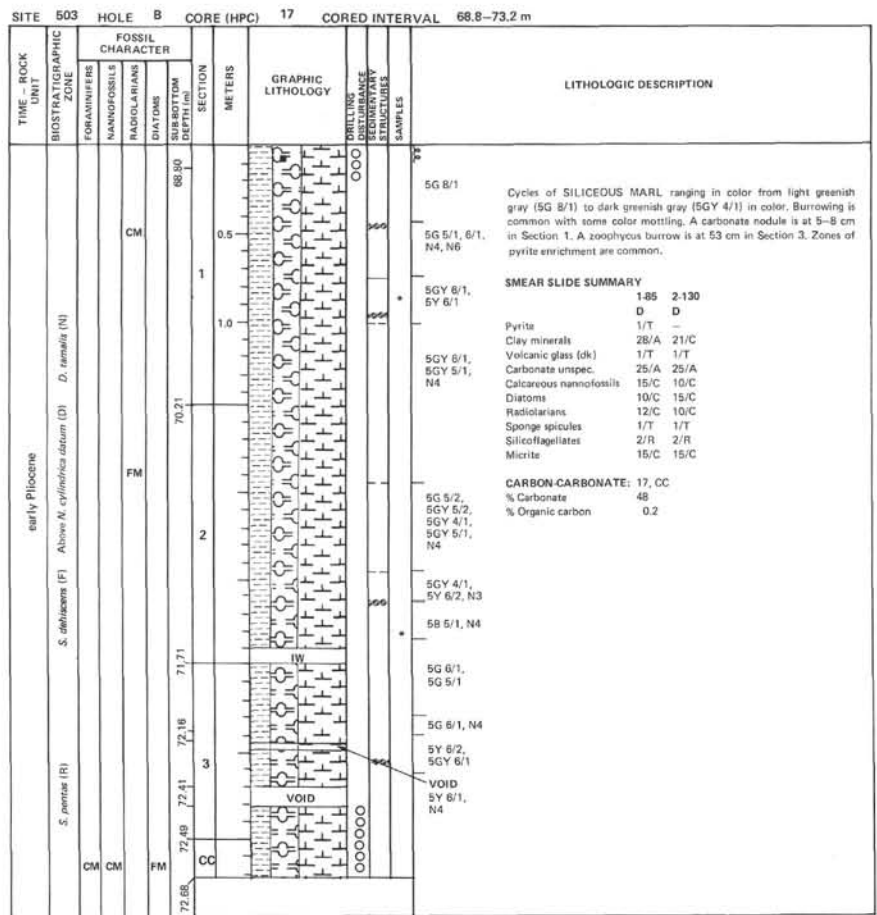


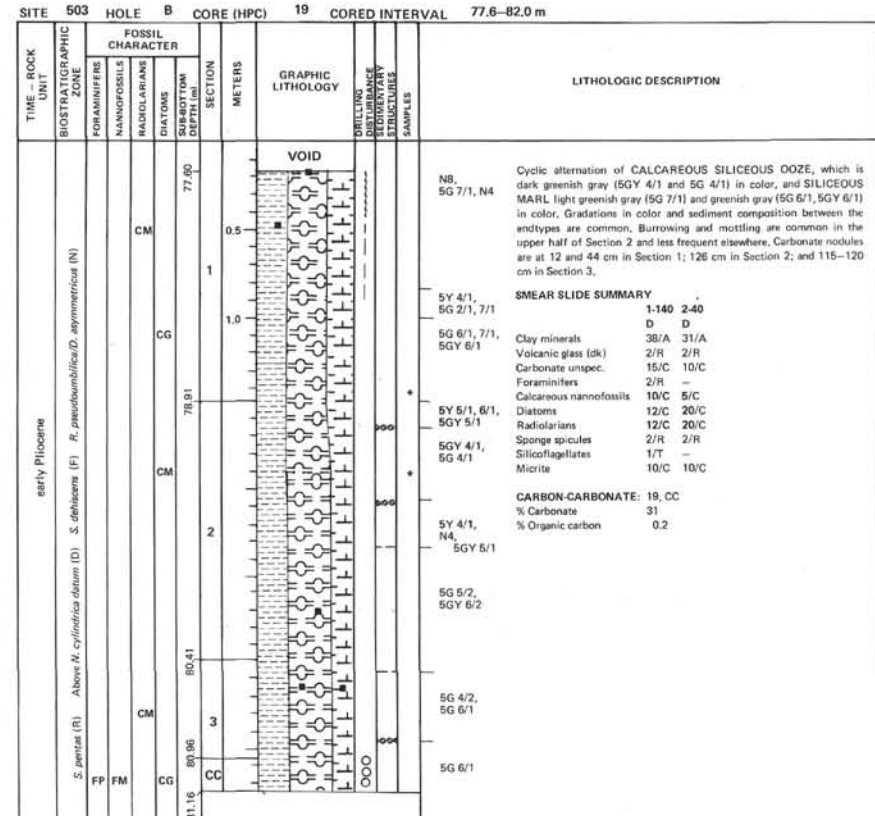
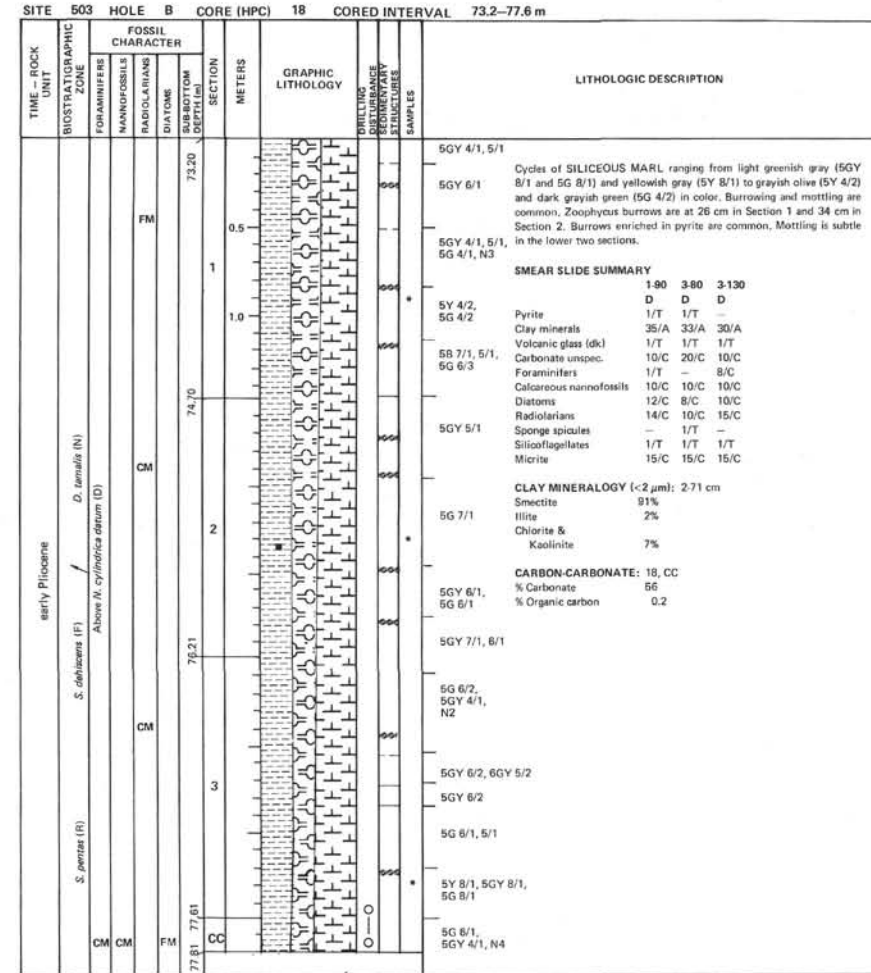
Note: Graphic lithology represents average composition derived from smear slides and does not reflect the detailed alternation of sediment types. Gradational changes between smear slides are arbitrary and do not imply actual lithologic trends. Color variations approximate lithologic changes.



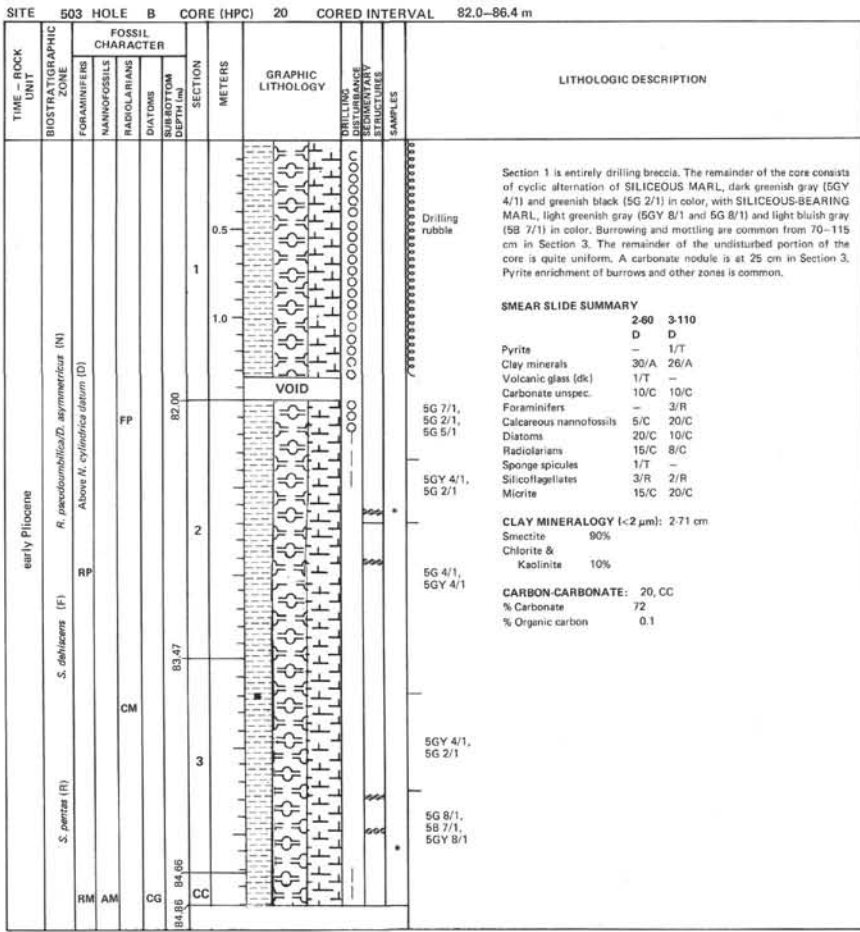


Note: Graphic lithology represents average composition derived from smear slides and does not reflect the detailed alternation of sediment types. Gradational changes between smear slides are arbitrary and do not imply actual lithologic trends. Color variations approximate lithologic changes.

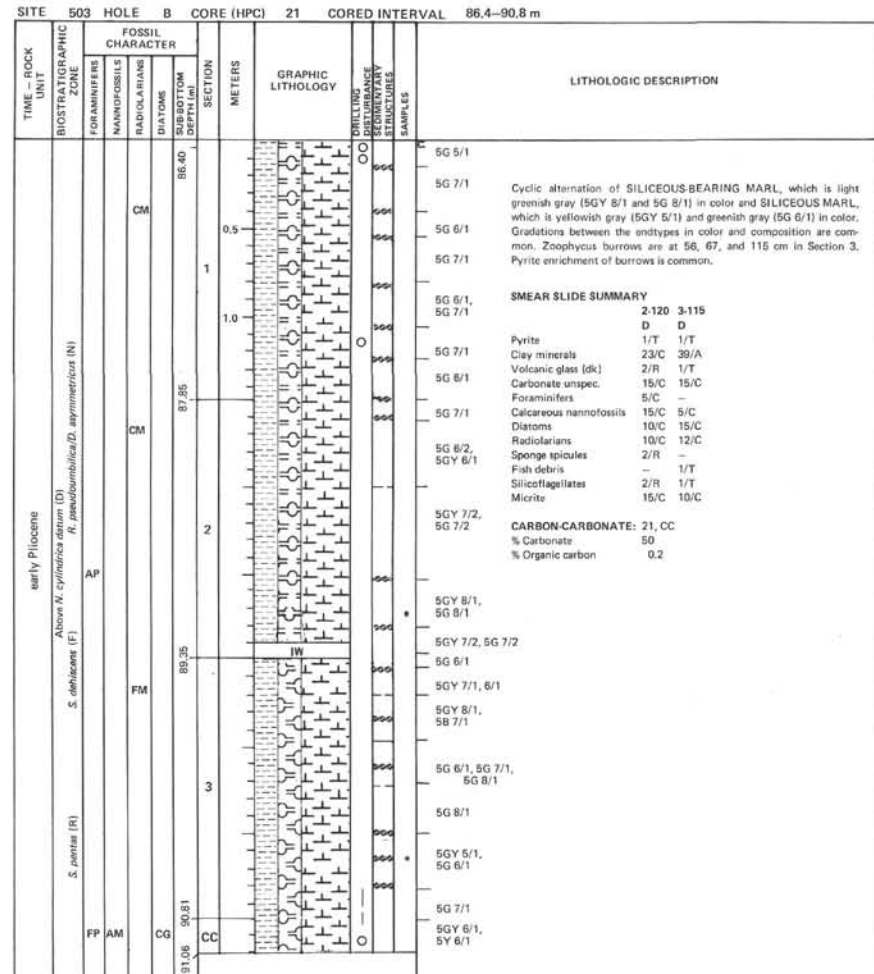


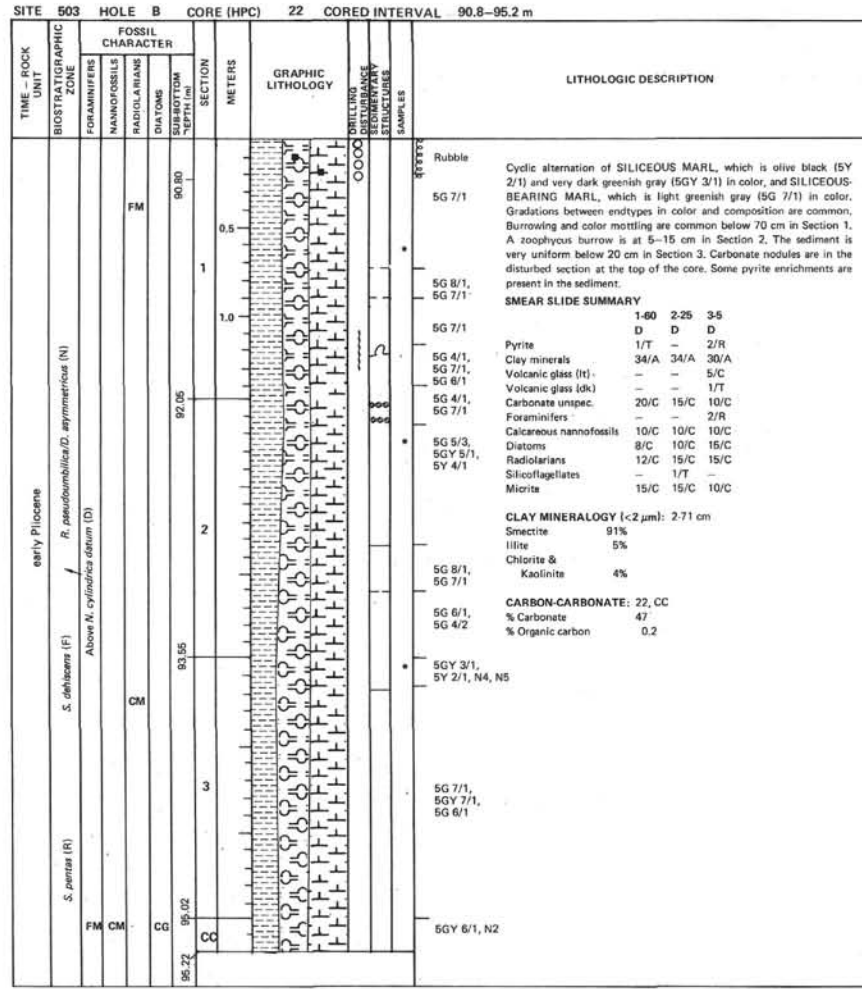


Note: Graphic lithology represents average composition derived from smear slides and does not reflect the detailed alternation of sediment types. Gradational changes between smear slides are arbitrary and do not imply actual lithologic trends. Color variations approximate lithologic changes.

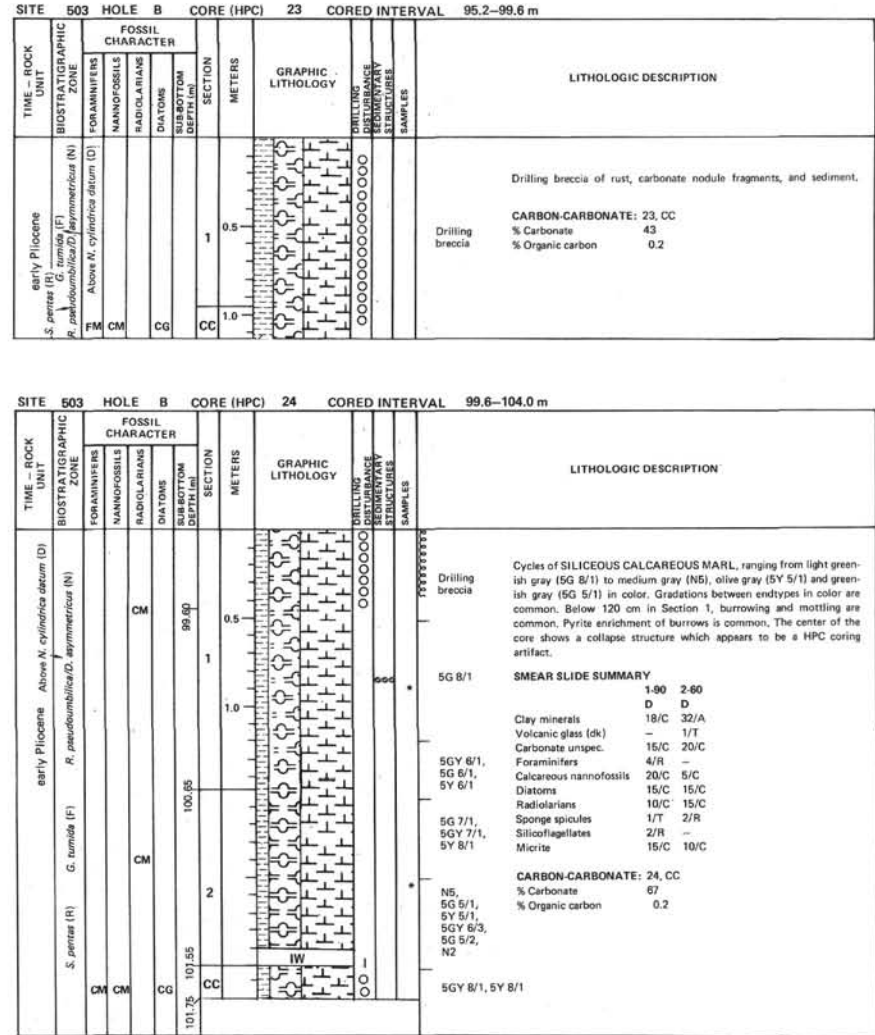


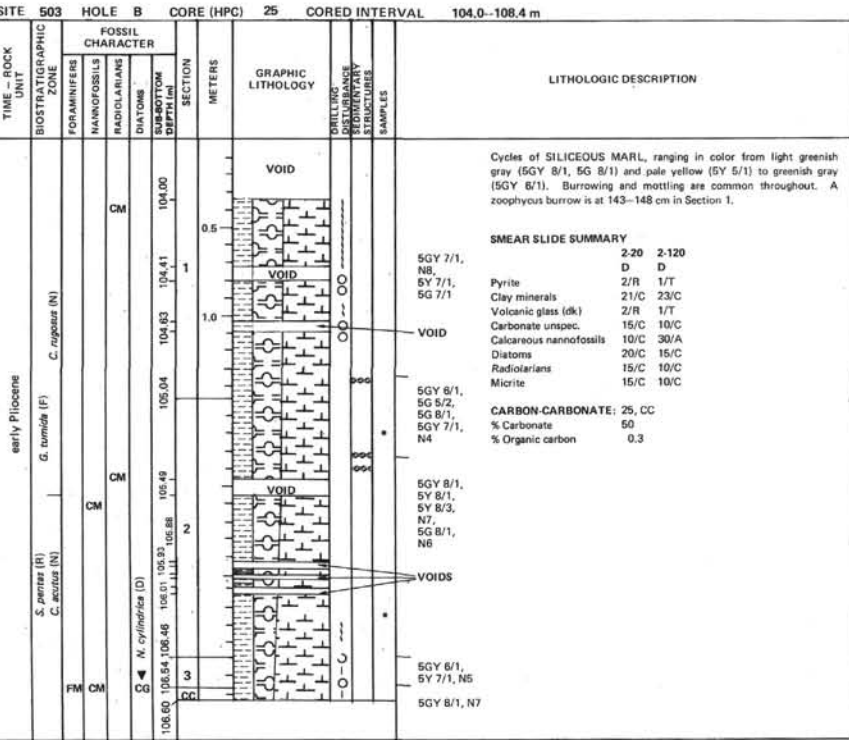
Note: Graphic lithology represents average composition derived from smear slides and does not reflect the detailed alternation of sediment types. Gradational changes between smear slides are arbitrary and do not imply actual lithologic trends. Color variations approximate lithologic changes.



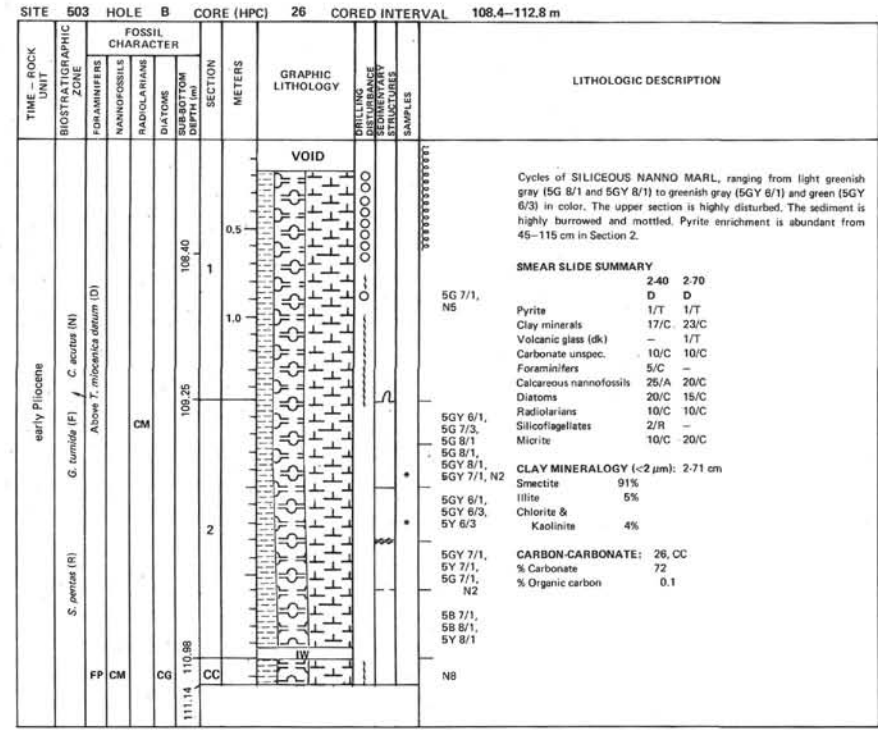


Note: Graphic lithology represents average composition derived from smear slides and does not reflect the detailed alternation of sediment types. Gradational changes between smear slides are arbitrary and do not imply actual lithologic trends. Color variations approximate lithologic changes.

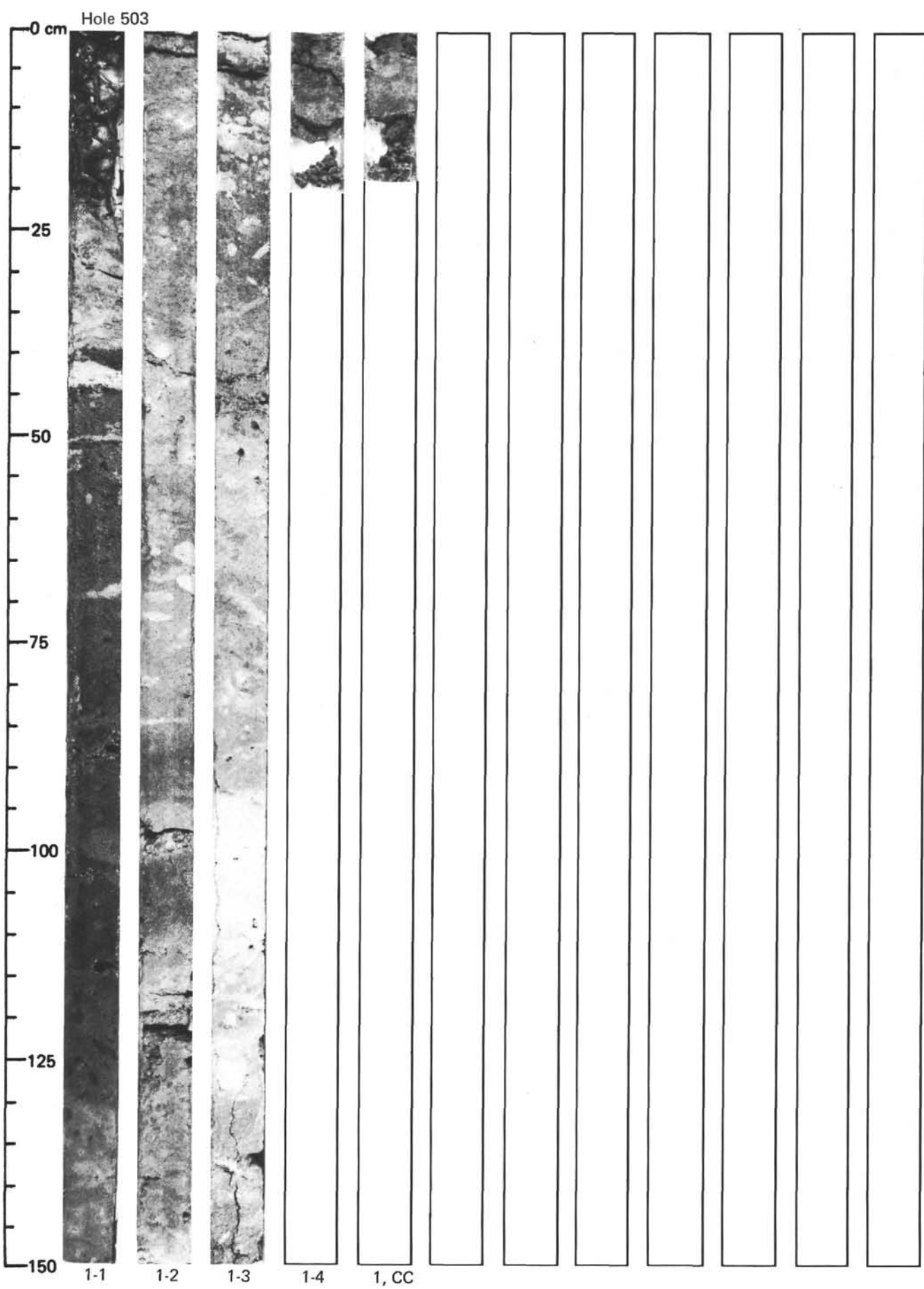


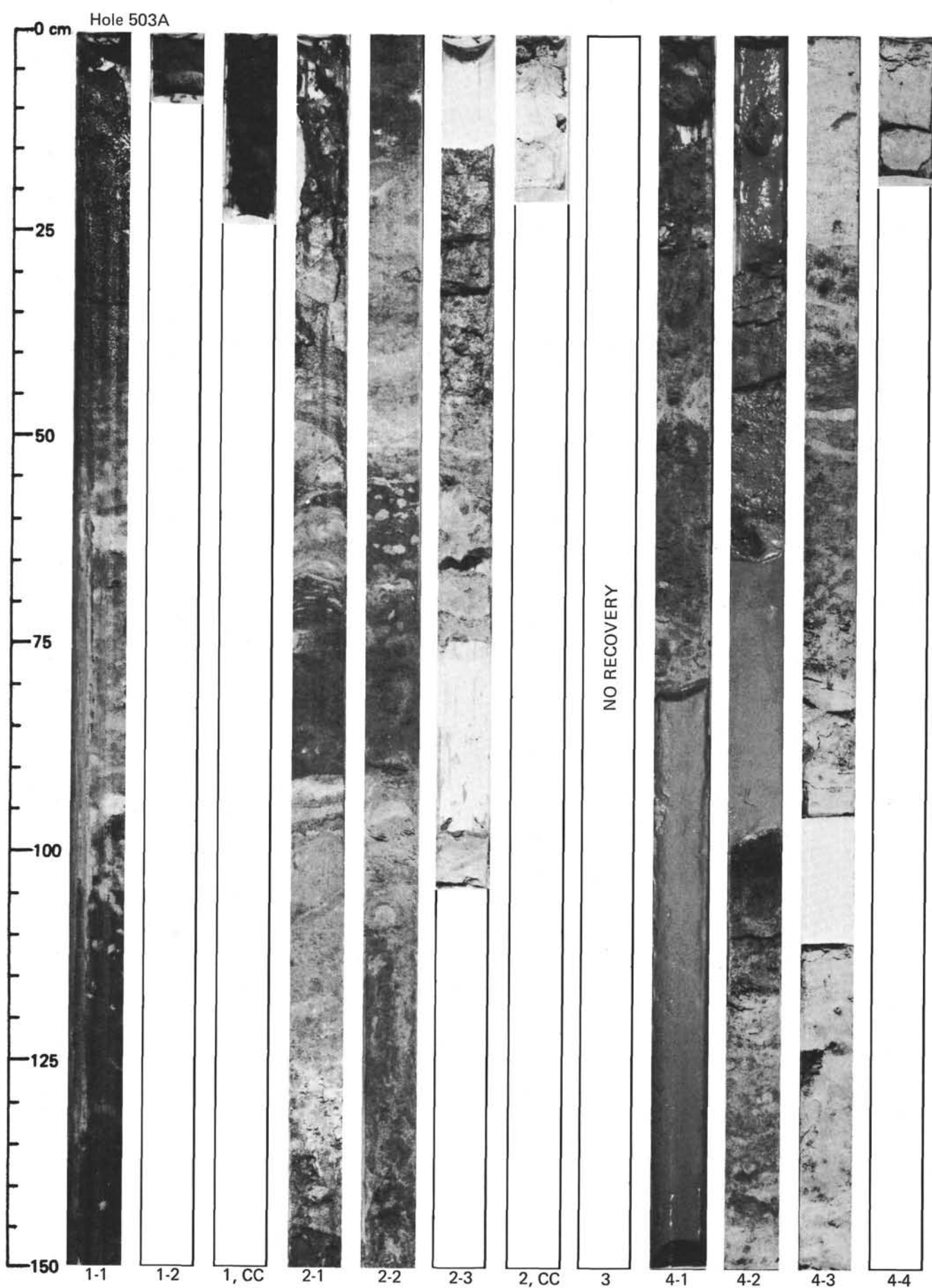


Note: Graphic lithology represents average composition derived from smear slides and does not reflect the detailed alternation of sediment types. Gradational changes between smear slides are arbitrary and do not imply actual lithologic trends. Color variations approximate lithologic changes.

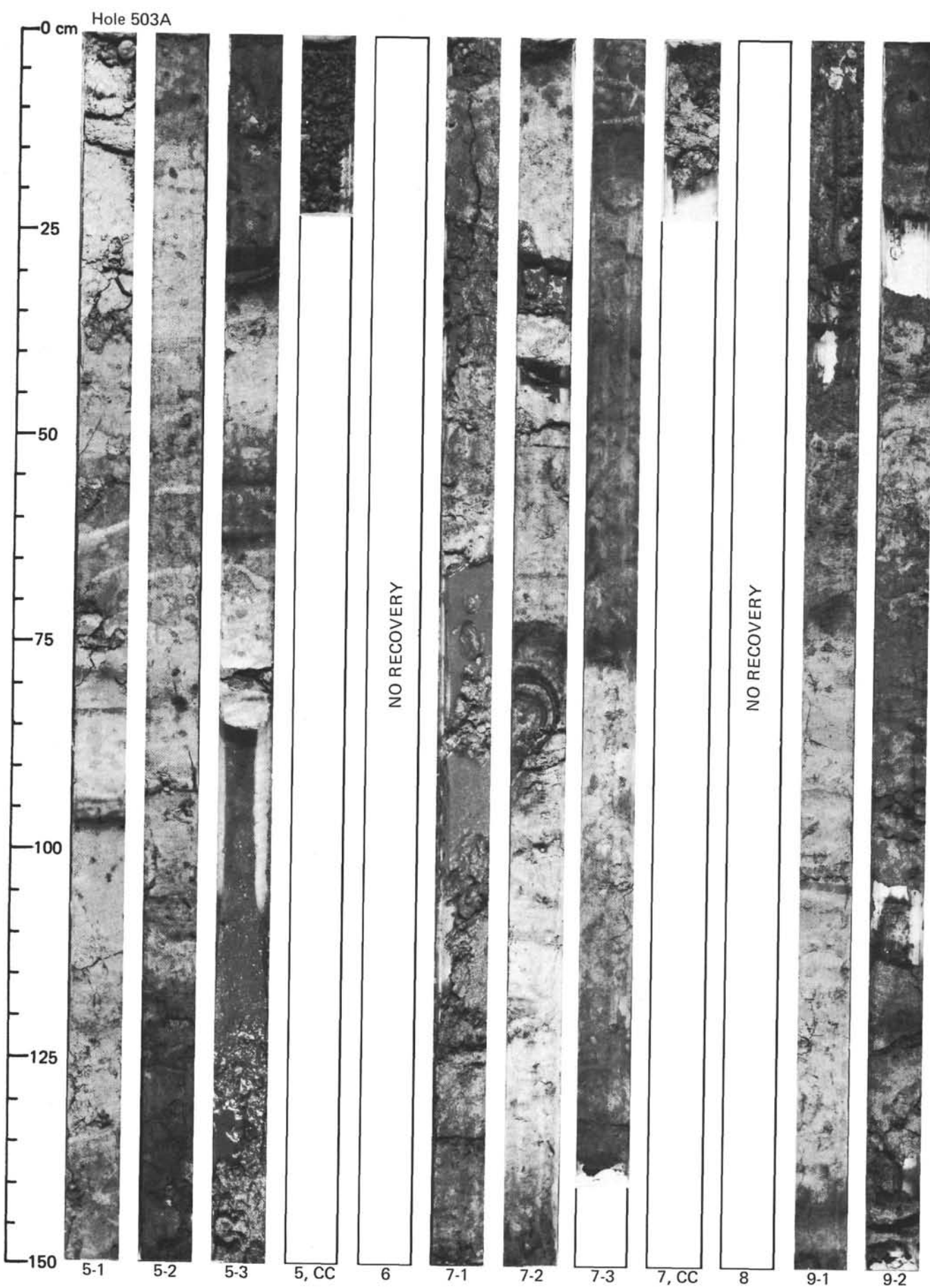


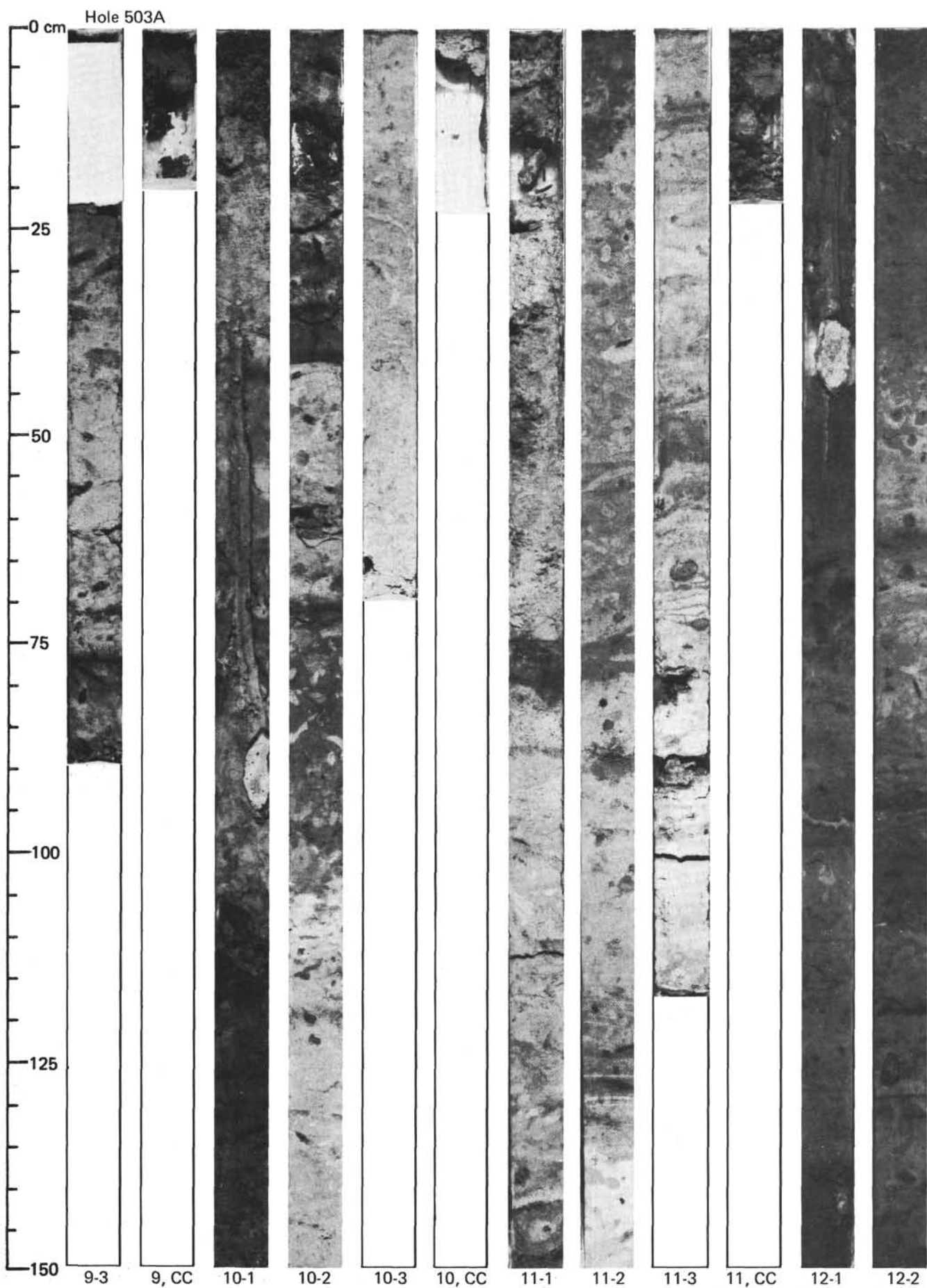
SITE 503

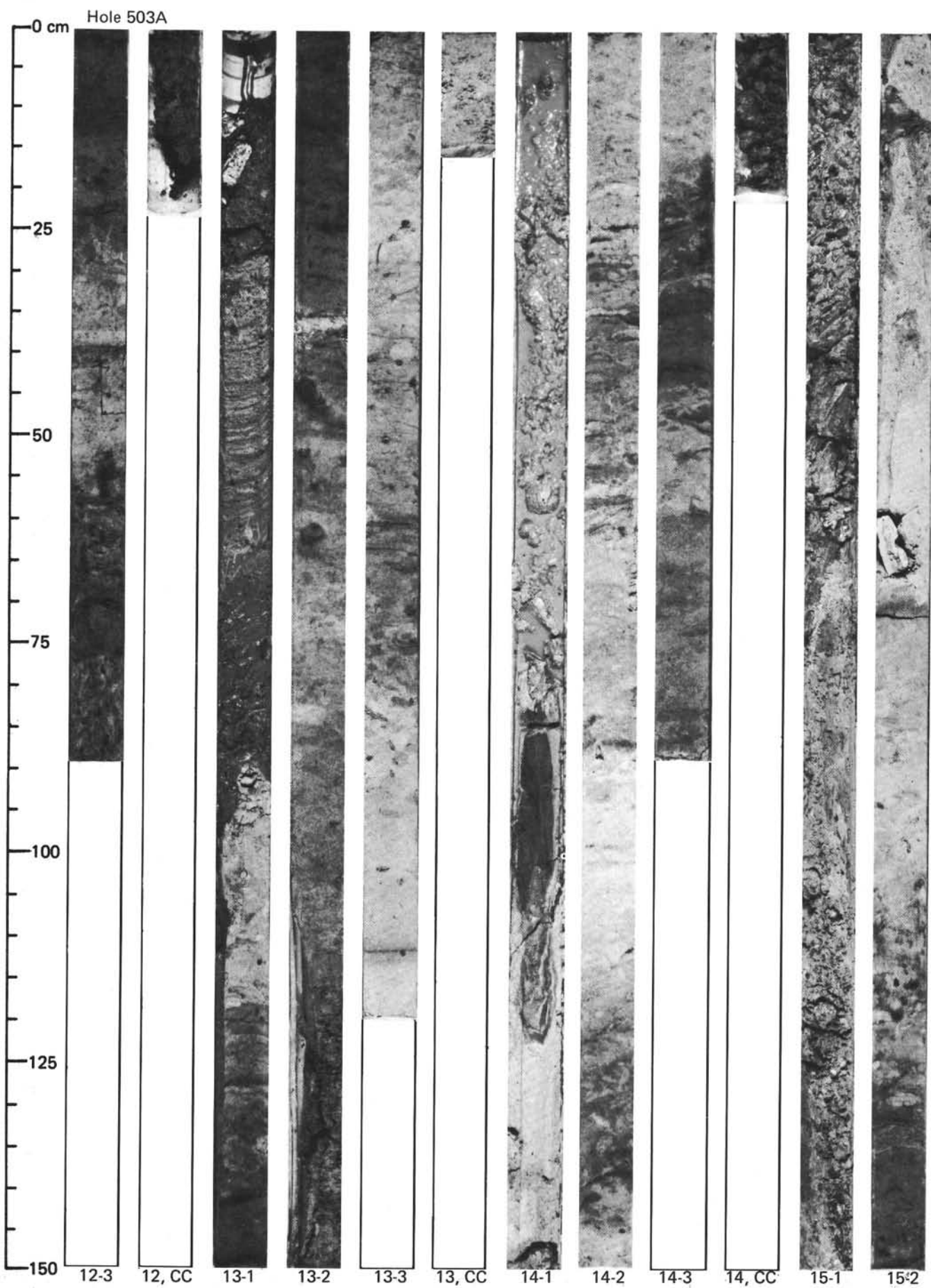


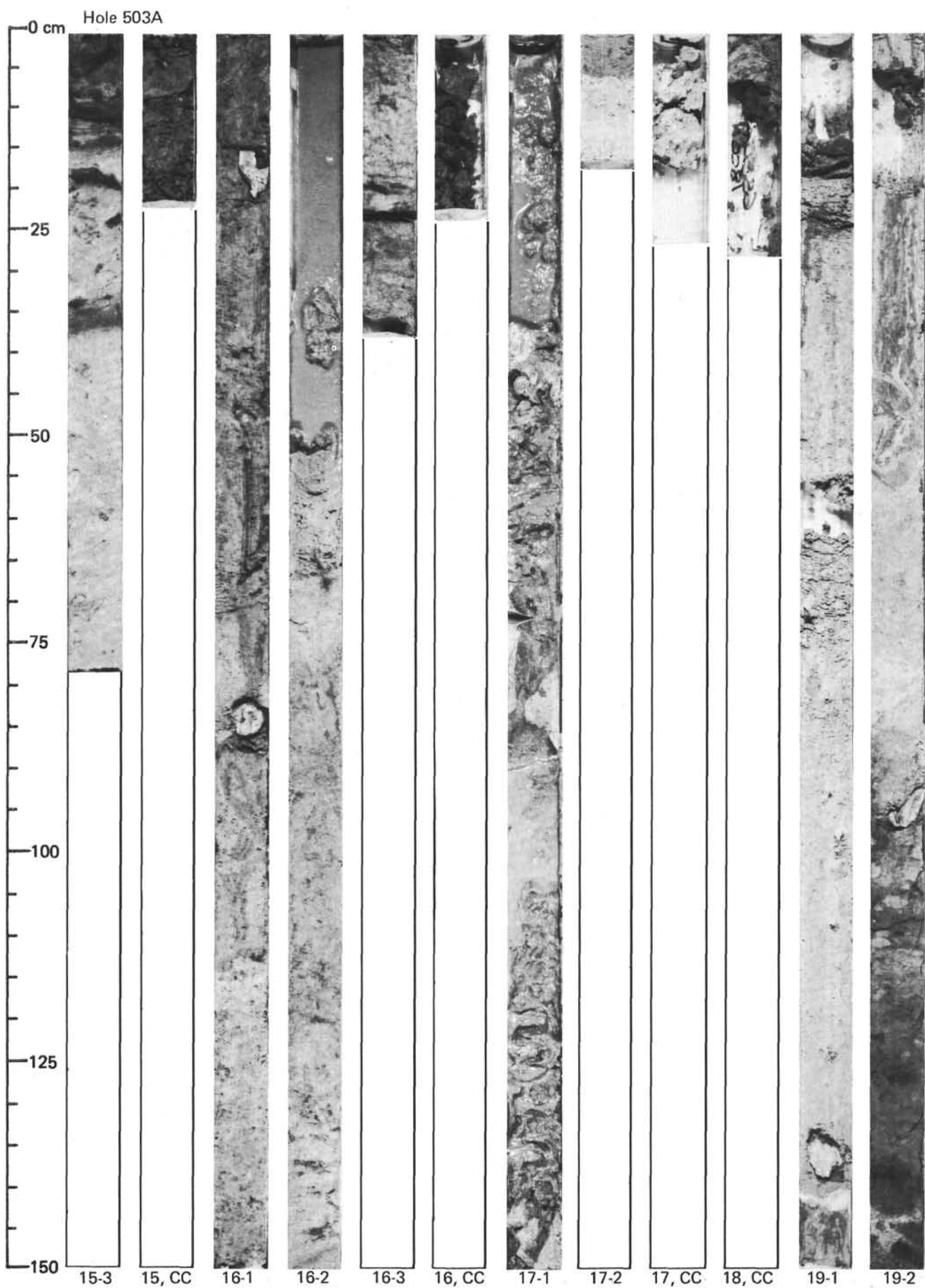


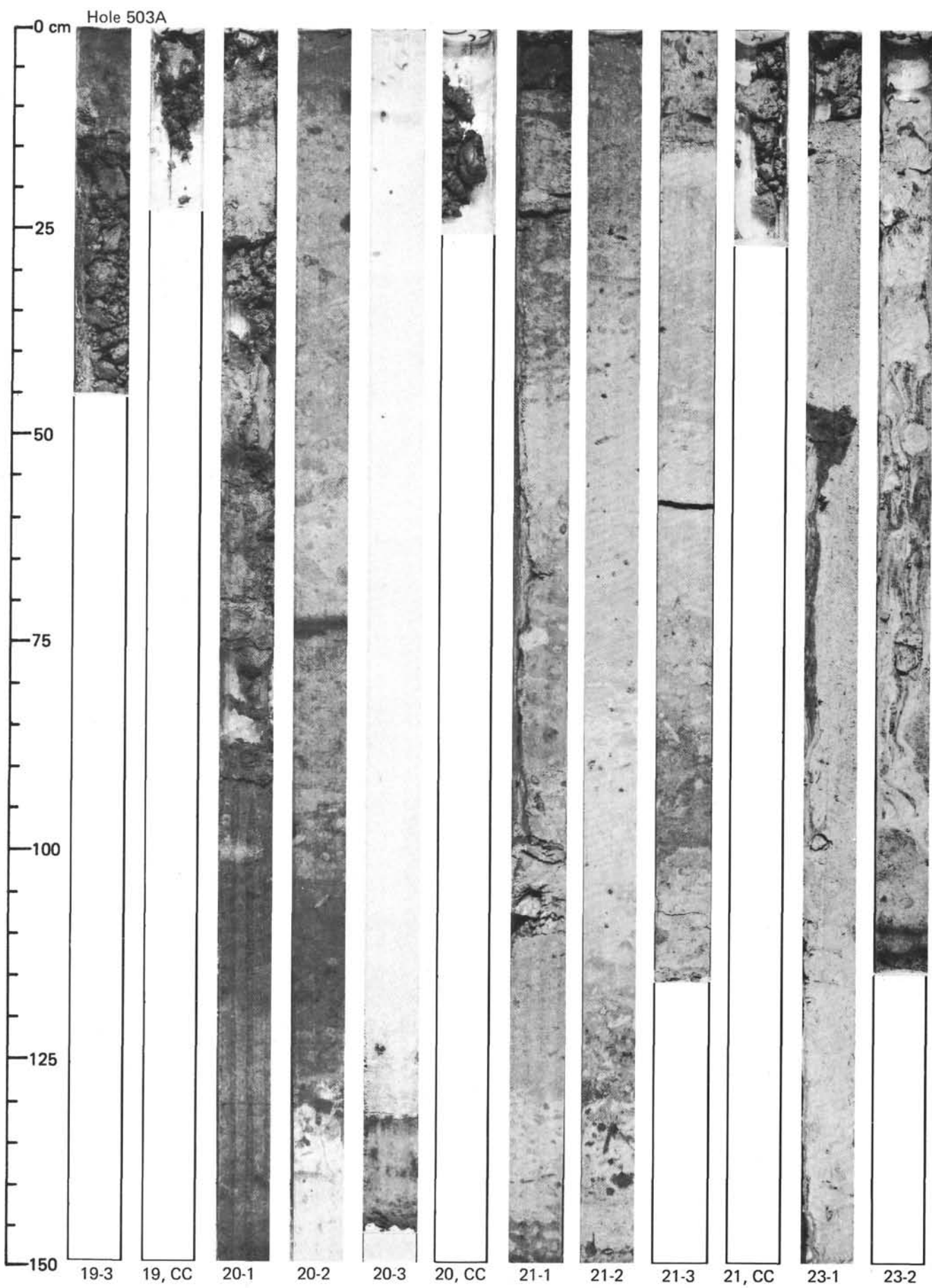
SITE 503

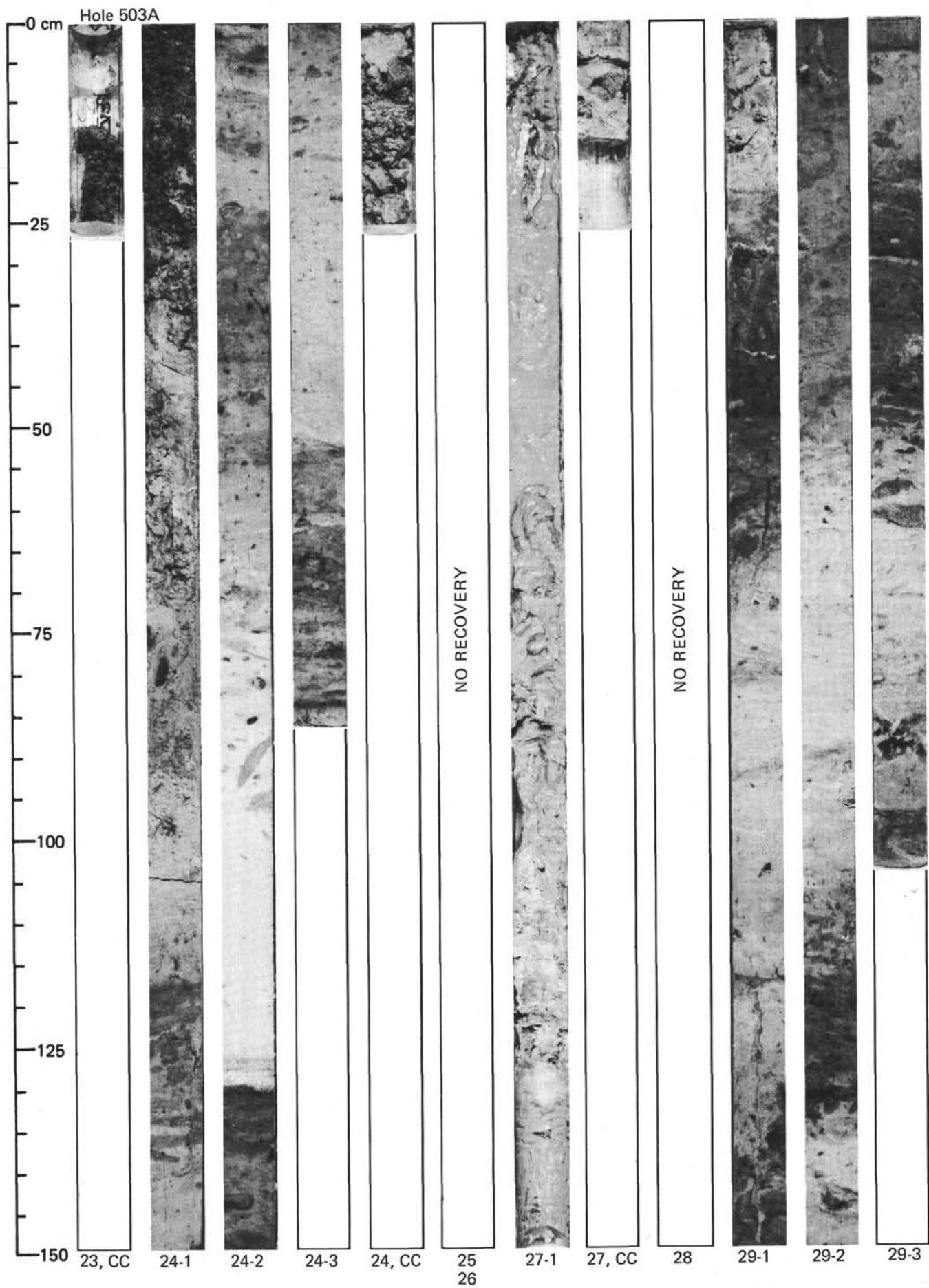


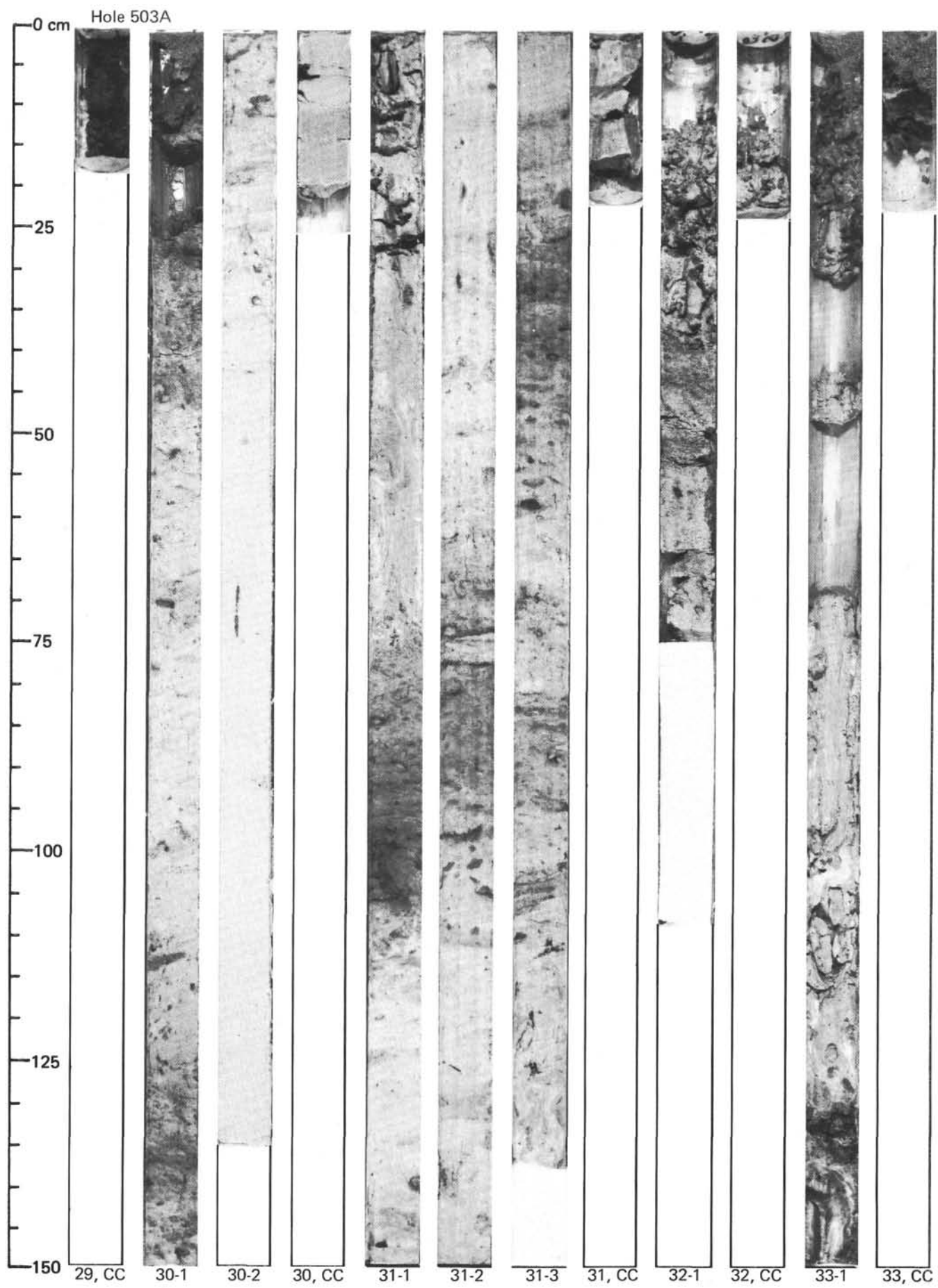


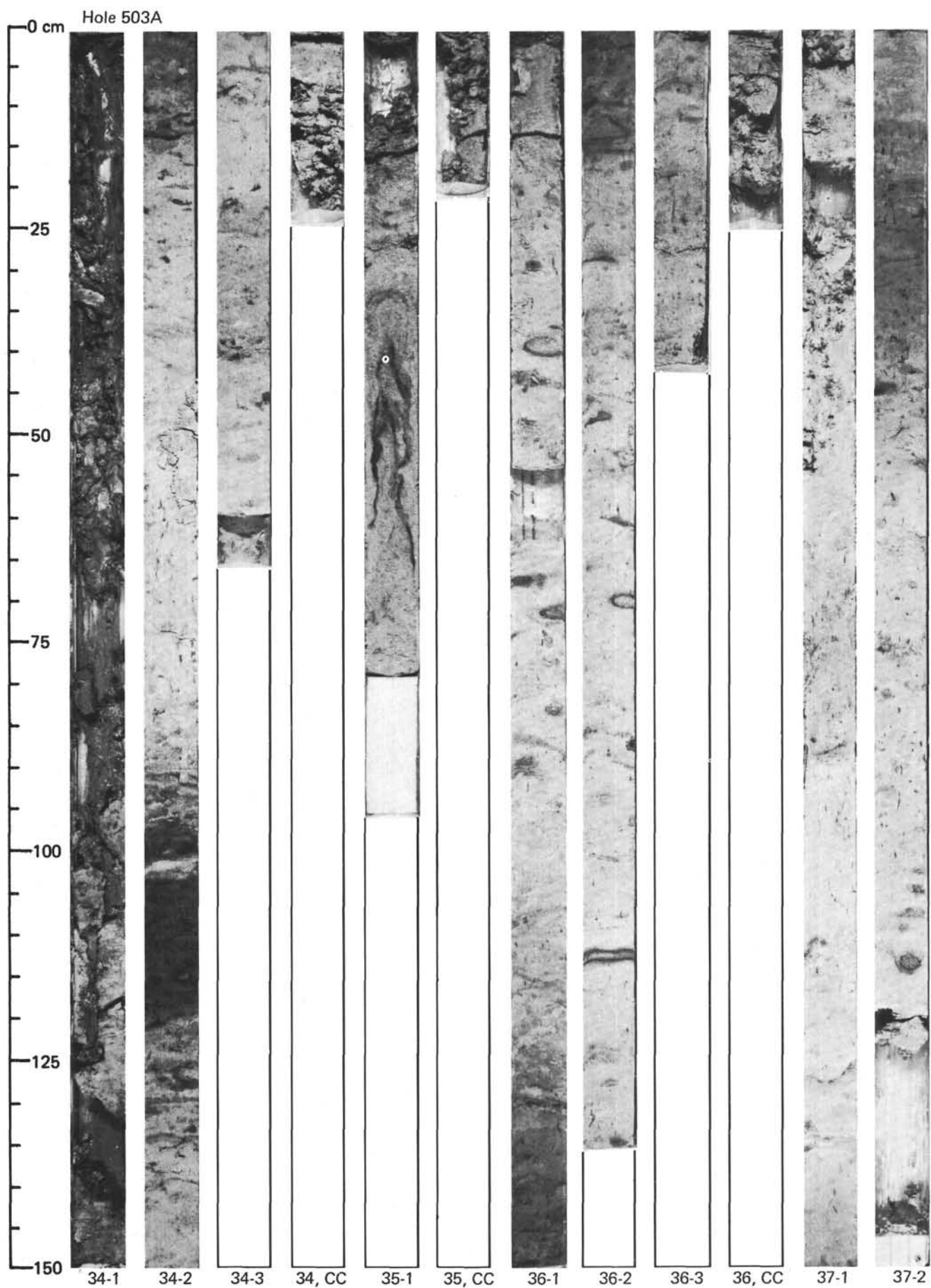




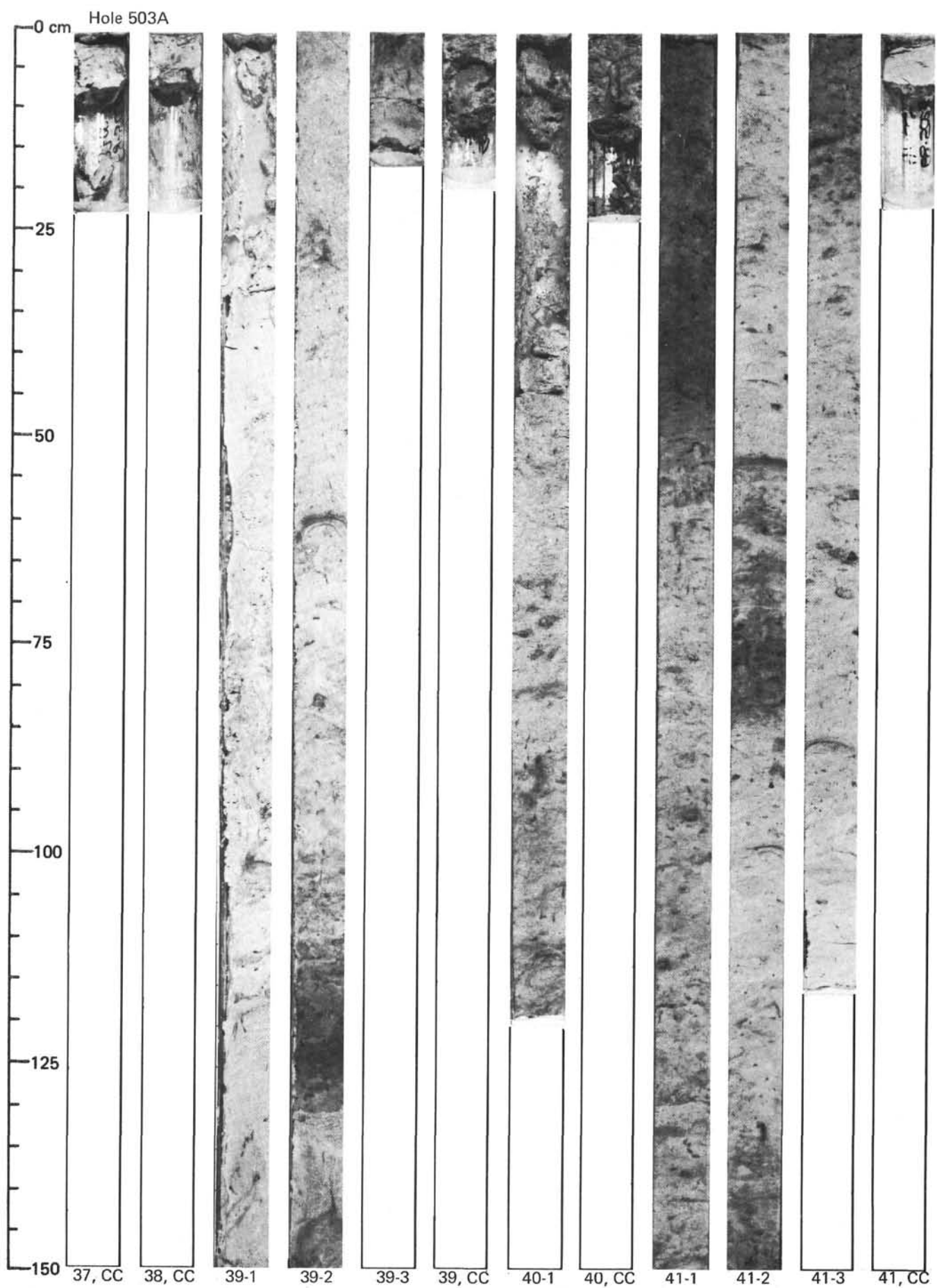


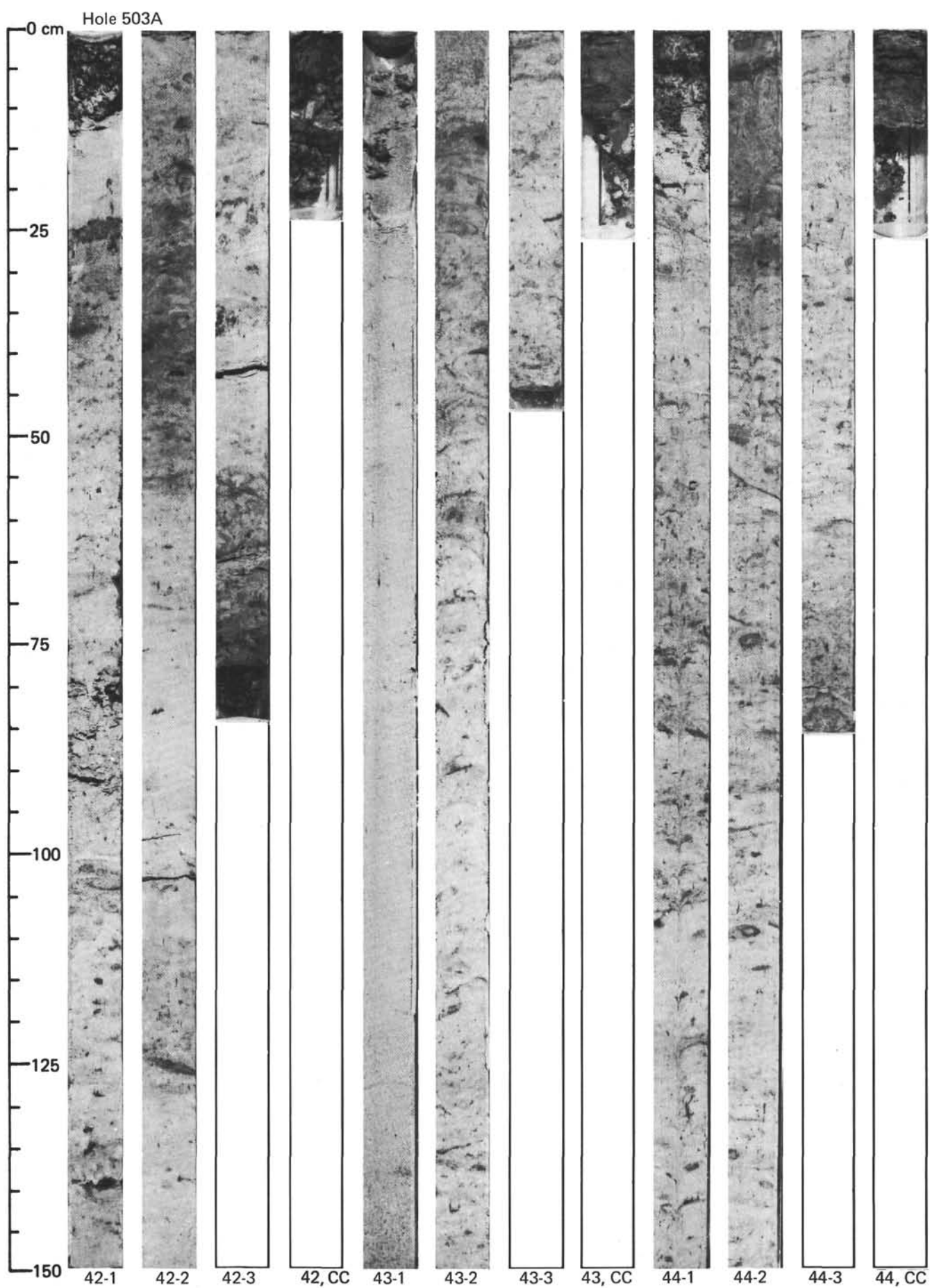




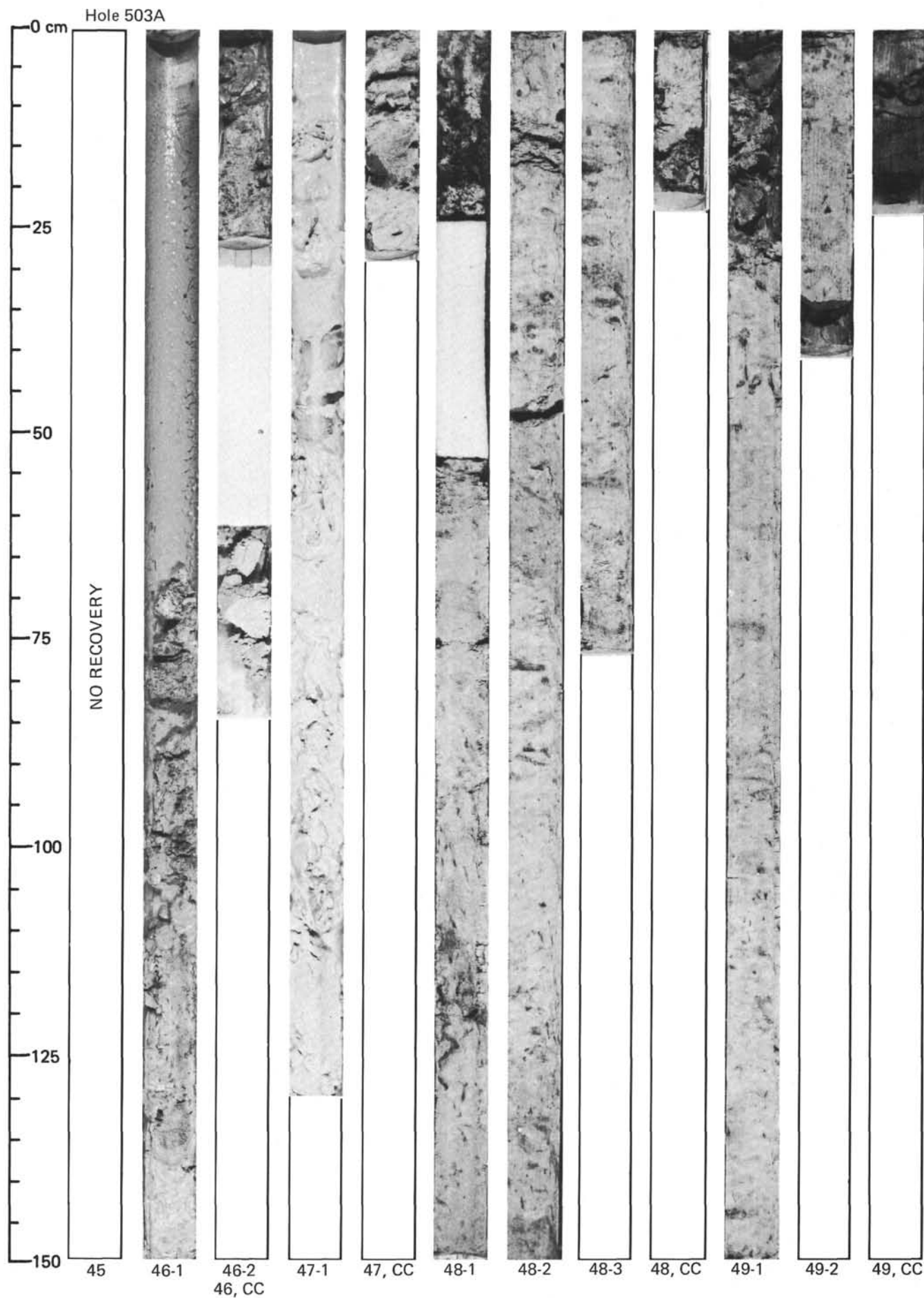


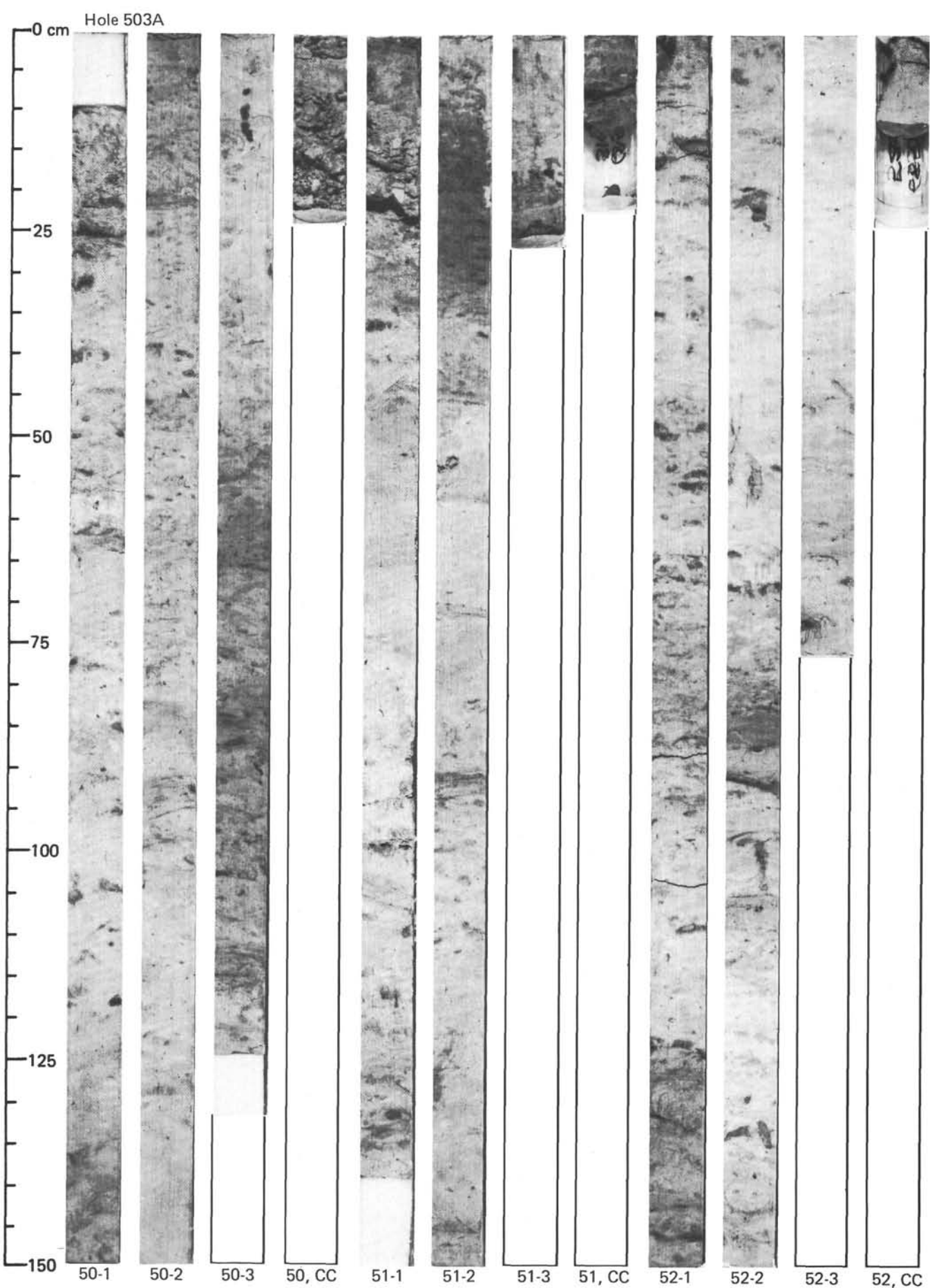
SITE 503





SITE 503





SITE 503

